ON THE TRANSMISSION PROPERTIES OF SYNAPSES MADE BETWEEN GRANULE CELLS AND CEREBELLAR PURKINJE CELLS

ROBERT SIMS

Doctor of Philosophy

ASTON UNIVERSITY

December 2003

ASTON UNIVERSITY

On the transmission properties of synapses made between granule cell axons and cerebellar Purkinje cells

Thesis submitted for the degree of Doctor of Philosophy, by Robert Edward Sims, December 2003.

In the cerebellar cortex, forms of both long-term depression (LTD) and long-term potentiation (LTP) can be observed at parallel fibre (PF) – Purkinje cell (PC) synapses. A presynaptic variant of cerebellar LTP can be evoked in PCs by raised frequency stimulation (RFS) of parallel fibres at 4-16Hz for 15s. This form of LTP is dependent on protein kinase A (PKA) and nitric oxide (NO), and can spread to distant synapses. Application of an extracellular NO scavenger, cPTIO, was found to prevent the spread of LTP to distant PF synapses in rat cerebellar slices.

G-substrate may be an important mediator of the NO-dependent pathway for LTD. 8-16Hz RFS of PFs without a high concentration of calcium chelator in the postsynaptic cell evokes LTD. In cerebellar slices from wild-type and transgenic, G-substrate knockout mice, 8Hz RFS was applied to PFs, with a low concentration of postsynaptic calcium chelator. In PCs from wild-type mice, LTD predominated, whereas in those from transgenic mice LTP predominated.

The ascending axon (AA) segment of the granule cell axon forms synapses with PCs as well as the PF segment. PPF and fluctuation analysis of EPSCs in rat PCs confirmed that the release sites of AA synapses have a greater probability of transmitter release than PF synapses. Furthermore, AA release sites have greater mean quantal amplitude than PF synapses, which is not due to a different type of postsynaptic receptor. AA synapses were found to have limited capacity to undergo the presynaptic variant of LTP, and were potentiated less than PF synapses in the presence of the PKA activator, forskolin. AA synapses also did not undergo the postsynaptic form of LTP, nor LTD induced by conjunctive stimulation of climbing fibre and PF.

Keywords: Cerebellum, Purkinje cell, granule cell, LTP, LTD.

Acknowledgements

I would like to thank the following people:

My supervisor, Dr. Nick Hartell, for his invaluable support and guidance throughout this project, and for undertaking several experiments that helped to elucidate work contained within this thesis.

Dr. S. Endo for supplying the transgenic G-substrate knockout mice.

Professor Ian Martin, Dr. David Poyner and Dr. Heather Cater for advice and assistance where required.

Contents

List of tables and figures

Abbreviations

AA	Granule cell ascending axon segment
AC	Adenylate cyclase
aCSF	Artificial cerebrospinal fluid
AMPA	DL-α-amino-3-hydroxy5-methyl-4-isoxazalone-proprionate
ArA	Arachidonic acid
Na_2ATP	Sodium adenosine-h'-triphosphate
BAPTA	1,2-bis(2-aminophenoxy)-ethane-N,N,N',N'-tetraacetic acid
cAMP	Cyclic adenosine-5'-monophosphate
CDR	Calcium-dependent recovery
CF	Climbing fibre
cGMP	Cyclic 3,5'-guanosine monophosphate
cPTIO	2-(4-carboxyphenyl)-4,4,5,5-tetramethylimidazoline-1-oxyl-3-oxide
CREB	cAMP response element-binding protein
CRF	Corticotrophin releasing factor
CV	Coefficient of variation
DMSO	Dimethylsulphoxide
DAG	Diacylglycerol
DPPX	1,3-dipropyl-8-phenylxanthine
EGTA	ethylene glycol-bis(2-aminoethylether)-N,N,N',N',-tetraacetic acid
EPSC	Excitatory postsynaptic current
GABA	γ-amino butyric acid
GC	Granule cell
GL	Granule cell layer
GRIP	Glutamate receptor binding protein
GTP	Guanosine-5'-triphosphate
HEPES	N-(2-hydroxyethyl)piperazine-N'-(2-ethanesulfonic acid)
IGF-1	Insulin-like growth factor 1
I_h	Holding current
IPSC	Inhibitory postsynaptic current
IP_3	Inositol-1,4,5-trisphosphate
LTD	Long-term depression
LTP	Long-term potentiation
mEPSC	Miniature excitatory postsynaptic current
MF	Mossy fibre
mGluR	Metabotropic glutamate receptor
N	Number of release sites
N_{min}	Minimum number of release sites
NBQX	1,2,3,4-tetrahydro-6-nitro-2,3-dioxo-benzo[f]quinoxaline-7-sulfonamide

NO	Nitric oxide
nNOS	Neuronal nitric oxide synthase
NOS	Nitric oxide synthase
OKR	Optokinetic reflex
PAF	Platelet activating factor
PC	Purkinje cell
PCL	Purkinje cell layer
PF	Parallel fibre
PICK1	Protein interacting with C kinase 1
PKA	Protein kinase A
PKC	Protein kinase C
PKG	Protein kinase G
PLA_2	Phospholipase A_2
PLC	Phospholipase C
PP	Protein phosphatase
PPD	Paired-pulse depression
PPF	Paired-pulse facilitation
PPR	Paired-pulse ratio
P_r	Probability of release at a release site
PTK	Protein tyrosine kinase
Q	Quantal amplitude
R_m	Input resistance
R_s	Series resistance
RFS	Raised-frequency stimulation
sGC	Soluble guanylate cyclase
STP	Short-term potentiation
τ_{decay}	Decay time constant
τ_{rise}	Rise time constant
VGCC	Voltage-gated calcium channel
V-M	Variance-mean
VM-M	Variance/mean-mean
VOR	Vestibulo-ocular reflex

Chapter 1

Introduction

1.1 The form and function of the cerebellum

The cerebellum is located in the hindbrain, connected to the brainstem. While it consists of only a tenth of the brain, it contains over half its neurones. The cerebellum functions as part of the motor system. Although it involves both motor and sensory components, it is necessary for neither movement nor sensation. Damage to the cerebellum causes a loss of co-ordination in limbs and eye movement, impaired balance and loss of muscle tone, as was demonstrated by lesion experiments (Dow & Moruzzi, 1958). This contrasts with damage to the motor cortex, which causes muscles to lose strength and speed, and even the inability to move muscles at all. The cerebellum acts unconsciously to improve smoothness and accuracy of movement, without requiring feedback. Instead, the cerebellum is thought to operate a 'feed-forward' mechanism, whereby signals from the motor cortex are compared to existing sensory data and corrections issued where necessary to ensure accuracy. Furthermore, the activity of the cerebellum is altered by experience, making it capable of learning motor tasks.

1.1.1 Gross anatomy of the cerebellum

The cerebellum has an external layer of grey matter, termed the cerebellar cortex. The interior region consists of white matter, and three pairs of deep nuclei. The cerebellum is connected to the pons by thick cerebellar peduncles. Each peduncle consists of the many axons that transmit afferent information to and efferent information from the cerebellum. The surface of the cerebellum is divided into lobes by parallel, transverse fissures. The primary fissure separates the cerebellum into posterior and anterior lobes. The posterolateral fissure then separates the large posterior lobe from the small flocculonodular lobe. Each lobe is then further subdivided by smaller

fissures into lobules. Each lobule consists of a branch of white matter extending from the centre of the cerebellum, surrounded by grey matter. There are further small offshoots of white matter and cortex from each lobule, termed 'folia'.

C

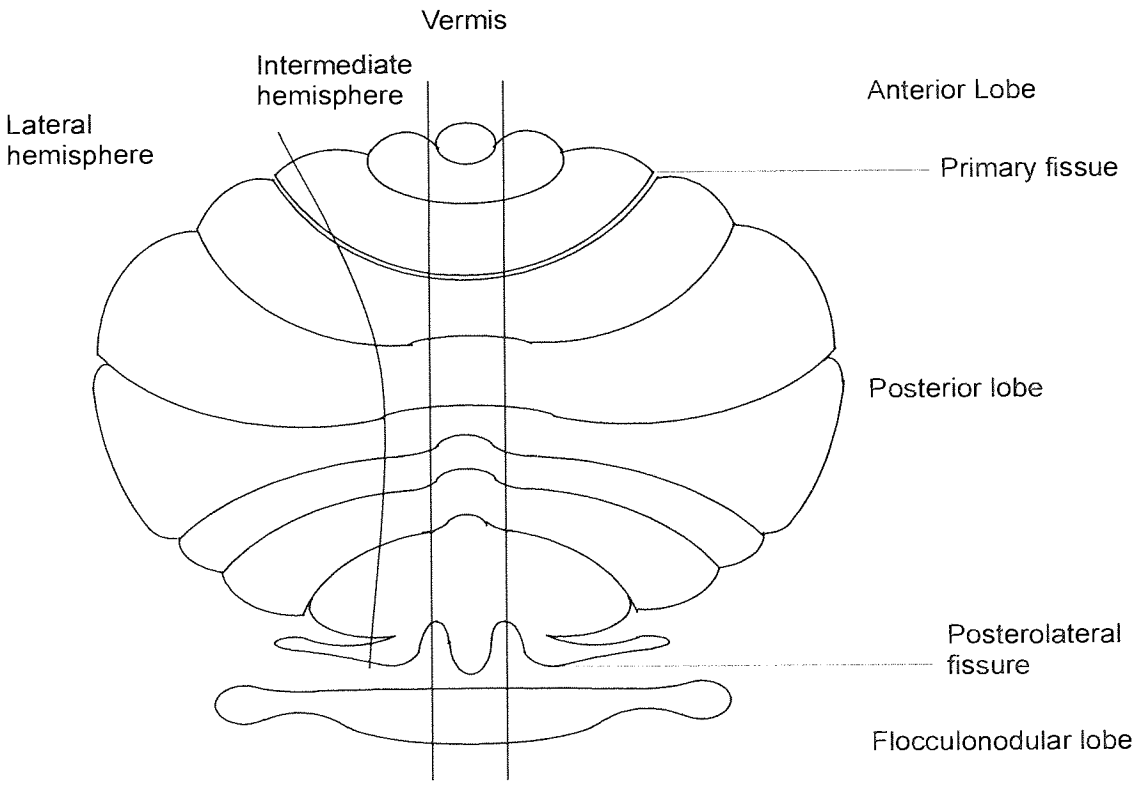

Figure 1.1 Gross cerebellar anatomy. *A* is a dorsal view of a human cerebellum, cut in a coronal plane at midway through the cerebellum with the anterior surface to the bottom of the picture. The '1' represents the pons of the brainstem. *B* is a human cerebellum cut in a sagittal plane mid-way through the vermis, demonstrating the lobules and folia branching out. *C* is a diagram of a posterior view of a human cerebellum. The longitudinal organisation is demonstrated on the top left of the picture, the transverse organisation on the right. The images of cerebellar sections in *A* and *B* have been reproduced from 'WebPath' (www.medlib.med.utah.edu/WebPath/) with the permission of Dr. E. Klatt, Florida State University.

The cerebellum is also divided longitudinally by two furrows, which separate the left and right cerebellar hemispheres from the central vermis. Each cerebellar hemisphere is further divided into an intermediate zone, next to the vermis, and lateral zone (Fig 1.1c). Each longitudinal section sends efferent information to different, distinct locations of the periphery via the deep cerebellar nuclei. Output from the vermis goes through the fastigial nucleus to the medial descending system, and is involved in the control of proximal muscles. Output from the intermediate zone of the cerebellar hemisphere is sent to the lateral descending system via the interposed nucleus, and is involved in control of the distal muscles in limbs. The lateral zone of the cerebellar hemisphere sends output to the dentate nucleus, which connects with the motor cortex, and is involved in the planning of voluntary movement.

1.1.2 The cerebellar cortex

There are three layers to the cerebellar cortex. The deepest layer, next to the white matter, is the granule cell layer (or granular layer; GL). It is densely populated by small granule cells (GCs) and a few inhibitory Golgi cells that lie near the upper boundary. Above it is the Purkinje cell layer (PCL), which is a monolayer of Purkinje cells (PCs), which are the sole output neurones of the cerebellar cortex. Their dendritic trees reach up into the molecular layer (ML) above that. The ML is a cell-sparse region, mostly comprising the axons of granule cells, with some inhibitory interneurones, stellate and basket cells. Beyond the ML is the pial surface.

The cerebellar cortex receives excitatory, glutamatergic input from two sources. The first are mossy fibres (MFs), which originate from the brainstem and spinal cord. Each MF excites many granule cells within a spatially restricted termination zone. Secondly there are the climbing fibres (CFs), which extend from the inferior olivary nucleus, and terminate on the soma and proximal dendrites of PCs. Both MFs and PFs also transmit information

to the deep cerebellar nuclei. Figure 1.2 illustrates the cerebellar neuronal circuit.

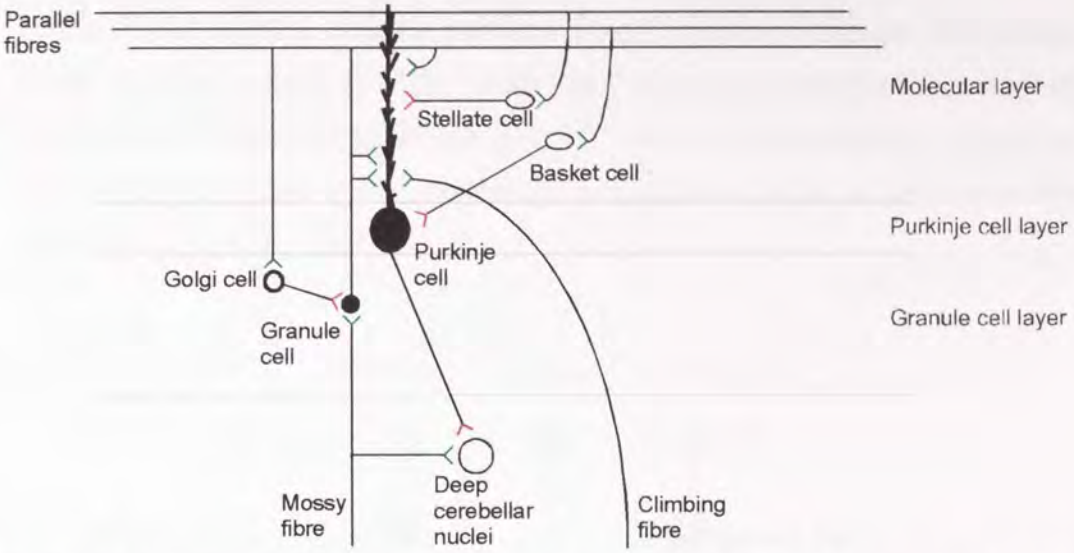

Figure 1.2 Representation of the cerebellar cortical circuit. This schematic diagram demonstrates the inputs to and the outputs from the cerebellar cortex. Excitatory synapses are illustrated by green lines and inhibitory synapses by red lines.

1.1.3 The cerebellar Purkinje cell.

PC dendritic trees are extensive, and planar. They rise to the pial layer, and can spread over 100μm in each direction yet are just a few μm thick (Rapp *et al.*, 1994). All PC dendritic trees are aligned similarly, with the plane of the dendritic tree in the sagittal plane. PCs are the sole output neurone of the cerebellar cortex, therefore understanding the inputs to PCs is essential to understanding the function of the cerebellar cortex. Excitatory, glutamatergic inputs to PCs are supplied by the CF and GCs. Additionally, there are inhibitory inputs from the interneurones of the ML.

Initially a PC is multiply innervated by several CFs, although after birth this swiftly declines to just one CF, although one CF may innervate several PCs. CF synapses are located on the proximal dendrites of the PC (Palay & Chan-Palay, 1974). Up to 26,000 CF synapses per PC has been estimated (Ito, 2001) according to the density of CF-PC varicosities on PC dendrites (Nieto-Bona *et al.*, 1997), although this is likely to be a huge overestimate as the CF

does not reach distal dendrites (Palay & Chan-Palay, 1974). Around 500 CF-PC transmitter release sites have been reported (Silver *et al.*, 1998), with 8-10 vesicle docking sites per CF-PC synapse (Xu-Friedman *et al.*, 2001). These would instead indicate perhaps 50-100 active synapses. CF activity elicits complex spikes in PCs, which consist of large depolarising sodium conductances superimposed with smaller calcium conductances (Eccles *et al.*, 1966b). Complex spikes discharge irregularly at rates of approximately 1Hz *in vivo* (Thatch, 1967).

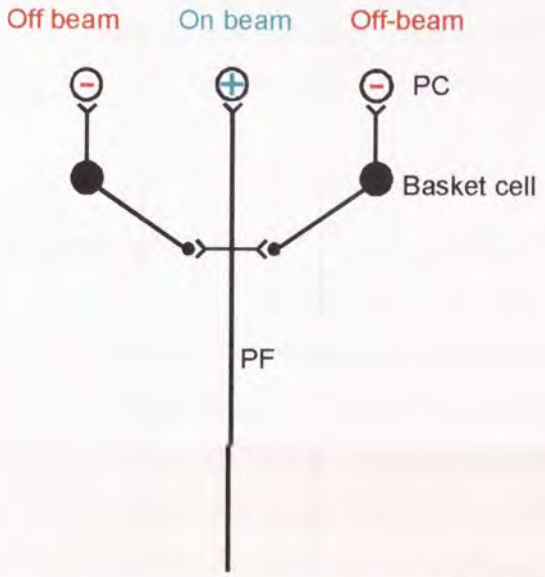

Figure 1.3 On-beam and off-beam stimulation. A parallel fibre transmits excitatory information to PCs and interneurones it forms synapses with, although the interneurones inhibit PCs to either side of those the PF excites.

GC axons have two segments. The ascending axon segment (AA) rises vertically past the PCL into the ML, forming multiple synapses with each PC (Napper & Harvey, 1988). In the ML, the axon bifurcates, and forms parallel fibres (PFs), which run in opposite directions for long distances, orthogonal to the plane of the PC dendrites. The length of PFs vary according to species, but in rats they extend 2-3mm in both directions from the bifurcation point (Harvey & Napper, 1988; Pitchitpornchai *et al.*, 1994). PFs form one or two synapses with each PC *en passant*, with multiple (maximum of two) synapses being more prevalent in the proximal region of the PF (Pitchitpornchai *et al.*, 1994). Each PC was once thought to receive about

60,000 synapses from GCs (Palay & Chan-Palay, 1974), although a more recent study suggests over 150,000 (Napper & Harvey, 1988). Up to 20% of these are estimated to be made by the AA (Gundappa-Sulur *et al.*, 1999). GC activity elicits simple spikes in PCs, which discharge at 50-100Hz. (Thatch, 1967).

PCs receive inhibitory signals from stellate and basket cells, which are also activated by GC axons. However, while a PF transmits excitatory information to the PCs it innervates ('on-beam' stimulation), the interneurones it stimulates transmit inhibitory signals to PCs either side of the PF beam ('off-beam' stimulation; fig 1.3.)

1.1.4 Cerebellar microcomplexes

The cerebellar cortex is organised into spatially discrete areas, termed 'microzones'. Microzone range from about 0.3 up to 1mm wide and can be much as $10mm^2$ in area (Oscarsson, 1979; Ito, 1998), containing thousands of PCs and many afferent MFs and CFs. Each microzone is 'paired' with a set of neurones in the deep cerebellar nuclei, as MFs afferent to particular microzones of the cerebellar cortex also activate the paired neurones in the deep nuclei via axon collaterals (Ito, 2001). A microzone is responsible for controlling the movement components of a certain area of the periphery. Each area of the periphery however is represented by several microzones, which are often not adjacent to each other (Shambes *et al.*, 1978).

The cerebellar microcomplex is postulated to work according to the following concepts (for a detailed account see Ito, 2001). MFs pass signals to GCs, and these control PC activity through patterns of excitatory and, via interneurones, inhibitory inputs. These MFs also control the activity of the paired deep cerebellar neurones, which are further modulated by inhibitory PC activity. In this model, errors are represented by CF signals to target PCs, which removes inappropriate MF-PC input to facilitate a learning element. This is consistent with data that reveal the PF receptive fields of PCs are

outside the local CF receptive field (Ekerot & Jorntell, 2001), which would depress PF synapses.

1.2 Plasticity at parallel fibre – Purkinje cell synapses

Synaptic plasticity was first postulated by Hebb (1949), who theorised that synchronous pre- and postsynaptic activity in mutually interconnected neurones increases the efficacy of both sides of the synapse. The first network theory of the cerebellar cortex was formed by Marr (1969), who suggested that the convergent GC and CF inputs to the cerebellum might act to cause pre- and postsynaptic stimulation, and thus potentiation. This was refined by Albus (1971), who theorised that depression, rather than potentiation, was caused by conjunctive stimulation of GC- and CF-PC synapses. However, experimental evidence for the existence of cerebellar long-term depression (LTD) was not acquired until the 1980s by Ito and colleagues (Ito & Kano, 1982; Ito *et al.*, 1982). Since then another form of plasticity has been discovered at PF-PC synapses, which is dependent on PF activity but not CF activity, long-term potentiation (LTP; Shibuki & Okada, 1992; Salin *et al.*, 1996; Jacoby *et al.*, 2001; Lev-Ram *et al.*, 2002).

1.2.1 Induction of long-term depression

There are three cellular requirements thought to be physiologically necessary for LTD. Firstly LTD requires activation of fast, ionotropic DL-α-amino-3-hydroxy5-methyl-4-isoxazalone-proprionate receptors (AMPARs; Linden *et al.*, 1993; Hemart *et al.*, 1995). Secondly, LTD requires activation of metabotropic glutamate receptors (mGluRs; Linden *et al.*, 1993; Conquet *et al.*, 1994; Hartell, 1994b; Shigemoto *et al.*, 1994). These first two requirements are met by glutamate release from PF synapses (Konnerth *et al.*, 1990; Batchelor *et al.*, 1994). The third requirement for LTD is postsynaptic calcium influx via voltage-gated calcium channels (Sakurai, 1990; Sugimori & Llinas, 1990; Linden *et al.*, 1991). The CF also releases glutamate to activate AMPARs, and because of the large number of

synapses this causes a huge depolarisation of the cell, hence the CF is considered the likeliest source of the increase in postsynaptic calcium (Ross & Werman, 1987; Sugimori & Llinas, 1990; Sakurai, 1990; Konnerth *et al.*, 1992). It has been demonstrated that depolarisation of the cell can be used in place of the CF to induce LTD *in vitro* (Crepel & Krupa, 1988; Hirano, 1990; Glaum *et al.*, 1992). However, depolarisation should not be considered equal to CF stimulation, as a number of neurotransmitters from the CF may affect LTD (as detailed below). Conjunction of depolarisation with PF stimulation has been reported as less effective at inducing LTD than conjunctive CF and PF stimulation (Reynolds & Hartell, 2000).

Conjunctive LTD is associative, in that it requires repetitive stimulation of CF and PFs within a certain time frame. Several studies have examined the relative timing of these two inputs that is most effective in inducing LTD. LTD can be induced by simultaneous stimulation of the CF and PFs, or activation of CFs up to 750ms before the PF (e.g. Ekerot & Kano, 1989; Karachot *et al.*, 1995; Chen & Thompson, 1995). However, other studies favour prior stimulation of PFs (Schreurs *et al.*, 1996; Wang *et al.*, 2000a). This is more fitting with the theory that the CF acts as an error signal and that, *in vivo*, CF signals appear to reach the cerebellar cortex up to 250ms after movement and MF activity has ceased (Kitazawa *et al.*, 1998; Kitazawa, 2002). While the PF-PC synapses are depressed in LTD, the CF-PC synapses are not. In cerebellar slices conjunctive LTD tends to develop gradually over the course of 10-60 minutes (e.g. Karachot *et al.*, 1995; Hartell, 2000; Wang *et al.*, 2000a). In some cultured preparations, however, LTD has been found to reach a maximal level within 5 minutes (Linden, 1995; Wang & Linden, 2000). In these experiments there was a two-phase LTD, with a peak in depression at about five minutes after induction that appeared to be absent in cerebellar slices.

A form of LTD can also be generated by activation of PFs alone, termed CF-independent LTD. This has been achieved by a number of protocols, involving raised frequency, or raised frequency and intensity stimulation (Hartell, 1996; Eilers *et al.*, 1997; Jacoby & Hartell, 1999). It is thought that

activation of sufficient PFs in close proximity can depolarise the PC sufficiently to allow calcium influx through voltage-gated calcium channels (VGCCs; Hartell, 1996; Eilers *et al.*, 1997), thus mimicking the action of the CF.

1.2.2 Secondary messenger pathways of long-term depression

mGluRs are G-protein-coupled receptors, and it is activation of the type 1 receptor that is thought to be necessary for LTD (Hartell, 1994b; Shigemoto *et al.*, 1994; Conquet *et al.*, 1994). They are characterised by activating phospholipase C (PLC; Schoepp & Conn, 1993; Nakanishi, 1994). PLC hydrolyses the membrane lipid phosphatidylinositol 4,5-bisphosphate to produce 1,2-diaglycerol (DAG) and IP_3. mGluR1s are also linked to the activation of phospholipase A_2 (PLA_2; Aramori & Nakanishi, 1992; Dumuis *et al.*, 1993; Lombardi *et al.*, 1996).

IP_3 receptors are abundant in PCs (Maeda *et al.*, 1990). IP_3 activates IP_3 receptors on the surface of intracellular calcium stores to open associated calcium channels, thus increasing intracellular calcium levels. Experiments on cultured PCs have questioned the role of IP_3 in LTD, as an inhibitor of IP_3 receptors failed to prevent LTD. Addition of synthetic DAG, however, combined with AMPAR activation and depolarisation produced LTD (Narasimhan *et al.*, 1998). In cerebellar slices LTD can be generated with IP_3 release replacing the need for mGluR activation in LTD induction (Kasono & Hirano, 1994; Khodakhah & Armstrong, 1997). LTD was prevented in cerebellar slices by both thapsigargin (a depletor of intracellular calcium stores; Hemart *et al.*, 1995), and LTD could be restored in mGluR1-deficient mice by photolytic release of IP_3 (Daniel *et al.*, 1999). Ryanodine receptors may also be important in calcium release for LTD, as they are responsible for calcium-induced calcium release from internal stores. The ryanodine receptor inhibitor ruthenium red has been demonstrated to block LTD (Kohda *et al.*, 1995)

DAG, with the presence of sufficiently raised intracellular calcium levels, is prominent in the activation of protein kinase C (PKC; Shinomura *et al.*, 1991). Synthetic DAG, when combined with depolarisation and AMPA pulses generated LTD in cultured PCs (Narasimhan *et al.*, 1998). PKC inhibition blocks LTD in cerebellar slices, whether induced by PF activation and depolarisation (Crepel & Jaillard, 1990; Hemart *et al.*, 1995; Freeman *et al.*, 1998), or conjunctive activation of PFs and CF (Hartell, 1994a), and also in cultured PC pairing glutamate application and depolarisation (Linden & Connor, 1991). Furthermore, activation of PKC by phorbol esters causes depression of glutamate currents (Crepel & Krupa, 1988). Activation of PKC may also be controlled by corticotrophin releasing factor (CRF; Miyata *et al.*, 1999). However, a transgenic knockout of PKC-γ did not block LTD (Chen *et al.*, 1995), although it may be that other types of PKC are involved in cerebellar LTD.

PLA_2 produces the release of arachidonic acid (ArA) and oleic acid from membrane phospholipids. LTD was weakened by inhibitors of PLA_2, but has been restored by addition of ArA or oleic acid in cultured PCs (Linden, 1995). ArA inhibitors also have also prevented LTD in cerebellar slices (Reynolds & Hartell, 2001). ArA stimulates PKC-γ (Shearman *et al.*, 1989) and possibly also guanylate cyclase (sGC; Tremblay *et al.*, 1988). However, it also downregulates DAG via DAG kinase, and therefore also downregulates PKC (Rao *et al.*, 1994).

Protein tyrosine kinases (PTKs) have also been implicated in LTD, as PTK inhibitors have been demonstrated to block LTD, possibly through involvement with PKC (Boxall *et al.*, 1996). This may be through inhibition of the PLC-mediated pathway, as it blocks IP_3 formation by the G-protein subtypes $G_{q/11}$ (Umemori *et al.*, 1999). PTKs may also be associated with insulin-like growth factor 1 (IGF-1) receptors, IGF-1 being released from the CF (Wang & Linden, 2000). A form of PTK, Lyn, is associated with AMPARs, and it may be this that is activated in LTD (Hayashi *et al.*, 1999). This study also found that PTKs may also activate the mitogen-activated protein kinase

pathway which would lead to transcriptional modifications (Hayashi *et al.*, 1999).

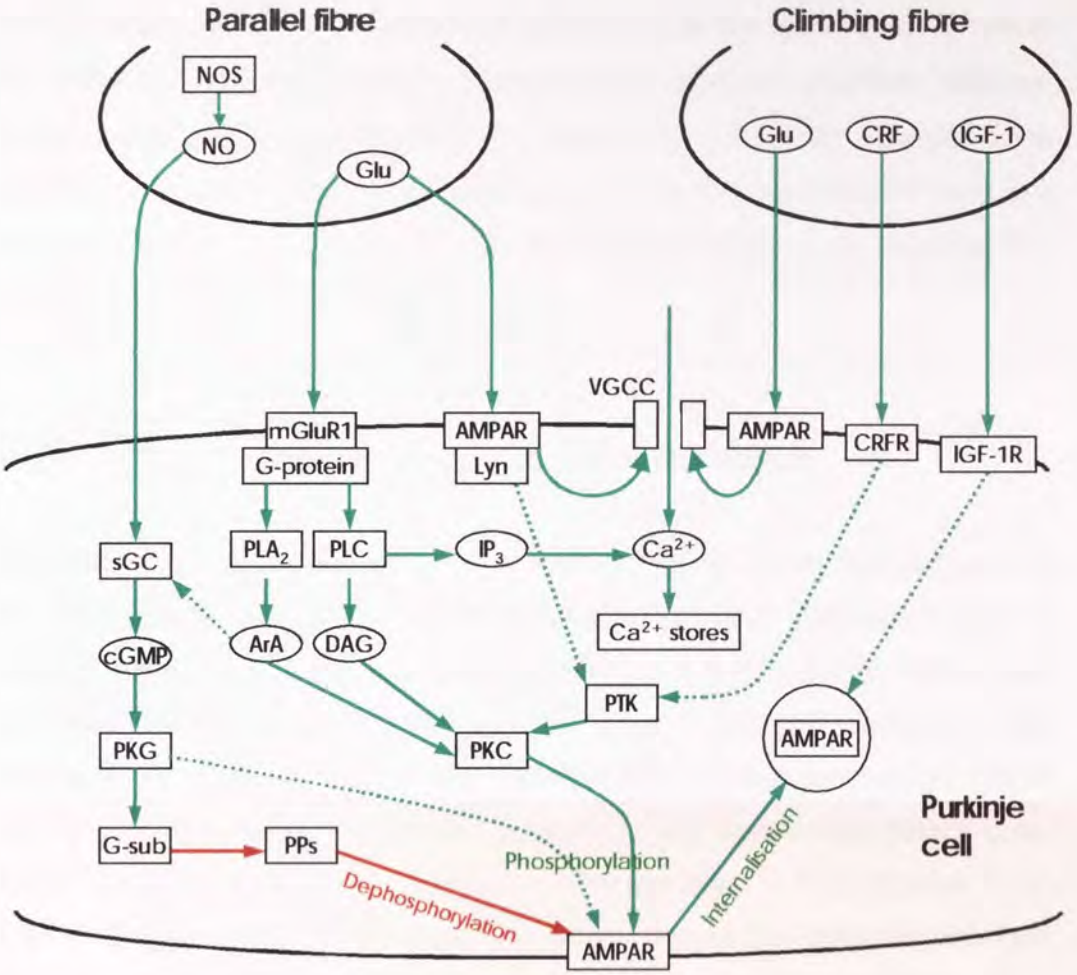

Figure 1.4 Signal transduction pathways involved in cerebellar LTD. This diagram summarises the major pathways involved in and leading to AMPAR phosphorylation and downregulation. Green arrows represent activation, and red arrows represent inhibition. Dotted lines indicate uncertain links. Abbreviations used: NOS, nitric oxide synthase; NO, nitric oxide; sGC, soluble guanylate cyclase; cGMP, cyclic guanosine monophosphate; PKG, protein kinase G; G-sub, G-substrate; PPs, protein phosphatases; Glu, glutamate; mGluR1, type 1 metabotropic glutamate receptor; PLA_2, phospholipase A_2; ArA, arachidonic acid; PLC, phospholipase C; DAG, diacylglycerol; PKC, protein kinase C; IP3, inositol 1,4,5-trisphosphate; Ca2+, calcium, PTK, protein tyrosine kinase; AMPAR, AMPA receptor, VGCC, voltage-gated calcium channel; CRF, corticotrophin-releasing factor; CRFR, CRF receptor; IGF-1, insulin-like growth factor 1; IGF-1R, IGF-1 receptor.

Also possibly involved in LTD is the δ_2 subunit of glutamate receptors. An antisense oligonucleotide against δ_2 mRNA prevented LTD in cultured neurones (Hirano *et al.*, 1994; Jeromin *et al.*, 1996). LTD was also impaired in PCs obtained from mice with a genetic knockout of δ_2 receptors in both cerebellar slices (Kashiwabuchi *et al.*, 1995) and cultured neurones (Hirano

et al., 1995). There is evidence that δ2 subunits may form heteromers with other AMPAR subunits, although glutamate sensitivity is greatly reduced (Kohler *et al.*, 2003). In cultured PCs, antibodies to the ligand-binding site of δ2 subunits reduced synaptic transmission, induced AMPAR receptor endocytosis, yet also abolished LTD (Hirai *et al.*, 2003). δ2 subunits have also been reported to have a developmental role in enhancing PF synapse formation on PCs, and restricting CF synapse formation to the proximal PC dendrites (Ichikawa *et al.*, 2002).

1.2.3 The nitric oxide pathway of long-term depression

The nitric oxide (NO) pathway of LTD appears to be largely independent of the AMPA/mGluR1/calcium dependent pathway. It is discussed fully in chapter 3, but is summarised briefly here. NO is produced by nitric oxide synthase (NOS), which exists in three forms: epithelial, inducible, and neuronal, of which only the latter is abundant in the cerebellum. While neuronal NOS was found to be present in GCs and basket cells (Bredt *et al.*, 1990; Southam *et al.*, 1992), it has not been identified in PCs (Crepel *et al.*, 1994). Consequently, NO is thought to diffuse across the synaptic cleft from PFs. The role of NO in LTD is demonstrated by the fact that NOS inhibitors prevented LTD (Crepel & Jaillard, 1990; Shibuki & Okada, 1991; Daniel *et al.*, 1993), and an NO donor induced depression (Shibuki & Okada, 1991). NO activates soluble guanylate cyclase (sGC) in the postsynaptic cell, which produces cyclic 3,5-guanosine monophosphate (cGMP; Daniel *et al.*, 1993; Boxall & Garthwaite, 1996), which in turn activates protein kinase G (Ito & Karachot, 1992; Hartell, 1994a). PKG activates G-substrate (Schlichter *et al.*, 1978; Aswad & Greengard, 1981a; Aswad & Greengard, 1981b) which is a potent inhibitor of protein phosphatase 2a (PP2a; Hall *et al.*, 1999; Endo *et al.*, 1999). As PP2a probably acts to dephosphorylate AMPARs, the NO pathway therefore contributes to phosphorylation of AMPARs.

1.2.4 Protein synthesis and gene regulation in long-term depression

A long-term requirement for protein synthesis has been demonstrated by translational inhibitors applied immediately after LTD induction, which blocked LTD after 45 minutes in cultured PCs (Linden, 1996). In cerebellar slices, however, translational inhibitors applied for 5 minutes around the induction period rapidly and persistently inhibited LTD. However, the same 5-minute treatment with the translational inhibitor failed to block LTD when applied 15 minutes after induction, suggesting an early role for protein synthesis as well (Karachot *et al.*, 2001).

There are a few instances of gene regulation identified in LTD. Application of AMPA and 8-bromo-cGMP to cerebellar slices causes a depression of AMPA sensitivity in PCs (Ito & Karachot, 1990) and also enhanced expression of the genes c-Fos and Jun-B (Nakazawa *et al.*, 1993). Jun-B has also been activated by AMPA application and CF stimulation (Yamamori *et al.*, 1995) and conjunctive CF-PF stimulation (Yano *et al.*, 1996). Jun-B and c-Fos form a complex that operates as a transcriptional factor (Morgan & Curran, 1989), but little more is known. The later phase of LTD may be controlled by cAMP response element-binding protein (CREB), which is activated at high calcium concentrations by calcium/calmodulin dependent kinase IV. When CREB was prevented from binding with DNA, the late phase of LTD after 45 minutes was abolished (Ahn *et al.*, 1999). Cultured PCs derived from mice with a CaMKIV knockout did not exhibit the late phase of LTD either (Ho *et al.*, 2000).

1.2.5 Inactivation of AMPA receptors

LTD results in a decrease in the activity of postsynaptic AMPARs at the PF-PC synapse. It has previously been reported that LTD is caused by desensitisation of the receptor (Hemart *et al.*, 1994), and AMPAR activity can be downregulated by PLA_2 (Bi *et al.*, 1998; Chabot *et al.*, 1998). However, desensitisation of AMPARs has since been refuted (Linden, 2001). As

desensitisation is also usually an activity-dependent process, it is doubly unlikely, as LTD can be generated without AMPAR activation (Hemart *et al.*, 1995; Finch & Augustine, 1998).

A more likely cause is AMPAR declustering (Matsuda *et al.*, 2000; Hirai, 2001) and/or internalisation (Wang & Linden, 2000). Both declustering and internalisation are dependent on the phosphorylation-mediated release of the intracellular area of AMPARs from cytoskeletal elements. The AMPAR is anchored to cytoskeletal proteins by glutamate receptor binding protein (GRIP), AMPA receptor binding protein (ABP), and protein interacting with C kinase 1 (PICK1; Dong *et al.*, 1997). Phosphorylation by protein PKC of the serine-880 residue of the AMPAR GluR2 subunit greatly reduces GRIP affinity for the receptor (Barria *et al.*, 1997; Matsuda *et al.*, 2000; Xia *et al.*, 2000).

1.2.6 Spread of long-term depression to distant synapses

The Marr-Albus theories of cerebellar cortical function assume synapse specificity, in that the only PF synapses depressed are those conjunctively activated with the CF. However, there is increasing evidence that this is in fact not the case. A reduction in AMPAR sensitivity to glutamate has been observed at PC synapses up to 100μm distant from PFs either conjunctively stimulated with the CF, (Reynolds & Hartell, 1998; Hartell, 2000; Wang *et al.*, 2000b), or stimulated with raised intensity and/or frequency (Hartell, 1996). As this spread most likely occurs through diffusion of an extracellular messenger (Wang *et al.* 2000b), it is possible that synapses on nearby PCs could also be affected, as well as synapses on the same PC. It has been postulated that synapse specificity in such circumstances may be maintained by temporal, rather than spatial, activity (Ito, 2001). A further suggestion in the same paper is that volume learning in a number of synapses or cells, rather than individual synapses, may be the mechanism of operation for motor learning.

1.2.7 Long-term potentiation of parallel fibre – Purkinje cell synapses

PF-PC synapses not only undergo LTD but also LTP. The mechanisms involved in long-term potentiation at PF-PC synapses are discussed fully in chapter 3. Briefly, LTP is most commonly observed in the presence of a high concentration of postsynaptic calcium chelator (Shibuki & Okada, 1992; Salin *et al.*, 1996; Lev-Ram *et al.*, 2002), and appear to exist in two forms at PF-PC synapses. A presynaptic variant is generated by a brief 4-16Hz stimulation and is thought to result in an increase of presynaptic transmitter release (Shibuki & Okada, 1992; Salin *et al.*, 1996; Jacoby *et al.*, 2001; Lev-Ram *et al.*, 2002). It is shown to be dependent firstly on presynaptic PKA (Salin *et al.*, 1996; Jacoby *et al.*, 2001) and also NO (Jacoby *et al.*, 2001), although the site of the actions of NO is disputed (Lev-Ram *et al.*, 2002). A postsynaptic variant can been initiated by stimulation of PFs, 300-600 times at 1Hz (Lev-Ram *et al.*, 2002). It has been shown to be NO-dependent, although no other mechanisms have yet been identified. Cerebellar LTP of a putative presynaptic origin has also been observed to spread to synapses up to around 160μm distant through an NO-dependent mechanism (Jacoby *et al.*, 2001).

The role of PF-PC LTP in cerebellar learning is less fully understood. Work on the receptive fields of PCs has revealed that PF stimulation increases the PC receptive field, but paired PF and CF stimulation reduces the PC receptive field (Jorntell & Ekerot, 2002). This may indicate that LTP, as well as LTD, does have an important role in cerebellar learning. It has been suggested that the postsynaptic variant of LTP may be capable of reversing the effects of LTD (Lev-Ram *et al.*, 2002).

1.3 Eye movement adaptation – examples of motor learning

The vestibulo-ocular reflex (VOR) is responsible for correcting the movement of the eye when the head turns to maintain focus on a point. Movements of

the head are sensed by the vestibular labyrinth, which then instructs the eyes to move in the opposite direction. A visual focus can be rotated. When a platform is rotated so that the head moves exactly with the focus (thereby making VOR redundant), adaptation of the VOR is stunted. If however the platform moves in the opposite direction to the focus, adaptation of VOR is demonstrated to increase. VOR is controlled by areas of the flocculus and is a common model used to examine motor learning (Ito, 1982; Ito, 1989). Numerous studies have demonstrated that LTD in PCs, with the CF as an error signal, is an important mechanism in motor learning. Application of haemoglobin (a NO scavenger) to the flocculus inhibited VOR in rabbits and monkeys (Nagao & Ito, 1991). Similarly, injection of a NOS inhibitor into the cerebella of goldfish also blocked the improvement in VOR (Li *et al.*, 1995). Finally, transgenic mice that selectively expressed a PKC-γ inhibitor had both LTD and VOR inhibited (DeZeeuw *et al.*, 1998). Another recent study has shown that mice deficient in cGMP-dependent protein kinase I (cgK1) also have impaired LTD and VOR, although motor performance was not adversely affected (Feil *et al.*, 2003).

Continued rotation of a visual field around a stationary animal increases the adaptation of the optokinetic reflex (OKR; Nagao, 1988). OKR adaptation was inhibited both in mice where the CF was depleted by 3-AP (Katoh *et al.*, 1998), and in mice that did not express nNOS (Katoh *et al.*, 2000). Mice lacking Fyn, one of a subfamily of genes encoding for non-receptor PTKs, did not demonstrate reduced OKR adaptation (Kitazawa *et al.*, 2000), although it may be that Fyn is not required to express the PTKs in LTD.

1.4 Aims and objectives

This thesis sets out to investigate two main areas. The first constitutes part of a larger study carried out in this laboratory, examining the role of NO in cerebellar plasticity (Jacoby & Hartell, 1999; Jacoby *et al.*, 2001). Two stimulating electrodes were used to stimulate two discrete bundles of PFs that formed synapses on the same PC. It was found by Jacoby *et al.* (2001)

that LTP generated at one set of PF synapses ('test' pathway) was capable of spreading to the distant PF synapses. Furthermore, LTP in both test and distant pathways was NO-dependent. Using the same protocol of stimulating LTP in one pathway with a 15s, 8-16Hz stimulation, this study recorded the distance that LTP spread to the distant pathway. Secondly, it also examined whether a NO scavenger in the extracellular medium could cause input-specific LTP of the test pathway. This 8-16Hz burst of PF activity will also induce LTD if a low concentration of calcium chelator is present in the postsynaptic cell (Jacoby & Hartell, 1999). G-substrate, activated by the NO-dependent pathway in LTD, in the cerebellum is almost unique to PCs (Detre *et al.*, 1984) and a potent inhibitor of PPs (Endo *et al.*, 1999). This means that G-substrate could be an important mediator of LTD as part of a pathway to prevent dephosphorylation of AMPARs. This study will also examine whether the absence of G-substrate can prevent LTD occurring in PCs that do not have high concentrations of calcium chelator. 8-16Hz stimulation was applied to PFs from wild-type and homozygous G-substrate knockout mice, in order to examine whether LTD was abolished in favour of LTP in the transgenic mice. These experiments are detailed in chapter 3.

The second area of investigation is based on the growing evidence that the AA of the GC may have a distinct role in cerebellar physiology from the PF. Peripheral or MF stimulation has been shown to lead to only a limited 'patch' of PC activity, far more restricted than the length of PF might suggest (Bower & Woolston, 1983; Cohen & Yarom, 1998). This has led to speculation that the PFs may not be as efficacious at transmission as supposed. Additionally, PF- and AA-PC synapses have been found to differ anatomically, both pre- and postsynaptically (Gundappa-Sulur *et al.,* 1999). Firstly, there was a greater number of presynaptic vesicles at AA synapses than PF synapses, which may indicate a greater probability of release at AA synapses (Murthy *et al.*, 1997). Secondly, there was a lack of correlation between pre- and postsynaptic anatomical characteristics of AA synapses compared to PF synapses. As co-ordination of pre-and postsynaptic environments may be important in both cerebellar LTD (Lev-Ram *et al.*, 1997a) and also LTP, this may indicate that AAs have limited susceptibility to synaptic plasticity. As a

consequence, this thesis intends to investigate physiological differences between AA- and PF-PC synapses. Chapter 4 describes the basic transmission properties (quantal amplitude, probability of transmitter release and number of release sites) at AA- and PF synapses. Chapter 5 examined the susceptibility of both synapse types to several forms of synaptic plasticity previously identified at PF-PC synapses – presynaptic LTP, postsynaptic LTP, and conjunctive LTD.

Chapter 2

Materials and Methods

2.1 Slice preparation

2.1.1 Extraction of the cerebellum

The majority of experiments undertaken in this study were carried out on 14-21 day old, male, Wistar rats. For experiments investigating the role of G-substrate on cerebellar plasticity (detailed in chapter 3), wild-type and G-substrate knockout C57/BL6 mice were used, aged between 3 and 8 weeks. Animals were sacrificed in accordance with Home Office procedures as detailed in the Animal (Scientific Procedures) Act 1986, and in a manner approved by the Aston University bioethics committee. Irrespective of species, slice preparation was the same. Both rats and mice were placed at the end of a tube emanating from a Boyle's apparatus and anaesthetized by inhalation of 5% halothane or isoflurane in a mixture of 2:1 NO_2:O_2 at a rate of 3 litres per minute. When pedal reflexes were absent, the animals were decapitated and the rear portion of the skull removed. The cerebellum was separated from the rest of the brain and immediately transferred to an isotonic solution maintained at below 4°C. The removal of the cerebellum was carried out as swiftly as possible (under 1 minute) to reduce cell damage from anoxia. In early experiments, in chapter 3, artificial cerebrospinal fluid (aCSF; see later for composition) was used. In later experiments a sucrose-based solution was used, comprising (in mM): sucrose, 250; KCl, 2.5; $NaHCO_3$, 26; glucose, 10; $NaHPO_4$, 1.25; $CaCl_2$, 2; $MgCl_2.6H_20$, 1; and equilibrated with 95% O_2, 5% CO_2 (see for example Cuttle *et al.*, 1998). The sucrose solution is designed to remove sodium from the cutting mixture whilst maintaining isotonicity. Reducing the sodium in the external solution prevents cells firing action potentials and thus reduces the release of transmitter. The rationale behind this is to prevent excitotoxic damage during the cutting process (for information on excitotoxic theory, see Siesjo, 1992; Erecinska & Silver, 1992). The number of healthy cells in slices was

observed to increase after sucrose solution replaced aCSF in this during this process.

2.1.2 Cutting of cerebellar slices

Cerebellar slices cut in a parasagittal plane have the dendritic trees of PCs parallel with the face of the slice (fig. 2.1), with the parallel fibres orthogonal. Thus the parallel fibres are severed, whereas PCs at the depth patched (>20μm deep) should have undamaged dendritic trees which can be clearly visualised. Sagittal slices were prepared using established methods (for instance see Edwards *et al.*, 1989) as follows. The isolated cerebellum was transferred onto a piece of 3% agar in 0.9% NaCl solution. Two parasagittal cuts were made either side of the vermis, the first approximately halfway along the cerebellar hemisphere, the other just beyond the paravermis. The cerebellum was then attached to a Teflon block with cyanoacrylate adhesive on the side cut halfway along the hemisphere. The cerebellum was orientated with the dorsal surface facing the blade and supported to the rear by a second section of agar. The cerebellum was then transferred to the holding chamber of a vibroslicer (Campden Instruments, Sileby, UK) filled with chilled sucrose-based solution (aCSF in earlier experiments) and maintained below 4°C by a peltier cooling device. 200μm thick slices were then cut at a slow forward speed with maximum lateral vibration, to reduce disruption to the slice. Slices were then transferred onto a platform of nylon netting in a holding chamber filled with aCSF bubbled with 95% O_2, 5% CO_2, kept at room temperature. Slices were left a minimum of one hour before use.

Preparation of coronal slices was essentially similar as described previously for sagittal slices except for the following. The lateral halves of the cerebellar hemispheres were removed with parasagittal cuts on an agar block. The cerebellum was then adhered to the Teflon block by its ventral surface, with the posterior facing the blade. To try to minimalise damage to the extensive

PC dendritic trees, which are orthogonal to the plane of cut, slices were cut to a thickness of 250μm. Initially, thicker slices (up to 400μm) were cut, but the associated reduction in cell visibility outweighed the benefit of increased cell viability.

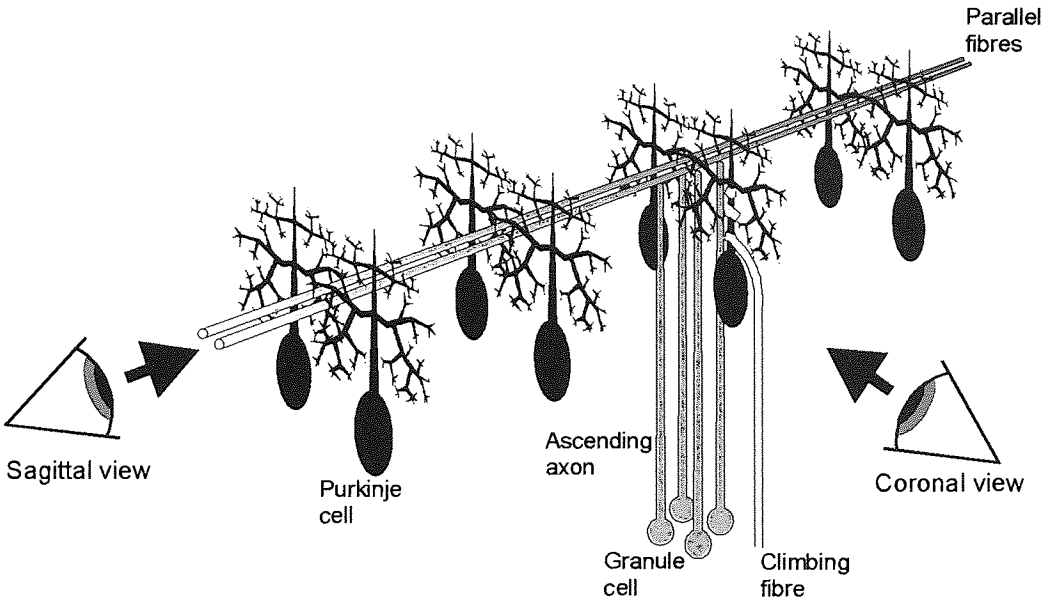

Figure 2.1 Differing views of coronal and sagittal slices. This figure illustrates the views of the cell provided by the two slice orientations. Sagittal slices can observe the entire 'face' of the PC dendritic tree, whereas coronal slices see the PC from the 'side'.

Coronal slices have several disadvantages. There is an increased likelihood of severed dendrites, and visualisation of PC dendritic trees is limited because they are observed side-on (fig 2.1). PCs that survive the cutting process tend to be deeper in the slice, so it is also harder to visualise the cell soma for patching. In coronal orientation, PFs run lengthways along the face of the slice and are not severed. Therefore placing a stimulating electrode distant from the recorded PC can selectively activate the PFs.

2.2 Experimental set-up

2.2.1 Slice set-up and visualisation.

After a suitable period of incubation, slices were transferred to a chamber fitted to the stage of an upright microscope (Olympus BX50WI), and held between two nylon nets to prevent movement. The recording chamber was

continually perfused with oxygenated aCSF at a flow rate of 1.5-2 $mlmin^{-1}$. Standard aCSF was composed of (in mM): NaCl, 120; KCl, 2.7; $CaCl_2.2H_20$, 2.5; $NaHCO_3$, 25; NaH_2PO_4, 1.2; $MgSO_4.7H_20$, 1.2; glucose, 11; picrotoxin 20μM; with pH 7.4 at room temperature. Picrotoxin was added to inhibit $GABA_A$ and glycine receptors. Other drugs were added to this aCSF as required by the experiment in question. Visualisation through the microscope was done with a 10x / 0.25 NA non-immersion, or 40x / 0.8 NA water immersion lens. A CCD camera (Hitachi Denshi Ltd., model KP-M1E/K) was also fitted to the microscope. The CCD camera was connected to a contrast enhancer unit (BRSL, model ADV-2), allowing images to be observed on a monitor, and captured on computer. Images were stored and calibrated using an image of a calibrated graticule.

2.2.2 Electrode preparation

Both stimulating and recording electrodes were prepared from borosilicate glass tubes, (outside diameter 1.5mm, inside diameter 1.17mm; Harvard Apparatus), and were pulled with a Flaming-Brown micropipette puller (Sutter Instruments, Model P-97.) Simulating electrodes were filled with aCSF and had resistances of 0.5-1.5MΩ. Recording electrodes were pulled to produce tip sizes with resistances of 3-5MΩ when filled with internal solution. The internal recording pipette solution comprised (in mM): KGluconate, 132; NaCl, 8; $MgCl_2.6H_20$, 2; HEPES, 30; Na_2ATP, 4; GTP, 0.3. One of two different calcium chelators was added to the solution at a concentration of 0.5 or 10mM, depending on the experiment. 10mM 1,2-bis(2-aminophenoxy)-ethane-N,N,N',N'-tetraacetic acid (BAPTA) was used in order to inhibit calcium-dependent processes of synaptic plasticity in the post-synaptic cell. 0.5mM BAPTA or ethylene glycol-bis(2-aminoethylether)-N,N,N',N',-tetraacetic acid (EGTA) was used otherwise. EGTA was used only for experiments investigating the role of G-substrate in synaptic plasticity, in order to ensure consistency with previously published data. The pH of the internal solution was adjusted to 7.3 with KOH.

2.2.3 Recording and stimulating apparatus

Electrophysiological signals were acquired with an Axopatch 200B amplifier (Axon Instruments) and converted from analogue to digital signals by a Digidata 1200A board (Axon Instruments). Data were filtered through a lowpass Bessel filter at 5kHz, and sampled at 10kHz. Initially, Clampex 6 software (Axon Instruments) was used to monitor seal and whole cell patch formation. 'The LTP Program' (Anderson & Collingridge, 1999) was used to observe and record the data during the experiment. Stimulation pulses were applied through isolated stimulator boxes (Digitimer Ltd.; type 2533, model DS2 or DS2A.)

2.3 Electrophysiology

2.3.1 Whole cell patch formation

The cerebellar cortex was examined for areas with a high concentration of healthy PCs under the 10x lens. Individual PCs were then located under the 40x water immersion lens. Healthy PCs were identified as having rounded somata of approximately 25μm. Dead or dying PCs tend to be swollen and with indistinct membranes, or shrunken with very clearly defined membranes. Whole cell patch clamp recordings were made from the somata of cells at depths of 20-120μM. Positive pressure was applied through the recording electrode until the tip was adjacent to the PC soma. The positive pressure was then released, and suction applied. Once a gigaseal was established, the cell membrane was disrupted with suction (and occasionally a 5ms, 26mV hyperpolarising pulse to the recording electrode) and the cell maintained in whole-cell configuration at –70mV. (For descriptions of patch clamp techniques, see Hamill *et al.*, 1981; Sakmann & Neher, 1984; Edwards *et al.*, 1989; Neher & Sakmann, 1992; Neher, 1992). The liquid junction potential was not corrected for, and was calculated as approximately 14.2mV, to an end membrane potential of approximately –84.2mV.

2.3.2 Electrode positioning

When the characteristics of synaptic plasticity at PF synapses was examined (chapter 3), two electrodes were placed on the surface of the slice in the ML to stimulate different bundles of PFs. They were separated by distances of 20-160μm. In most cases they were placed either side of the proximal dendrite, mid-way between the PCL and pial surface (fig. 2.3). On occasions where responses could not be acquired at large electrode separations, one electrode was placed near the PC soma and the other near the pial surface.

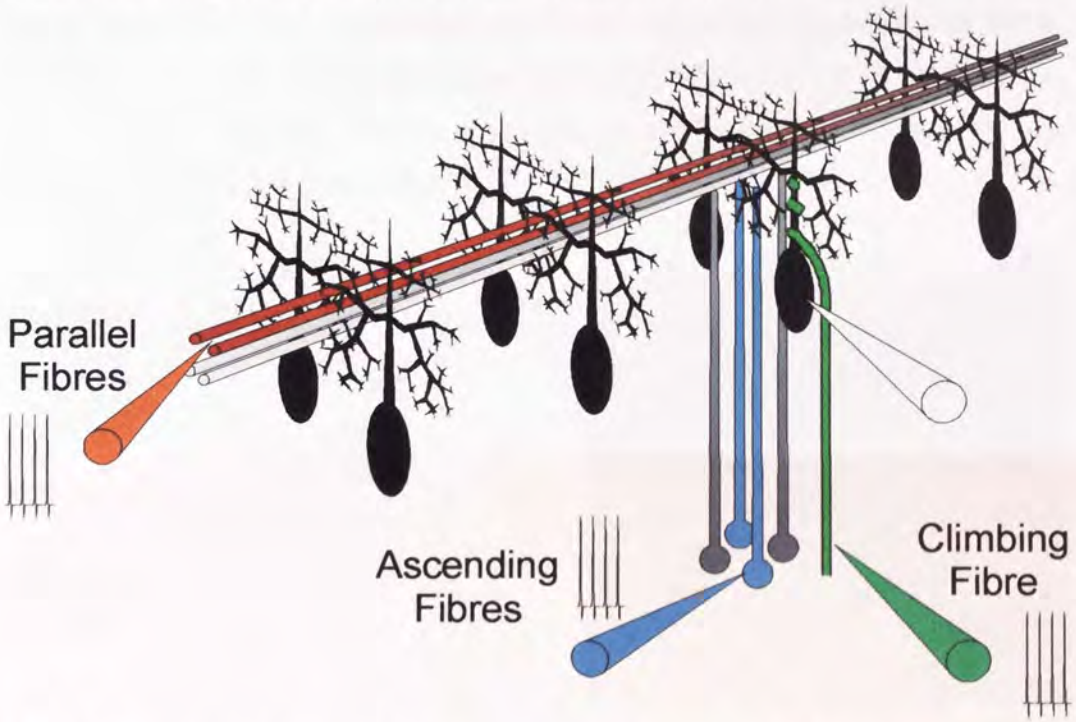

Figure 2.2 Illustration of electrode positioning. The electrode placement for stimulating parallel fibres, ascending axons, and the climbing fibre are shown. The unfilled electrode represents the recording electrode.

In chapters 4 and 5, the characteristics of two different sets of GC axons were examined, so electrodes were placed to stimulate AAs and PFs selectively. To activate PFs in sagittal slices, electrodes were placed on the surface of the slice in the ML, midway between the PCL and pial surface. To selectively activate PFs in coronal slices, electrodes were placed approximately 100μm deep in the slice, mid-way between the PCL and pial surface, over 100μm distant from the recorded PC. In both sagittal and coronal orientation slices, to selectively activate AA segments electrodes

were placed in the GL 20-100μm behind the PC in the same plane as the PC dendritic tree. Care was taken to avoid stimulation of the CF or retrograde activation of the PC axon. Stimulation of the CF generated characteristic large excitatory postsynaptic currents (EPSCs) over 1nA. Retrograde activation of the PC axon produced large responses (>500pA), which occurred less than 1ms after stimulation.

Electrodes to stimulate the CF were placed in the GL 20-100μm behind the PCL. When both the CF and AAs needed to be activated in the course of the same experiment, the stimulating electrodes were kept separated as far as possible to limit the likelihood of one electrode activating the other pathway. Fig. 2.2 illustrates the relative positions of stimulating electrodes for the activation of CFs, PFs and AAs.

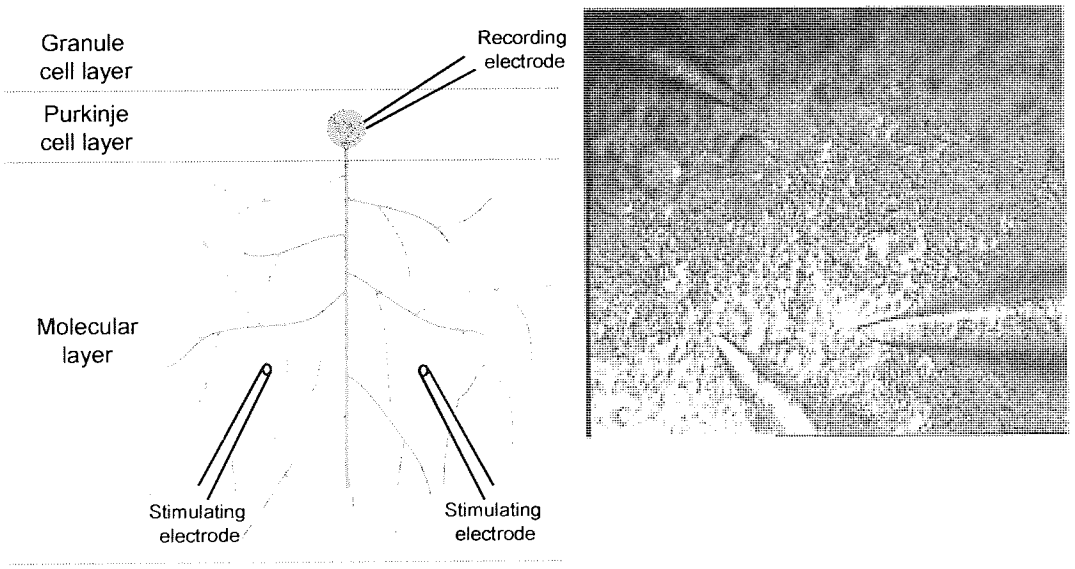

Figure 2.3 Example of electrode positioning to stimulate two PF pathways in sagittal slices. On the left is a schematic diagram showing electrode positioning either side of the proximal dendrite, mid-way between the PCL and pial surface. On the right is a bright field image of this captured from an experiment.

2.3.3 Baseline stimulation protocol

Sweeps consisted of two parts. Firstly, a command pulse was passed through the recording electrode, and then after 40ms, a series of pulses to one or other pathway was applied through a stimulating electrode (fig. 2.4).

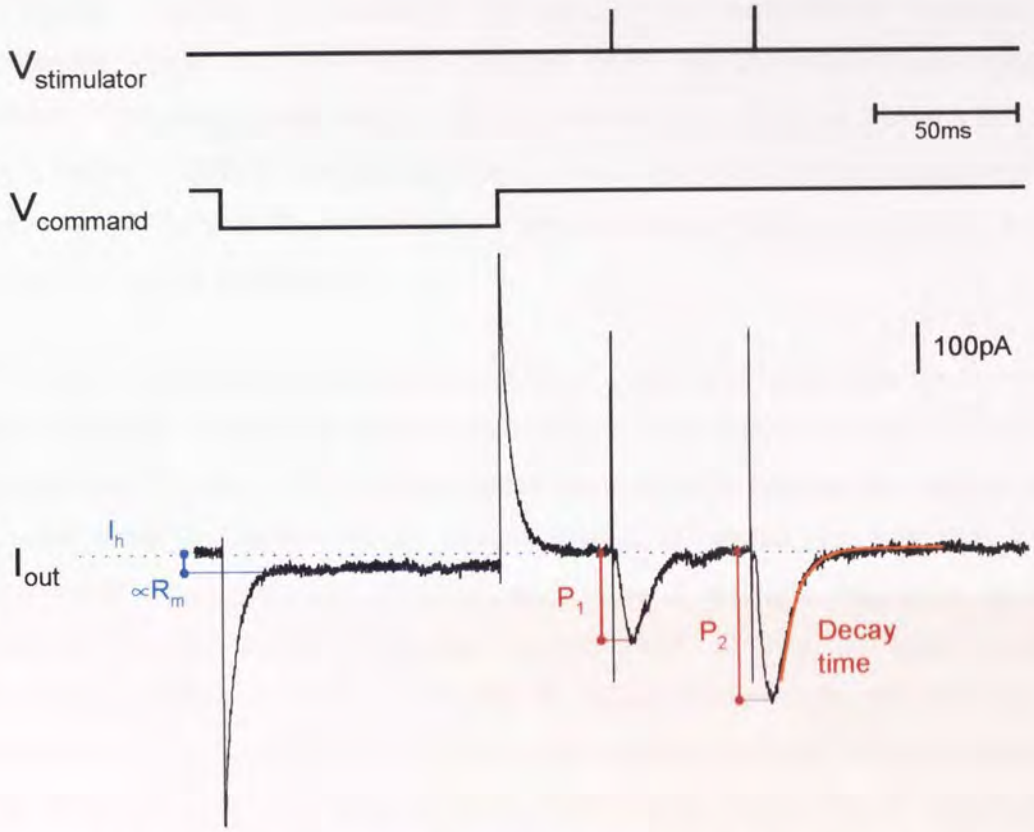

Figure 2.4 Baseline stimulation protocol and analysis of generated sweeps. This example demonstrates a basic paired-pulse protocol. Stimulation comprises a 4mV hyperpolarizing pulse through the recording electrode ($V_{command}$), and then pulses to the stimulator ($V_{stimulator}$) in one pathway. Below is an example of a data sweep of the currents evoked in the PC (I_{out}) by this protocol. The methods of calculating R_m, I_h, P_1, P_2 and τ_{decay} are also graphically demonstrated.

Holding current (I_h) was measured as the average current applied to keep the cell at –70mV before the command pulse. The 100ms, 4mV, hyperpolarizing command pulse was applied to the cell through the recording electrode. This allowed the measurement of input resistance (R_m), which is relative to the membrane resistance, and series resistance (R_s). R_s was compensated for using the amplifier (compensation >80%, lag 20μs). Changes in R_s during the experiment were monitored online and adjusted manually during recordings.

Experiments were terminated if R_s exceeded 15-20 MΩ (i.e. approximately four times the resistance of the recording electrode.) Immediately after patching, healthy PCs had an initial I_h of –400 to 200pA, and an initial R_m of 100-200MΩ. A gradual decline in R_m was usually observed that developed over about 30 minutes, and that stabilised at 40-100MΩ. I_h was often seen to gradually increase or decrease throughout the experiment, stabilising between –1000 and 0pA. Such changes were not observed to adversely affect EPSC responses (see fig. 3.5). However, if R_m declined below 40MΩ, or I_h below –1000pA, the cell was deemed too unhealthy and the experiment terminated. If either R_m or I_h changed considerably (>10%) and abruptly, the experiment was terminated.

A series of stimulation pulses with widths of 200μs and intensities up to 30V were applied. Pulses are termed according to their position in the series of pulses (i.e. P_1, P_2 ... P_n.) Paired pulses were used to assess the degree of paired-pulse facilitation (PPF). Unless stated otherwise, an interstimulus interval of 50ms was used. Several parameters of synaptic responses were measured. The peak amplitudes of individual EPSCs ($EPSC_A$) were measured online. In chapters 3 and 5 where experiments recorded the changes in $EPSC_A$ and PPR over time, six individual sweeps were averaged for each data point. $EPSC_A$ in these experiments measured the absolute peak of the six sweeps. Where individual sweeps were to be analysed (chapter 4 and coefficient of variation analysis in chapter 5), $EPSC_A$ measured the average EPSC amplitude of 1ms at the peak. The latter was considered advantageous for eliminating noise for individual EPSCs, whereas in the former noise would be compensated for by the averaging of six points. The rise times (τ_{rise}) and decay times (τ_{decay}) were also calculated from EPSCs by fitting exponential curves. Results are presented as the value ± the standard error of the mean (s.e.m.) unless otherwise stated.

Regardless of which section of the GC axon was stimulated, pathways were stimulated at 0.05-0.2Hz alternately (fig 2.5). Five to ten minute baseline periods with stable $EPSC_A$ responses were obtained from both pathways

before any plasticity-inducing protocols were applied. This was to help ensure that the responses from the cell were unlikely to change except from the applied protocols or drugs. Baseline $EPSC_A$s were maintained below 300pA in order to prevent localised calcium influx through VGCCs (Eilers *et al.*, 1995; Hartell, 1996).

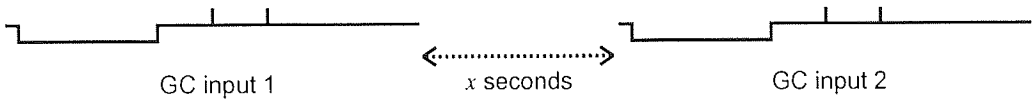

Figure 2.5 Alternate stimulation of two pathways. An example of paired pulse stimulation of two GC inputs is demonstrated. The separation between pulses (x) depends on the rate of stimulation and the length of the stimulation and recording period (GC input). The length of the recording period is subtracted from the time between pulses to achieve the rate of stimulation: for instance, with a 300ms recording period and 0.2Hz stimulation, x = 2.2s.

2.3.4 Plasticity-inducing protocols

Three different protocols were used to assess plasticity and its spread between sets of GC synapses. The first, which is thought to generate a presynaptic form of LTP (Salin *et al.*, 1996; Jacoby *et al.*, 2001), was a raised-frequency stimulation (RFS) of 8 or 16Hz for 15s to one pathway. The second pathway was not stimulated during this period. Stimulation was then resumed at baseline rates. 16Hz stimulation was preferentially used, except for the investigation of G-substrate on synaptic plasticity, where 8Hz stimulation was used for consistency with published material.

A form of LTP that is reportedly postsynaptic was induced by 300 pulses at 1Hz delivered to one pathway (Lev-Ram *et al.*, 2002). This protocol to the first pathway was carried out in two conditions. In one set of experiments no stimulation was applied to the second pathway. In the other, the second pathway was stimulated at the baseline rate of 0.1Hz to establish whether continued, low-rate stimulation was important.

The third protocol was used to generate conjunctive long-term depression. Since calcium entry through VGCCs is one of the requirements for LTD, and since CF stimulation rather than cell depolarisation was used, the induction phase of these experiments was performed in current clamp mode. A protocol based on Wang *et al.* (2000a) was applied. Cells were held at a potential of –70mV by injecting current. A 100ms hyperpolarizing pulse (100pA) was applied to ensure that the amplifier was correctly balanced and to assess the health of the cell and the recording conditions. After 40ms, five pulses were applied at 100Hz to one GC pathway, followed by stimulation of the climbing fibre 100ms later (fig 2.6). The other pathway was not stimulated during this period.

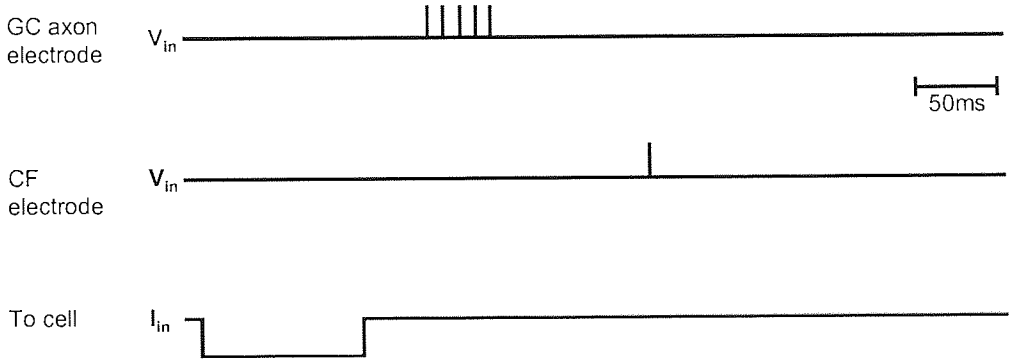

Figure 2.6 Stimulus parameters for LTD induction. This protocol was carried out in current clamp conditions. A 100ms hyperpolarizing pulse was applied to the cell to monitor health. 50ms later, 5 pulses were applied to the AA- or PF-pathway at 10ms intervals, and finally 100ms afterwards, the CF was activated.

2.4 Data Analysis

Initial analyses of $EPSC_A$, R_m, I_h and R_s were done online by 'The LTP Program'. Further analysis was done using customised procedures on Igor Pro (Wavemetrics), and later Microsoft Excel. Six sweeps were averaged for each data point in analyses of the change in EPSCs over time. $EPSC_A$, PPR and τ_{decay} from the 10-minute baseline were averaged. Each data point was then expressed as a percentage of the baseline average. Sweeps were analysed individually in all other data analyses. Curve fitting for τ_{rise} and τ_{decay} was performed by Igor Pro. Graphical representation and all other curve

fitting was done by SigmaPlot (SPSS Inc.). Statistical analysis was calculated by SPSS v10.0 (SPSS Inc.).

2.4.1 Paired-pulse facilitation

PPF is a phenomenon observed where a second pulse applied shortly after a first generates a larger response. Release of neurotransmitter is dependent on calcium influx to the presynaptic terminal, and PPF is thought to be due to a residual elevated calcium concentration in the presynaptic terminal increasing the probability of transmitter release on the second pulse (for reviews, see Zucker, 1989; Thomson, 2000). PPR is used to determine differences in the presynaptic release probability (Kullmann *et al.*, 1992), where a decrease in PPR is thought to signify an increased release probability. If the change in response is postsynaptic, PPR should not be altered. Mean PPR was calculated by the method of (mean P_2 / mean P_1) as opposed to mean (P_1/P_2). This is to compensate for natural random fluctuation, which skews PPR to unnaturally high values as responses become smaller (Kim & Alger, 2001).

PPR may be affected by factors other than release probability. If more presynaptic fibres are recruited by the later stimulation due to increase excitability, as has been reported in PFs (Merrill *et al.*, 1978; Kocsis *et al.*, 1983) this will cause an increase in PPR. Also possible is a residual glutamate concentration in the postsynaptic cleft from the earlier pulse, which may cause an abnormally large second EPSC. Receptor occupancy limits paired-pulse depression (PPD) at climbing fibres (Harrison & Jahr, 2003), although GC-PC release sites have much lower release probabilities, so it is unlikely that there will be such a great glutamate build-up. There may be increased spillover of glutamate to distant synapses (Barbour *et al.*, 1994) which could be a more significant effect on later pulses.

2.4.2 Fluctuation analysis

Fluctuation analysis depends upon the 'quantal' hypothesis of transmitter release, initially postulated by del Castillo & Katz (del Castillo & Katz, 1954). They found that the size of postsynaptic responses at a muscle fibre consisted of varying multiples of spontaneous miniature events. Briefly, the response at a synapse depends upon three variables: *i*, the probability of release of a presynaptic vesicle (P_r); *ii*, the number of independent vesicle release sites (N); and *iii*, the postsynaptic response to a quantum of transmitter (Q). Differences in synaptic strength can therefore be explained in terms of these variables. Quantal analysis is derived from binomial statistics, such that as Q, N or P_r differ, so the distribution of generated responses will also differ.

Several techniques have been developed for analysis of fluctuations of synaptic response (for instance Redman, 1990; Voronin, 1994). In this study (V-M) analysis was used, and carried out as detailed previously (Silver *et al.*, 1998; for a full explanation, see Clements & Silver, 2000). It is explained in more detail in chapter 4. Also used was analysis of coefficient of variation following Bekkers & Stevens (1990) and this is explained fully in chapter 5.

2.4.3 Statistics

Two variations of non-parametric ranking tests were used. For comparison of the two pathways within a series of cells, the Wilcoxon matched pair test was performed. For comparison of responses from two independent groups of cells, the Mann-Whitney U-test was preferentially used. In diagrams a single asterisk represents *P* values significant under 0.05, double asterisks represent *P* values significant under 0.01.

2.5 Materials

2-(4-carboxyphenyl)-4,4,5,5-tetramethylimidazoline-1-oxyl-3-oxide (cPTIO) was used to scavenge diffusible extracellular NO (Akaike *et al.*, 1993; Yoshida *et al.*, 1994; Tsunoda *et al.*, 1994). The solid was directly dissolved into aCSF to a concentration of 30μM, and was added prior to the baseline being recorded.

100nM 1,3-dipropyl-8-phenylxanthine (DPPX), a selective adenosine A1 antagonist (Daly *et al.*, 1985), was used to increase calcium influx at the presynaptic termini and thus increase release probability (Dittman & Regehr, 1996). DPPX also acts a phosphodiesterase inhibitor, although it is only effective at concentrations sufficiently greater than these used in this study so it should not affect results (Ukena *et al.*, 1993). Solid DPPX was dissolved in ethanol to a concentration of 100mM, and added to aCSF at a volume relationship of 1:1000, with an end ethanol concentration of 0.1%.

0.2μM H-89 dihydrochloride was added to the aCSF to inhibit PKA (Kawasaki *et al.*, 1998; de Rooij *et al.*, 1998) and thus prevent LTP (Salin *et al.*, 1996; Jacoby *et al.*, 2001). The solid was dissolved in a 1:1 mixture of ethanol and distilled water to make a stock concentration of 0.2mM. This was added to aCSF at a volume relationship of 1:1000, with an end ethanol concentration of 0.05%.

75nM 1,2,3,4-tetrahydro-6-nitro-2,3-dioxo-benzo[f]quinoxaline-7-sulfonamide (NBQX) was used to inhibit AMPARs, although it also will inhibit kainate receptors (Gill *et al.*, 1992; Zeman & Lodge, 1992; Namba *et al.*, 1994). Solid NBQX was dissolved in dimethylsulfoxide (DMSO) to a 2.5mM solution, which was further diluted to a 75μM stock solution with distilled water, which was added to aCSF at a volume relationship of 1:1000, with an end DMSO concentration of 0.003%.

H-89 was obtained from Calbiochem. DPPX, NBQX, cPTIO and forskolin were supplied by Tocris Cookson. Picrotoxin, EGTA and BAPTA were supplied by Sigma.

Chapter 3

Elucidation of the role of nitric oxide and nitric oxide dependent processes in cerebellar plasticity

NO is not produced in PCs, so to activate NO-dependent intracellular processes it must act as a freely diffusible transcellular messenger. It is an important mediator of synaptic plasticity at GC-PC synapses, influencing both LTP and LTD. In the former NO is thought to have possibly both pre- and postsynaptic effects, through mechanisms that are not clearly defined. In the latter, it acts postsynaptically through the sGC-cGMP-PKG-G-substrate pathway. Both forms of plasticity have been observed to spread to distant synapses, and the diffusible nature of NO also makes it a likely mediator of spread of plasticity to distant synapses in LTP and LTD. In this chapter, application of a NO scavenger to the extracellular environment was examined to see if it prevented the spread of LTP to distant synapses. Secondly, when subjected to an 8Hz RFS, it was examined whether LTD was prevented, allowing LTP to predominate, in PCs of mice with a genetic knockout of G-substrate.

3.1 Introduction

3.1.1 Long-term depression at parallel fibre – Purkinje cell synapses.

The first experimentally observed form of synaptic plasticity in the cerebellar cortex was LTD (Ito & Kano, 1982; Ito *et al.*, 1982). It is associative, requiring repetitive, temporally conjunctive stimulation of CF and PFs, although the precise timing requirement for this conjunction is debated. Some studies have found that LTD is best induced if the CF is stimulated before the PFs (Ekerot & Kano, 1989; Karachot *et al.*, 1995), while others suggest that PF stimulation should precede CF stimulation (Schreurs *et al.*, 1996; Wang *et al.*, 2000a). LTD is synapse specific, in that it results in a prolonged depression of transmission at the PF-PC synapse. The reduction in synaptic transmission is due to a decrease in post-synaptic AMPAR activity. While

desensitisation of AMPARs has been suggested as an expression mechanism for LTD (Hemart *et al.*, 1994), this is now thought unlikely (Linden, 2001). Prevailing thought favours dissipation of receptor clustering at the synapse (Matsuda *et al.*, 2000; Hirai, 2001) and/or receptor internalisation (Wang & Linden, 2000). LTD is considered to involve three important initial steps. These are raised postsynaptic calcium levels (Sakurai, 1990; Sugimori & Llinas, 1990; Linden *et al.*, 1991) combined with activation of AMPARs (Linden *et al.*, 1993; Hemart *et al.*, 1995) and mGluRs (Linden *et al.*, 1994; Conquet *et al.*, 1994; Hartell, 1994b; Shigemoto *et al.*, 1994). Physiologically, in conjunctive LTD the CF is thought to be responsible for elevating calcium (Ross & Werman, 1987; Sugimori & Llinas, 1990; Konnerth *et al.*, 1992) as *in vitro*, depolarisation of the PC can mimic CF activation, although is not directly equivalent. PFs are thought to be responsible for activating the AMPARs and mGluRs required.

There has also been discovered a form of LTD that does not require conjunctive activation of the CF or concurrent depolarisation: CF-independent LTD. Raising the intensity and frequency of PF stimulation has been demonstrated to induce LTD (Hartell, 1996; Eilers *et al.*, 1997). Stimulation of sufficient PFs in close proximity may depolarise the PC to allow localised calcium influx through voltage-gated calcium channels (Eilers *et al.*, 1995; Hartell, 1996). Eilers *et al.* (1995) estimated that 20-30 PFs are required to produce calcium influxes, based on the size of responses elicited by individual GC stimulation (Barbour, 1993), A more recent study of PF synapse strength (Isope & Barbour, 2002) suggests that around 30-50 fibres might be required. The number of fibres required to elevate postsynaptic calcium can be reduced if the frequency of stimulation is increased (Eilers *et al.*, 1997) because the PFs undergo facilitation at stimulation rates above 4Hz (Shibuki & Okada, 1992; Salin *et al.*, 1996). Higher rates of stimulation also activate mGluRs (Batchelor *et al.*, 1994), and lead to a further localised calcium response mediated by IP_3 (Finch & Augustine, 1998; Takechi *et al.*, 1998). As PFs also activate AMPARs (Konnerth *et al.*, 1990), all the conditions necessary to generate LTD can be met by PF stimulation alone.

3.1.2 The role of nitric oxide in long-term depression.

Latterly a number of second messenger intermediates and pathways have also been implicated in LTD (see chapter 1 for full details), amongst them NO, produced by NOS. nNOS is expressed in GCs, basket cells and Bergman glia (Bredt *et al.*, 1990; Southam *et al.*, 1992; Rodrigo *et al.*, 1994). While NOS mRNA was extracted from GCs, none was found in PCs (Crepel *et al.*, 1994). Consequently, if NO is to contribute to LTD, it must diffuse transcellularly, probably from PFs (Shibuki & Kimura, 1997). NO is known to activate sGC, present in PCs (Ariano *et al.*, 1982), which produces cGMP (Daniel *et al.*, 1993; Boxall & Garthwaite, 1996). cGMP may then activate PKG, which is thought to have few targets, amongst them G-substrate (fig. 1.4; Aswad & Greengard, 1981a; Aswad & Greengard, 1981b). Inhibition of NOS, sGC or PKG has previously been demonstrated to prevent LTD in cerebellar slices (Daniel *et al.*, 1993; Hartell, 1994a; Hartell, 1994b; Lev-Ram *et al.*, 1995; Lev-Ram *et al.*, 1997b). Conversely, application of NO donors or cGMP analogues will evoke a LTD in cerebellar slices (Crepel & Jaillard, 1990; Daniel *et al.*, 1993; Hartell, 1994a; Hartell, 1994b; Blond *et al.*, 1997; Lev-Ram *et al.*, 1997a). However, while LTD was inhibited in cerebellar slices prepared from mice deficient in nNOS, it was not restored by photolytic release on NO (Lev-Ram *et al.*, 1997b). This may however be due to adaptation of the NO signalling pathway to long-term absence of nNOS. Cultured PCs do not appear to require NO for LTD either. No difference was observed in LTD between PCs harvested from nNOS-deficient and wild-type mice (Linden *et al.*, 1995). Nor was LTD affected by NOS donors, NO scavengers or NOS inhibitors in other cultured preparations (Linden & Connor, 1992).

The intracellular environment of the AMPAR is connected to cytoskeletal elements, and release of the AMPAR from the cytoskeleton is likely to be integral to receptor internalisation (Nishimune *et al.*, 1998; Luthi *et al.*, 1999). Phosphorylation at the ser-880 site of the AMPA GluR2 subunit carboxy-terminus by PKC has been found to greatly diminish the binding of GRIP (Chung *et al.*, 2000; Xia *et al.*, 2000; Matsuda *et al.*, 2000). PKG has not

been found to exert a direct influence on receptor phosphorylation although it readily phosphorylates G-substrate (Schlichter *et al.*, 1978; Aswad & Greengard, 1981a; Aswad & Greengard, 1981b). G-substrate in the brain is almost unique to PCs (Schlichter *et al.*, 1980; Detre *et al.*, 1984) which alone suggests an important role. It is an inhibitor of protein phosphatases 1 and 2a (Hall *et al.*, 1999; Endo *et al.*, 1999) and thus may act to reinforce phosphorylation of AMPARs by kinases. Application of a NO donor has been demonstrated to enhance phosphorylation of G-substrate (Endo *et al.*, 2003), reinforcing the possibility that NO is involved in LTD. G-substrate also may exert a positive effect on gene transcription through inhibition of protein phosphatases, enhancing phosphorylation-dependent transcription pathways. The major pathways identified in LTD are illustrated in fig. 1.4.

3.1.3 Parallel fibre long-term potentiation

PF-PC synapses can also undergo LTP (Sakurai, 1987; Crepel & Jaillard, 1991; Shibuki & Okada, 1992; Salin *et al.*, 1996). Cerebellar LTP is more frequently observed when postsynaptic calcium levels are chelated or reduced (Salin *et al.*, 1996; Lev-Ram *et al.*, 2002). Both pre- and postsynaptic components may exist. The presynaptic form of LTP can be generated at the PF-PC synapse by a brief period of RFS at frequencies between 4 and 16Hz (Sakurai, 1987; Shibuki & Okada, 1992; Salin *et al.*, 1996; Jacoby *et al.*, 2001). It is dependent on cAMP and PKA – activation of adenylate cyclase (AC) by forskolin causes a potentiation which RFS will not further increase and the PKA inhibitor H-89 prevents LTP (Salin *et al.*, 1996). Evidence that this form of LTP is presynaptic comes from the observation that it is accompanied by a decrease in PPR, and thus thought to be due to increased probability of transmitter release. The newly discovered postsynaptic effect is reported as NO-dependent, and operates through an unidentified cGMP- and cAMP-independent mechanism (Lev-Ram *et al.*, 2002). It can be elicited by a minimum of 300 pulses at 1Hz. The 15s 8Hz RFS that evokes LTP can also generate LTD in PF-PC synapses (Jacoby & Hartell, 1999). LTP prevails under conditions where LTD is inhibited, such as

hyperpolarisation during the RFS to prevent calcium influx, inhibition of PKG, or high BAPTA concentrations.

3.1.4 The role of nitric oxide in long-term potentiation.

NO also appears to play an important role in PF-PC potentiation, as it does in some other central synapses (Haley *et al.*, 1992; Nowicky & Bindman, 1993; Arancio *et al.*, 1996; Son *et al.*, 1996). Inhibition of NOS has been found to block presynaptic LTP, and NO donors cause a potentiation of EPSCs with associated decrease in PPR (Jacoby *et al.*, 2001). Production of NO also shares similarities with presynaptic LTP generation, being both PKA-dependent and also potentiated by tetanic stimulation (Kimura *et al.*, 1998). NO may be considered to act downstream of cAMP/PKA, because application of a NO donor caused potentiation even in the presence of the PKA inhibitor H-89 (Jacoby *et al.*, 2001). Evidence that PKA can directly influence NOS is, however, dubious. NOS has several consensus binding sites that may be phosphorylated by kinases (Bredt *et al.*, 1992). Evidence that PKA can enhance the activity of NOS (Inada *et al.*, 1998; Inada *et al.*, 1999) is disputed (Brune & Lapetina, 1991). Possibly PKA could act through an indirect means involving other signalling pathways, or may simply increase the sensitivity of NOS to calcium/calmodulin, as is the case for PKC (Okada, 1995). Lev-Ram *et al.* (2002) found that though postsynaptic LTP is dependent on NO, presynaptic LTP is independent of it. Evidence of platelet-aggregating factor (PAF) acting as a retrograde messenger in LTP has also been suggested (Reynolds & Hartell, 2001), as has been observed in the hippocampus (Kato *et al.*, 1994). PAF is activated through the mGluR/PLA_2 pathway.

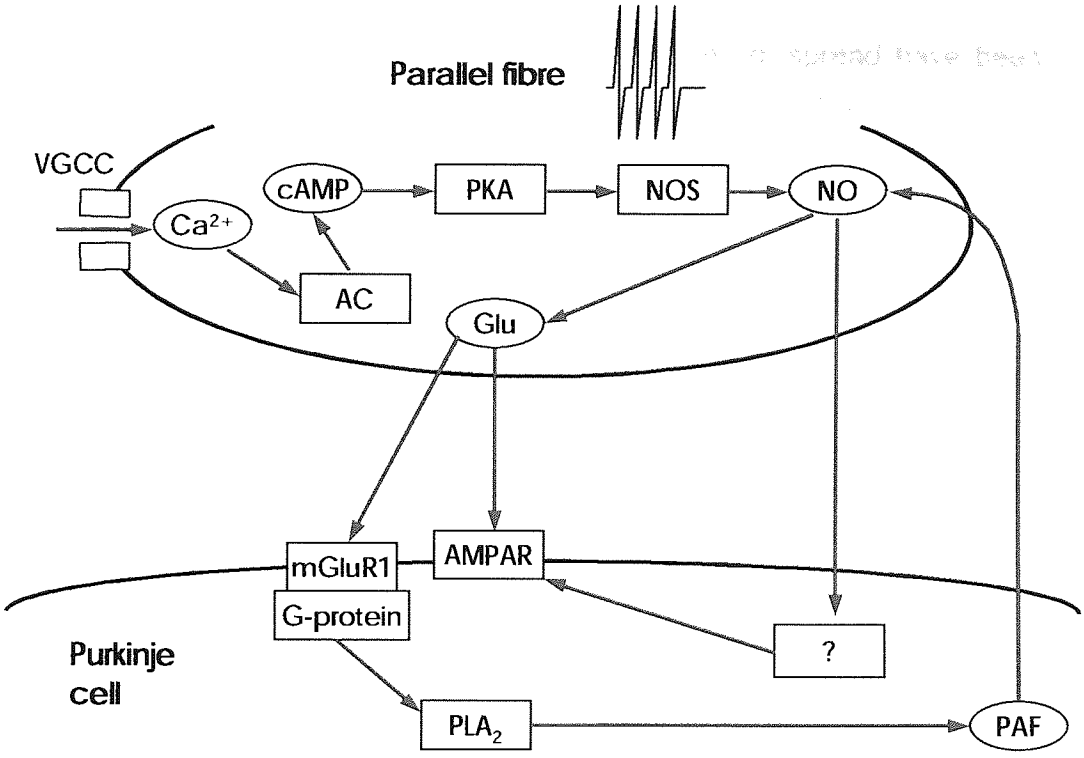

Figure 3.1 A summary of signal transduction processes in LTP. The scheme illustrates the proposed mechanism of action of NO-dependent pathways as per Jacoby *et al.* (2001). Abbreviations: VGCC, voltage-gated calcium channel; Ca^{2+}, calcium; AC, adenylate cyclase; cAMP, cyclic adenosine-5'-monphosphate; PKA, protein kinase A; NOS, nitric oxide synthase; NO, nitric oxide; Glu, glutamate; AMPAR, AMPA receptor; mGluR1, metabotropic glutamate receptor type 1; PLA2, phospholipase A_2; PAF, platelet aggregating factor.

3.1.5 Heterosynaptic plasticity at parallel fibre – Purkinje cell synapses

Plasticity has been observed to spread to distant synapses in both LTD and LTP. CF-independent LTD can spread distances of 40-100μm from bundles of PFs subjected to 1Hz raised intensity stimulation (Hartell, 1996; Hartell, 2000). There is a limited, localised increase in dendritic intracellular calcium concentration that spreads beyond spiny branchlets through VGCCs (Hartell, 1996) or IP_3 release (Finch & Augustine, 1998). However, it is too restricted to explain the distances observed in spread of LTD. LTD has also been observed to spread up to 100μm with conjunctive activation of PFs and either the CF or depolarisation (Reynolds & Hartell, 2000; Wang *et al.*, 2000b). The former showed a depression of distant PF responses, and the latter that depression of uncaged glutamate responses was attenuated with distance

from the site of LTD induction. Several other causes of spread have been proposed, such as ArA or PAF (Reynolds & Hartell, 2001). The NO cascade is a strong candidate, as inhibition of NOS, sGC or PKG has been found to prevent LTD spreading without affecting LTD at the test pathway (Hartell, 2000). This suggests that phosphatase inhibition via the NO pathway in LTD acts in parallel to and independent from the kinase pathway initiated by increased intracellular calcium. LTP has been observed at distances up to 168μm and again NO was involved (Jacoby *et al.*, 2001). As NO is capable of facilitating vesicle release at synapses (Meffert *et al.*, 1994; Meffert *et al.*, 1996), it is likely that NO alone could cause potentiation at a distant site.

3.1.6 Aims and objectives.

The work reviewed above provides evidence that both LTP and LTD are capable of spreading to distant PF pathways via mechanisms involving NO. In this chapter a series of experiments are described, some of which formed part of a larger study (Jacoby *et al.* 2001), in which the contribution of NO to the spread of LTP was explored. Firstly, evidence will be presented that shows LTP spreads to synapses tens of micrometres distant from those activated during LTP induction. Secondly, evidence will be presented to demonstrate that this spread requires the extracellular diffusion of NO.

G-substrate is abundant only in PCs, and it is a likely target for phosphorylation by PKG. G-substrate acts as an inhibitor of PPs (Endo *et al.*, 1999) which dephosphorylate AMPARs. Consequently, a role for G-substrate in LTD has been hypothesised. Experiments were carried out on slices from mice with a PC-specific knockout of G-substrate. 8-16Hz RFS induces LTP when LTD is prevented. Thus it is hypothesised that this RFS should generate LTP in PCs from animals that lack G-substrate, whereas cause LTD in PCs from wild-type animals.

3.2 Methods

Most of the methods for this chapter are fully detailed in chapter 2. Briefly, cerebellar slices were obtained from 14-21 day-old, male, Wistar rats for experiments described in section 3.3.1 investigating the role of NO. Slices were obtained from 21-60 day-old C57BL/6 mice (wild-type and G-substrate knock-out) for experiments described in section 3.3.2, investigating the effect of G-substrate on LTD. All experiments were carried out on 200μm thick sagittal slices in standard aCSF with 20μM picrotoxin. When stated, the NO scavenger cPTIO was present in this aCSF at a concentration of 30μM, which should be capable of scavenging all extracellular NO (Grassi & Pettorossi, 2000).

PCs were held in voltage-clamp configuration at –70mV. Baseline stimulation was a 100ms, 4mV hyperpolarizing command pulse to monitor cell conditions, followed 50ms later by paired pulses (stimulus width 100μs, 50ms interstimulus interval) applied to one pathway. Pathways were activated by this protocol alternately at 0.2Hz. At least 10 minutes stable $EPSC_A$s were acquired before experiments were initiated. The electrodes were termed PF_1 and PF_2; where required, a RFS consisting of a 15s train at 8 or 16Hz was applied to the PF_1 (test) pathway. The PF_2 (distant) pathway was not stimulated during this period, and subsequently baseline stimulation was resumed in both pathways. Each data point was constructed from the averages of six individual traces. The paired-pulse ratio was calculated as mean P_2 / mean P_1 for each data point. I_h, R_m, τ_{decay} and R_s were monitored throughout. Fluctuations in R_s were manually compensated for during the experiment. Experiments were discounted if I_h or R_m declined too far (see chapter 2 for details). The distances between electrodes were calculated as explained in chapter 2.

3.2.1 The creation of G-substrate knockout mice

The G-substrate knockout mice were created and supplied by S. Endo, RIKEN, Japan. Firstly, the cDNA for mouse G-substrate was acquired by polymerase chain reaction from primer sets based on human (Endo *et al.*, 1999) and rat (Endo *et al.*, 2003) cDNA. A C57/BL6 mouse genomic library was constructed in bacterial artificial plasmids (Osoegawa *et al.*, 2000) and screened with a random-primed cDNA probe for mouse G-substrate. Positive clones were then analysed by restriction mapping and sequencing.

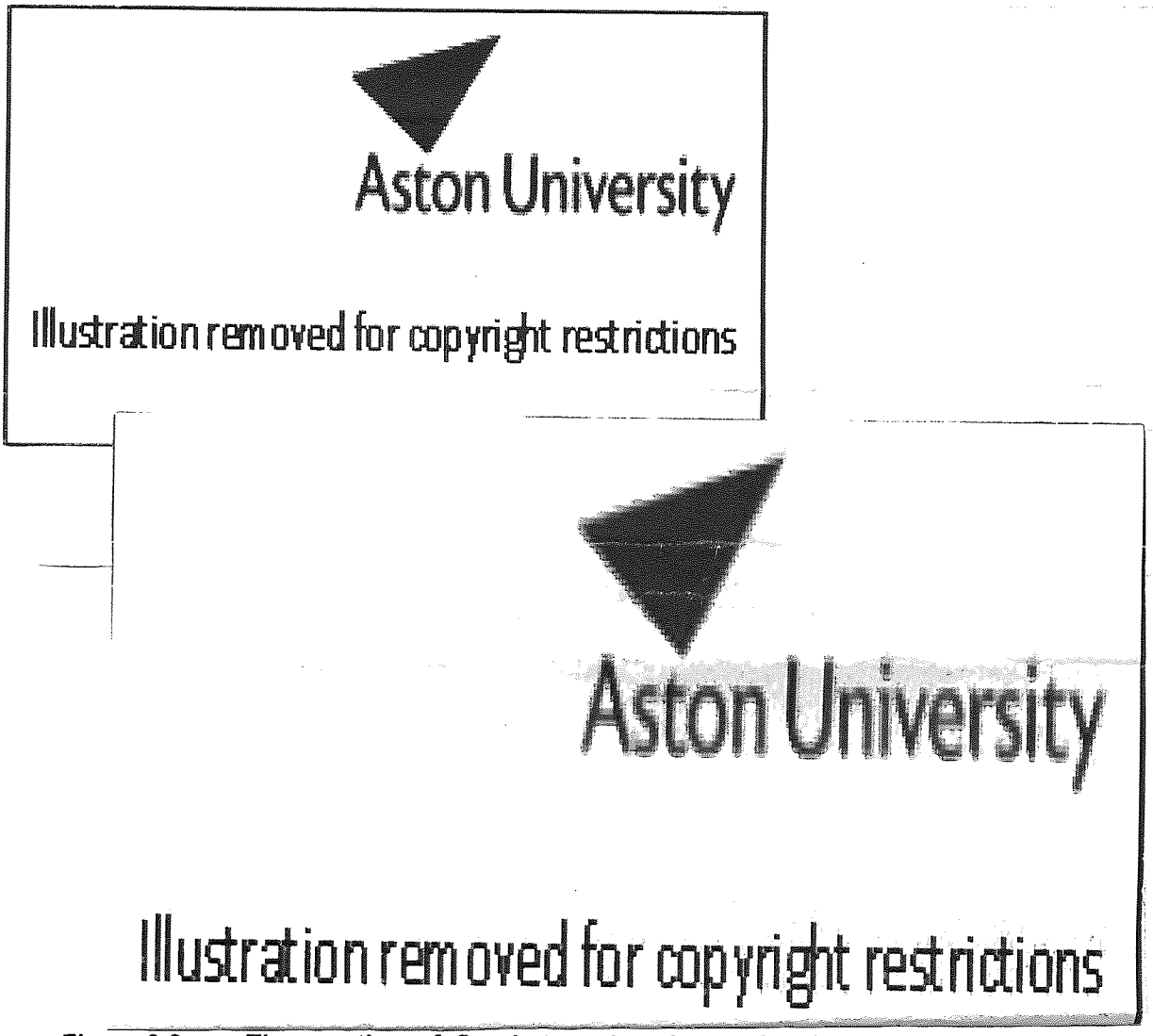

Figure 3.2 The creation of G-substrate knockout mice. The insertion of the tau-AFAP-pgk-Neo cassette into exon 2 of the G-substrate gene is demonstrated. Below, a picture of Purkinje cells in G-substrate knockout mice under fluorescence microscopy showing the presence of the fluorescent protein. Both are presented with permission from S. Endo (unpublished data.)

Targeting vectors were constructed to replace exon 2, containing the initiation site *Met*, of the G-substrate gene. This was replaced with a cassette containing tau-AFAP-pgk-Neo, which expressed a green fluorescent protein (fig. 3.2). This targeting vector was then inserted into MS12 embryonic stem cells. Southern blot analysis was used to find clones, via probes specific to the 5'- and 3'-ends of the recombination site. Embryonic stem cells that had positive clones were injected into blastocysts, to produce chimeric mice. Mice with the knockout were then bred with C57/BL6 mice, and the offspring genotyped for the presence of the knockout.

3.3 Results

Initially a series of control data were acquired to establish that recording conditions and synaptic transmission were stable. The concentration of BAPTA in the recording pipette ($BAPTA_i$) was 10mM. Pathways were stimulated alternately at 0.2Hz for over 30 minutes after a 10-minute stable baseline was established. Electrode positioning in the slice and a representative sweep are illustrated in fig. 2.3. Six consecutive sweeps for each pathway were averaged for each data point, and $EPSC_A$, PPR, I_h, R_m, and τ_{decay} were then plotted out over time. $EPSC_A$ and PPR were normalised, and expressed as a percentage of the baseline average. A representative example of a single control experiment is shown in fig. 3.3. Stable $EPSC_A$, PPR and τ_{decay} are recorded while I_h and R_m remain within acceptable parameters. During experiments in this chapter, decay time was not observed to alter significantly in any experiments, and consequently is not further represented.

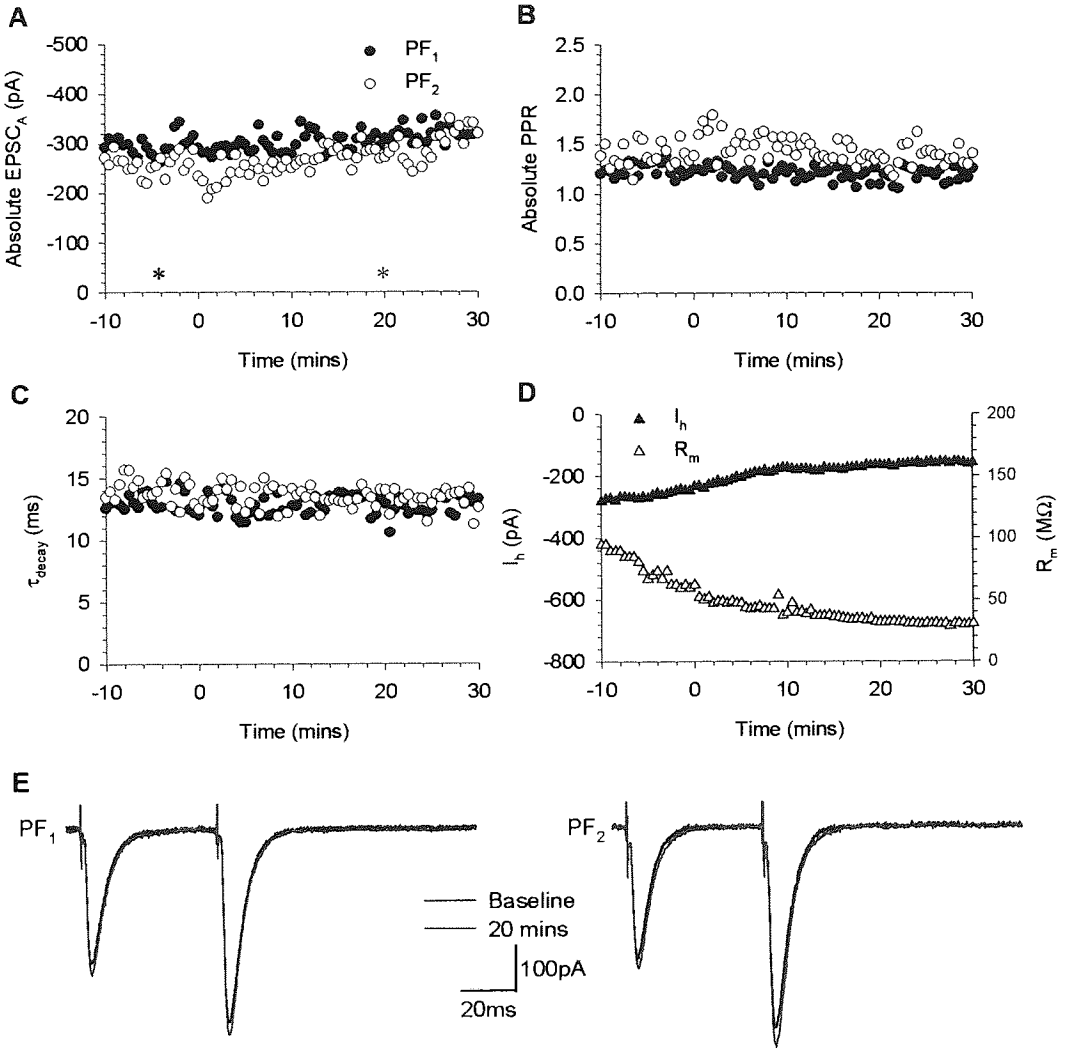

Figure 3.3 An example of a typical recording from a Purkinje cell with 10mM $BAPTA_i$. Two stimulating electrodes, PF_1 and PF_2, were placed in the ML, and both pathways were stimulated alternately at 0.2 Hz. The panels show absolute P_1 $EPSC_A$ (*A*), PPR (*B*), τ_{decay} (*C*) and I_h and R_m (*D*) in both pathways. The EPSCs in both pathways at baseline and after 20 minutes are illustrated in *E*. The traces are averages of 6 sweeps comprising the single time point, and asterisks denote the time points where the traces were sampled.

In 11 control cells, 20 minutes after baseline, $EPSC_A$ was 97.2 ± 2.6% of baseline levels in the PF_1 pathway, and 97.5 ± 5.4% in the PF_2 pathway. PPR at the same point was 98.0 ± 2.0% of baseline in the PF_1 pathway, and 101.3 ± 2.6%in the PF_2 pathway (fig. 3.4).

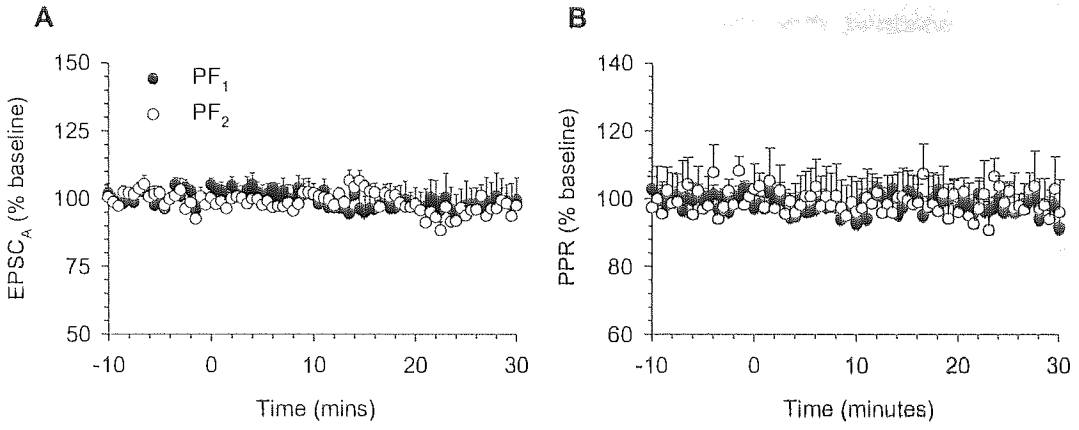

Figure 3.4 The effects of 0.2Hz alternate stimulation of two PF pathways with 10mM $BAPTA_i$. Two stimulating electrodes were placed in the molecular layer, and both pathways were stimulated alternately at 0.2 Hz. The mean values for $EPSC_A$ (*A*) and PPR (*B*) from 11 cells are illustrated.

3.3.1 The role of nitric oxide in the spread of long-term potentiation to distant synapses.

The effects of 16Hz RFS to one of two independent pathways were initially examined with 10mM BAPTA in the recording pipette. Of 17 experiments undertaken 10 underwent potentiation. Six of these showed an increase in normalised $EPSC_A$ at 20 minutes after LTP induction in the test pathway, which spread to the distant pathway (PF_1, 131.5 ± 8.4%; PF_2, 123.14.5 ± 5.4%; fig. 3.5). This potentiation was accompanied by a decrease in the PPR (PF_1, 91.7 ± 2.4%; PF_2, 92.9 ± 2.8%). $EPSC_A$ was significantly greater and PPR significantly lower when compared to control data sampled 20 minutes after baseline in both pathways (Mann-Whitney *U*-test, $p<0.05$, $n = 6$ RFS vs. 11 control), suggesting a presynaptic origin for the potentiation. Neither $EPSC_A$ nor PPR were significantly different between PF_1 and PF_2 pathways (Wilcoxon signed-rank test, $n=6$, $p<0.05$). In these six experiments that generated LTP the mean spatial separation between PF_1 and PF_2 electrodes was 91μm (range 22 to 158μm) The relationship between the separation of the PF_1 electrode and the PF_2, the pathways of which did and did not undergo 16Hz RFS respectively, is shown in fig. 3.9c. As can be seen, over

separations ranging from 22-158μm no evidence for a pathway-specific potentiation was observed, nor did specificity increase with distance.

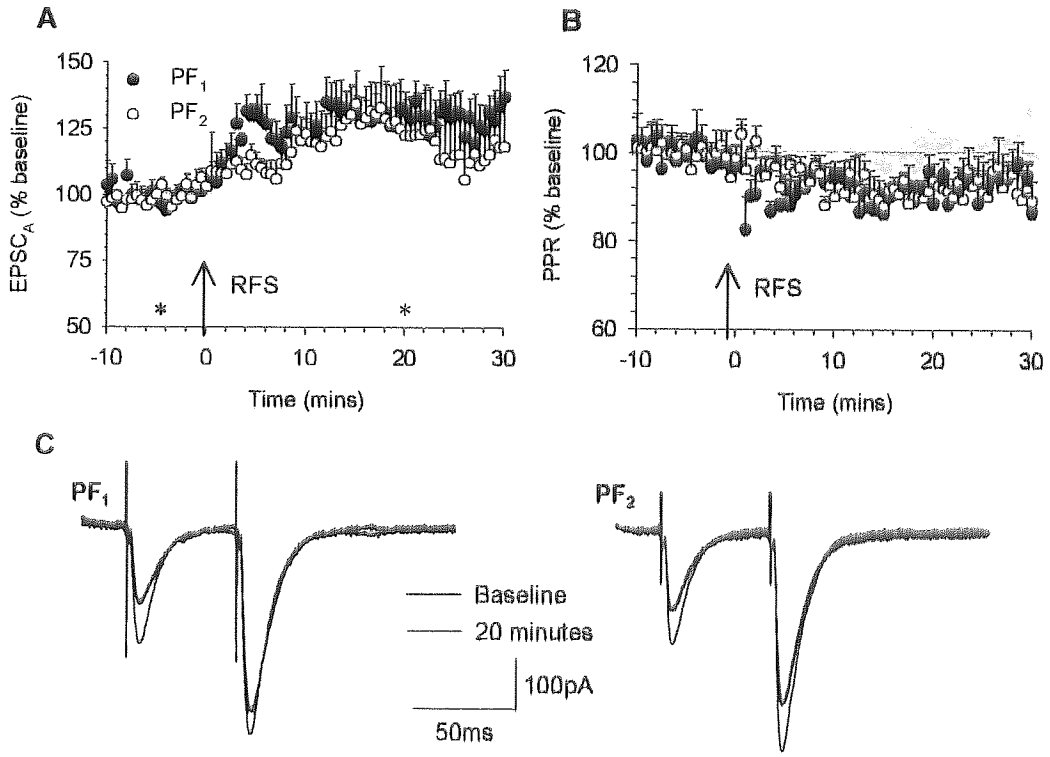

Figure 3.5 Long-term potentiation induced by 16Hz RFS with 10mM BAPTA$_i$. The effects of 16Hz RFS are illustrated, showing changes in EPSC$_A$ (*A*) and PPR (*B*) in both test (PF$_1$) and distant (PF$_2$) pathways (n=6). Representative traces of EPSCs at baseline and 20 minutes in the PF$_1$ and PF$_2$ pathways are shown in *C*. The traces are averages of 6 sweeps comprising the single time point, and asterisks denote the time points where the traces were sampled.

16Hz RFS in four cells evoked a transient increase in EPSC$_A$ that peaked within 5 minutes in the RFS-activated pathway and a smaller peak was observed later in the distant pathway. EPSC$_A$ measured at 4.5 minutes after RFS in the test pathway was 128.6 ± 6.9%, with the PPR being 87.8 ± 2.9% of baseline levels. Both parameters were significantly different compared to control data sampled at a similar time (Mann-Whiney U-test, $p<0.05$, $n = 4$ RFS vs. 11 control). The test pathway was also significantly different to the distant pathway at this time point (Wilcoxon signed-rank test, $p<0.05$ n=4). The EPSC$_A$ gradually declined back to baseline levels within 20 minutes (EPSC$_A$: PF$_1$, 96.3 ± 3.2%; PF$_2$, 97.3 ± 10.0%; PPR: PF$_1$, 102.6 ± 1.6%; PF$_2$,

99.1 ± 3.3%; fig. 3.6). Of the 17 experiments these 4 were the only ones to show any degree of synapse specificity, albeit transient.

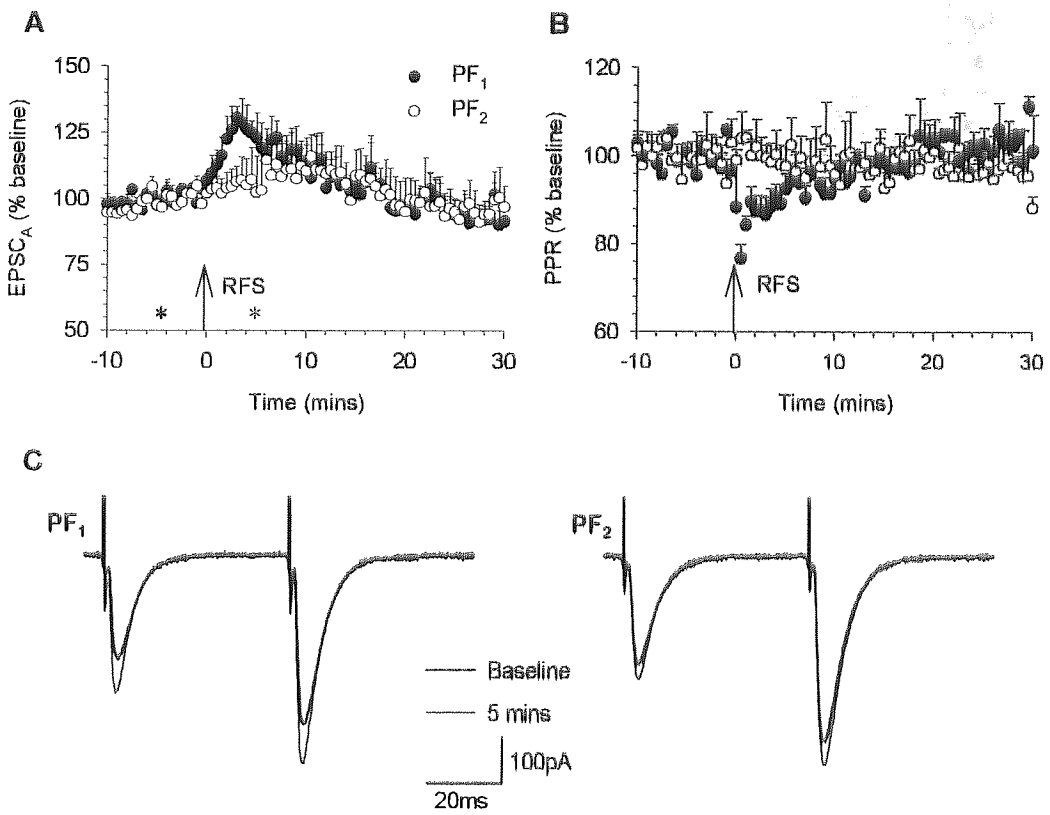

Figure 3.6 Short-term potentiation induced by 15s, 16Hz RFS with 10mM BAPTA$_i$. The effects of 16Hz RFS are illustrated, showing changes in EPSC$_A$ (*A*) and PPR (*B*) in both test (PF$_1$) and distant (PF$_2$) pathways (n=4). Representative traces of EPSCs at baseline and 20 minutes in the PF$_1$ and PF$_2$ pathways are shown in *C*. The traces are averages of 6 sweeps comprising the single time point, and asterisks denote the time points where the traces were sampled.

In the remaining seven cells no change in synaptic strength was observed in four cases, and in three others a long-term depression emerged in both pathways (EPSC$_A$: PF$_1$, 52.0 ± 6.0%; PF$_2$, 79.0 ± 6.7%; PPR: PF$_1$, 109.8 ± 6.9%; PF$_2$, 102.2 ± 1.4%; fig 3.7).

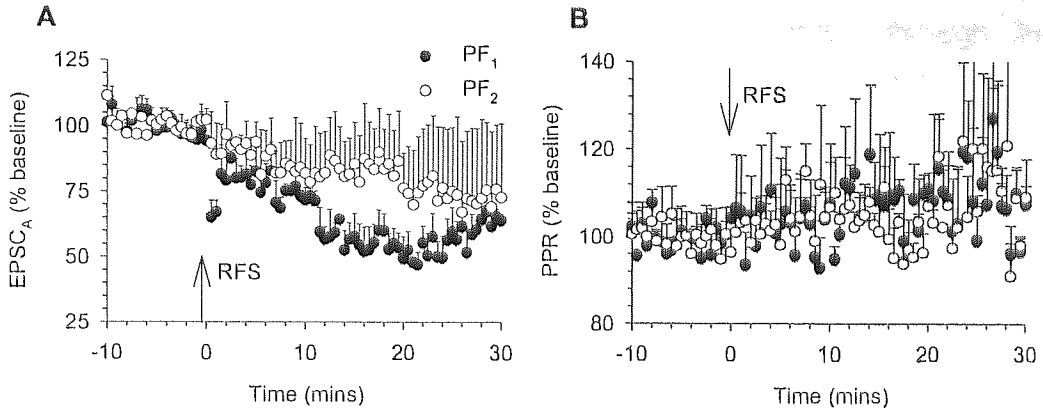

Figure 3.7 Long-term depression induced by 15s 16Hz RFS with 10mM BAPTA$_i$. The effects of 16Hz RFS are illustrated, showing changes in EPSC$_A$ (*A*) and PPR (*B*) in both test (PF$_1$) and distant (PF$_2$) pathways (n=6).

Work conducted previously by Jacoby *et al.* (2001) has demonstrated that inhibition of NOS prevents potentiation in either the test (PF$_1$) or distant (PF$_2$) pathway, and that the NO-donor spermine NONOate will mimic the effect of RFS in both pathways. However, this still leaves unanswered whether NO is responsible for the spread of potentiation. To address this 30μM cPTIO was added to the extracellular aCSF to scavenge any diffusible NO that may be released from PFs and the same LTP-generating protocol was applied. While there is no definitive evidence of it being unable to cross the cell membrane, its size and ionic charge makes it extremely unlikely it would be capable of doing so.

Under these conditions the PF$_1$ pathway showed a lasting potentiation of EPSC$_A$ (121.8 ± 7.2%) with a concurrent decrease in PPR (92.2 ± 2.8%) measured 20 minutes after induction, whereas the distant PF$_2$ pathway showed no evidence of LTP (EPSC$_A$, 96.2% ± 6.8%; PPR 101.6 ± 3.6%; fig. 3.8). In the PF$_1$ pathway, EPSC$_A$ and PPR were not significantly different from the 6 experiments where LTP was generated in the absence of cPTIO at 20 minutes after RFS. In the PF$_2$ pathway, EPSC$_A$ was significantly lower and PPR significantly higher than in the experiments where LTP was generated in the absence of cPTIO (Mann-Whitney *U*-test, $p<0.05$, $n = 7$ +cPTIO vs. 6 –cPTIO; fig. 3.9). The PF$_1$ and PF$_2$ pathways were significantly

different from each other in both $EPSC_A$ and PPR in the presence of 30μM cPTIO (Wilcoxon signed-rank test, $p<0.05$). It can be concluded therefore that diffusion of NO, presumably to distant parallel fibres, through the extracellular environment is critical for the spread of this form of LTP.

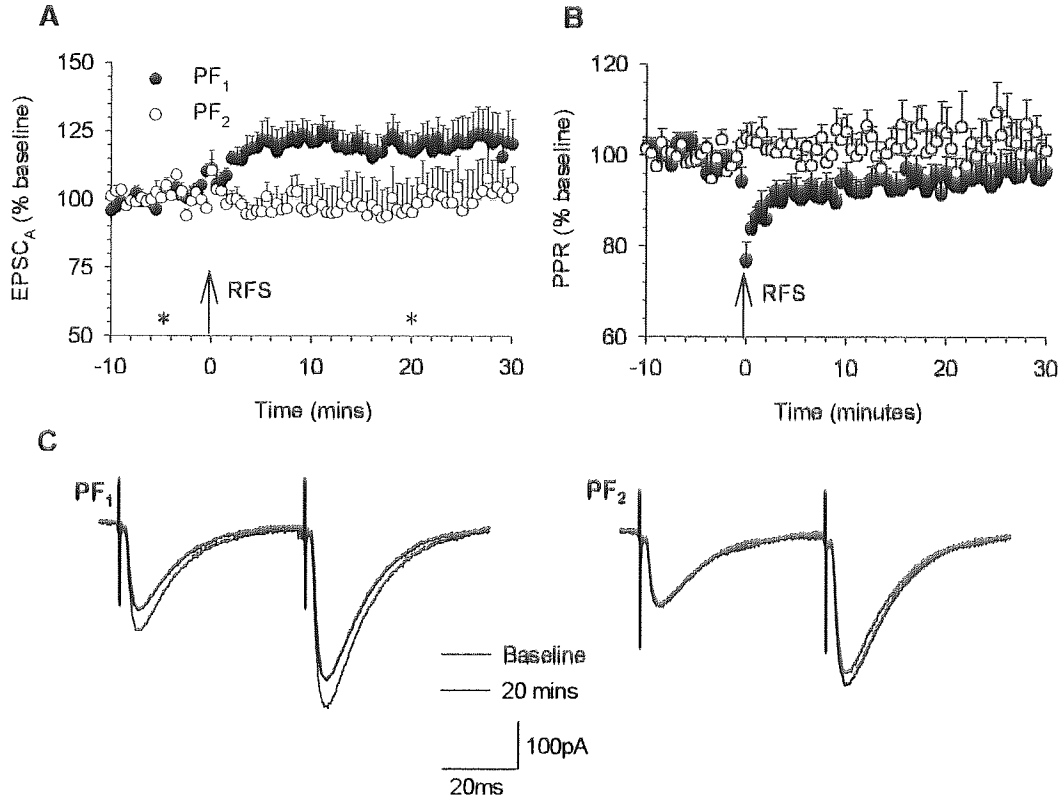

Figure 3.8 Pathway-specific potentiation of PF responses in the presence of cPTIO. The effects of 16Hz RFS are illustrated, showing changes in $EPSC_A$ (*A*) and PPR (*B*) in both test (PF_1) and distant (PF_2) pathways (n=7). Representative traces of EPSCs at baseline and 20 minutes in the PF_1 and PF_2 pathways are shown in *C*. The traces are averages of 6 sweeps comprising the single time point, and asterisks denote the time points where the traces were sampled.

LTP generation in the RFS-activated pathway was considerably more reliable in the presence of cPTIO, with only three out of nine cells failing to potentiate long-term. The electrode separations in these experiments were similar to those used in the absence of cPTIO that generated LTP, with mean 89μm (range 64 to 140μm; fig. 3.9c). The ratio of $EPSC_A$ as calculated by PF_1/PF_2 is greater than in the absence of cPTIO, which confirms that potentiation at the distant site was inhibited. Contrary to expectation, the ratio decreases as electrode separation increases, implying potentiation at distant pathways

increases with distance. This is possibly due to inaccuracies from the small sample number. The regression lines for data in the absence and presence of cPTIO were analysed for significance by the Fisher test. In the absence of cPTIO, there was no correlation between distance and the ratio of potentiation, and in the presence of cPTIO inconclusive evidence of correlation.

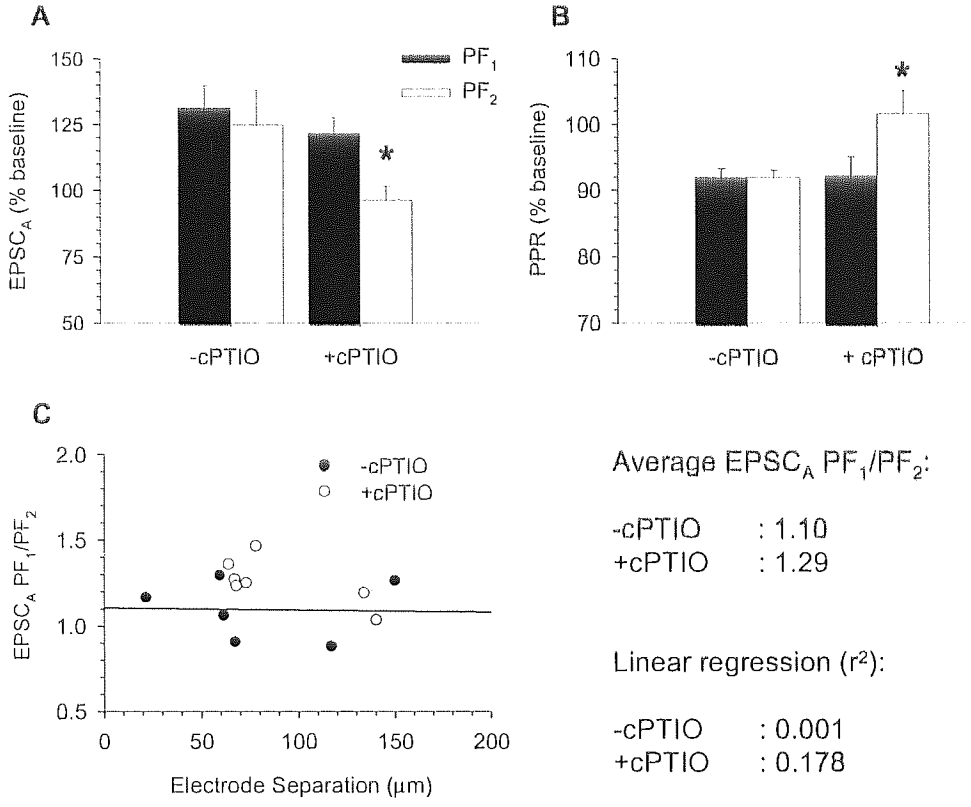

Figure 3.9 cPTIO prevents the spread of LTP to distant synapses. All results shown were taken 20 minutes after RFS and with 10mM $BAPTA_i$. The $EPSC_A$ (*A*) and PPR (*B*) of the test (PF_1) and distant (PF_2) pathways are illustrated in the absence (-cPTIO; n=6) and presence (+cPTIO; n=7) of cPTIO. Asterisks represent significant differences between +cPTIO and -cPTIO (Mann-Whitney U-test, $p<0.05$.) The ratio of potentiation at the PF_2 site compared to that at the test PF_1 site is plotted against the electrode distance for each experiment, in *C*. The Fisher test of the linear regressions showed no correlation between the ratio of potentiation and distance between data in the presence and absence of cPTIO.

3.3.2 G-substrate knockout mice do not undergo long-term depression when subjected to 16Hz raised frequency stimulation

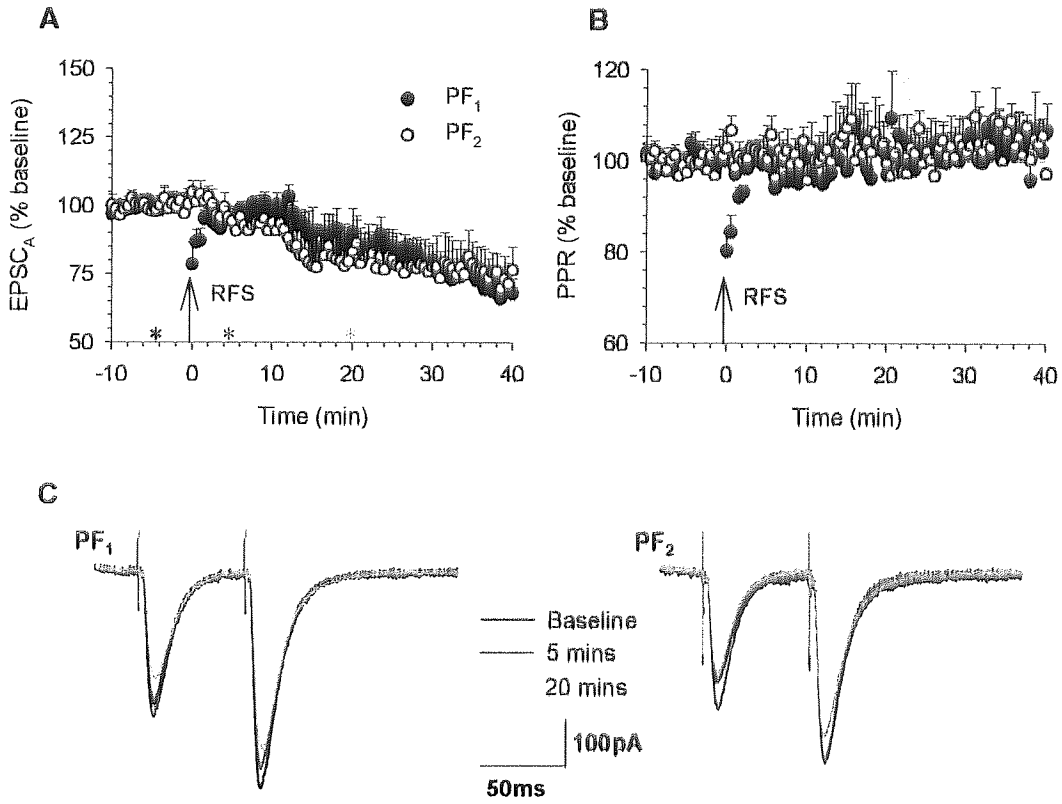

Figure 3.10 16Hz RFS generates LTD with 0.5mM BAPTA$_i$. The effects of 16Hz RFS are illustrated, showing changes in EPSC$_A$ (*A*) and PPR (*B*) in both test (PF$_1$) and distant (PF$_2$) pathways (n=6). Representative traces of EPSCs at baseline and 20 minutes in the PF$_1$ and PF$_2$ pathways are shown in *C*. The traces are averages of 6 sweeps comprising the single time point, and asterisks denote the time points where the traces were sampled.

It has previously been demonstrated that an 8Hz RFS that will generate LTD of PF-PC synapses will generate LTP in the presence of a high concentration of postsynaptic calcium chelator (Jacoby & Hartell, 1999). Furthermore, it has been demonstrated that the same protocol under low chelator concentrations will induce LTP when sGC is inhibited (Jacoby, 2001). It was hypothesised that when LTD is inhibited, LTP should be predominant when 16Hz RFS is applied. Consequently if LTP is evoked by 16Hz RFS in PCs of homozygous G-substrate knockout mice, it provides evidence that G-substrate is an important mediator of LTD, but not LTP.

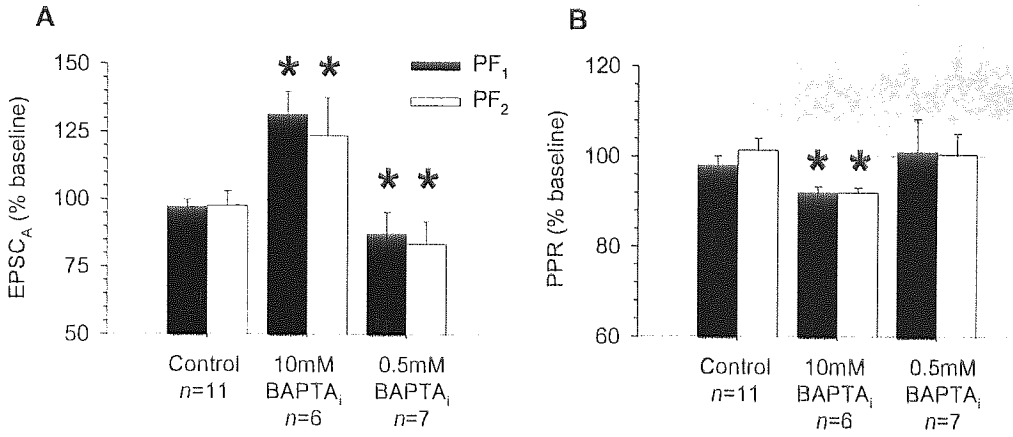

Figure 3.11 The predominance of LTP or LTD after 16Hz RFS can be determined by postsynaptic calcium chelation. All results shown are taken 20 minutes after the end of the baseline ceased. The $EPSC_A$ (*A*) and PPR (*B*) of the test (PF_1) and distant (PF_2) pathways are illustrated, with no RFS (control), with 16Hz RFS and 10mM $BAPTA_i$, and 16Hz RFS with 0.5mM $BAPTA_i$. Asterisks indicate significant difference from control data (Mann-Whitney U-test, $p<0.05$.)

Initially, the 16Hz RFS protocol previously used to generate LTP was applied to rat Purkinje cells, but with only 0.5mM BAPTA in the recording pipette (Fig. 3.10). In some cells, a small, transient potentiation in the PF_1 pathway was observed with concurrent decrease in PPR. However, 20 minutes after RFS $EPSC_A$ was depressed compared to baseline levels in all cells. After 20 minutes normalised $EPSC_A$ at the PF_1 pathway was slightly depressed (87.3 ± 7.9%), and depression was also evident at the distant pathway (83.4 ± 8.4%). PPR at 20 minutes was similar to baseline levels in both pathways (PF_1, 101.0 ± 7.3%; PF_2, 100.4 ± 4.7%). $EPSC_A$ in both pathways was significantly reduced when compared to control experiments with no RFS, as summarised in fig. 3.11 (Mann-Whitney U-test, $p<0.05$, n = 7 vs. 11 control). The LTD was observed to develop gradually over the course of the 40 minutes after induction. It can be concluded that in the absence of a high concentration of postsynaptic calcium chelator, LTD predominates over LTP when 16Hz RFS is applied. Furthermore, this depression is not synapse specific, also spreading to distant synapses.

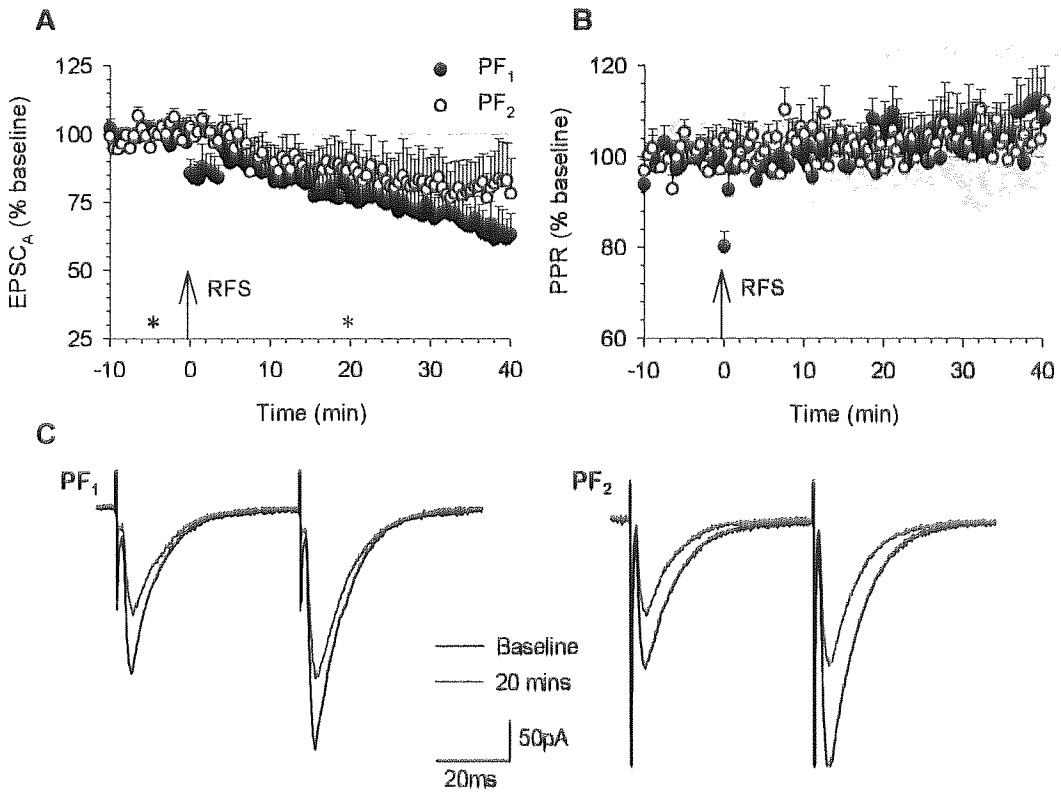

Figure 3.12 LTD is induced by 15s 16Hz RFS in wild-type mouse PCs with 0.5mM $EGTA_i$. The effects of 16Hz RFS are illustrated, showing changes in $EPSC_A$ (*A*) and PPR (*B*) in both test (PF_1) and distant (PF_2) pathways (n=6). Representative traces of EPSCs at baseline and 20 minutes in the PF_1 and PF_2 pathways are shown in *C*. The traces are averages of 6 sweeps comprising the single time point, and asterisks denote the time points where the traces were sampled.

In order to investigate the role of G-substrate in plasticity between PFs and PCs, two sets of C57/BL6 mice, one set wild-type and the other with a PC-specific knockout of G-substrate were used. To assess whether a G-substrate knockout similarly blocks LTD in favour of LTP, subsequent experiments were carried out in the presence of 0.5mM EGTA, and the RFS protocol applied to the PF_1 pathway was 15s at 8Hz. In the wild-type mice (*n*=6; fig. 3.12) the PF_1 pathway showed a long-term depression in $EPSC_A$ (79.0 ± 7.0%) with unchanged PPR (104.1 ± 4.4%). This depression spread to the distant PF_2 pathway, where $EPSC_A$ at 20 minutes was also depressed (88.7 ± 8.7%) with no change to PPR (99.8 ± 3.7%).

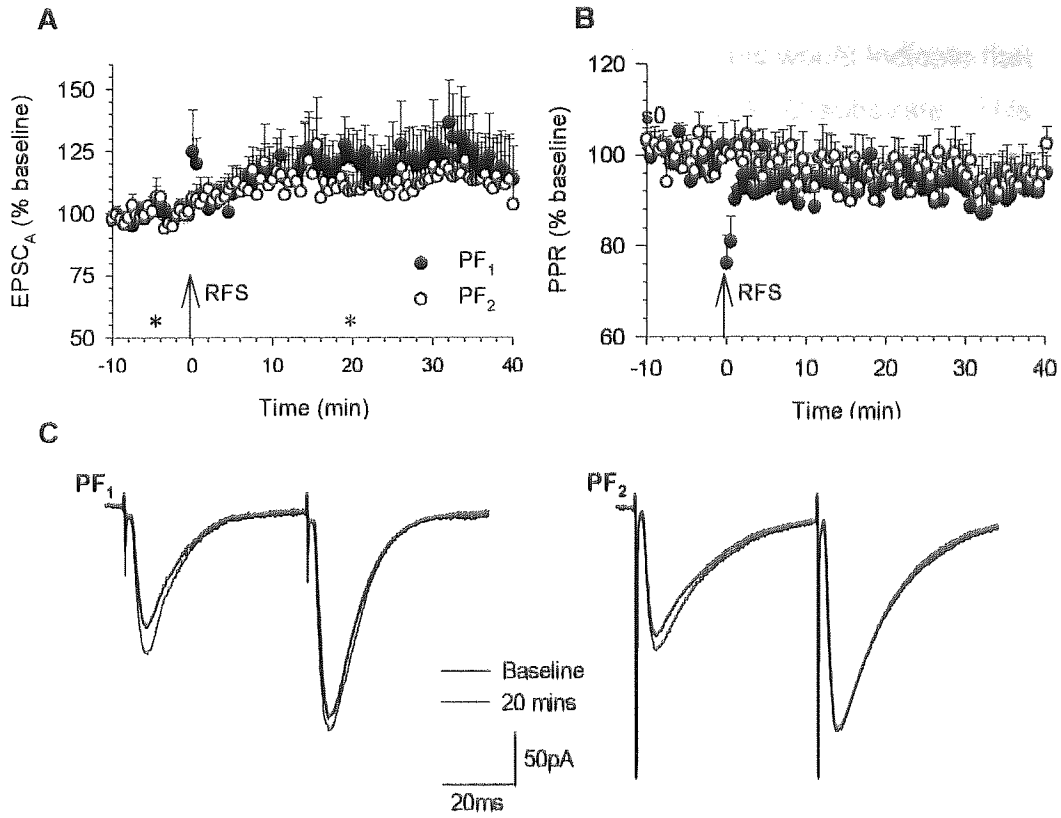

Figure 3.13 LTP is induced by 15s 16Hz RFS in homozygous G-substrate knockout mouse PCs with 0.5mM EGTA$_i$. The effects of 16Hz RFS are illustrated, showing changes in EPSC$_A$ (*A*) and PPR (*B*) in both test (PF$_1$) and distant (PF$_2$) pathways (*n*=7). Representative traces of EPSCs at baseline and 20 minutes in the PF$_1$ and PF$_2$ pathways are shown in *C*. The traces are averages of 6 sweeps comprising the single time point, and asterisks denote the time points where the traces were sampled.

In the G-substrate knockout mice (fig. 3.13; *n*=7), however, the same protocol induced LTP rather than the depression observed in wild-type mice. EPSC$_A$ in the PF$_1$ pathway was greater than baseline levels 20 minutes after RFS (123.5 ± 10.0%) and was coupled with a decrease in PPR (94.3 ± 2.9%). This potentiation also spread to the distant pathway, where EPSC$_A$ was slightly enhanced (109.7 ± 6.5%) and the PPR slightly depressed (95.9 ± 3.7%).

There was a statistically significant difference between the EPSC$_A$s of the PF$_1$ and PF$_2$ pathways between wild-type and homozygous mice (Mann-Whitney U-test: PF$_1$, $p<0.01$; PF$_2$ $p<0.05$). The PPRs of the PF$_1$ pathway were significantly different between wild-type and homozygous mice, although the PPRs of the PF$_2$ pathway were not. (Mann-Whitney U-test,

$p<0.05$; n = 6 wild-type vs. 7 homozygous; fig. 3.14). This would indicate that CF-independent LTD is prevented in mice that lack G-substrate. This suggests that G-substrate is involved in LTD, both at the stimulated and distant pathways.

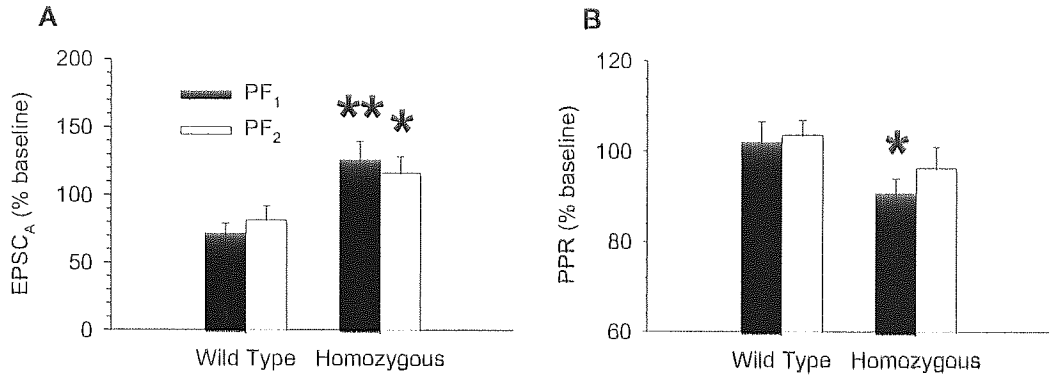

Figure 3.14 The effects of 8Hz RFS on wild-type and homozygous G-substrate knockout mice. All results shown are taken 20 minutes after baseline ceased, with 0.5mM EGTA$_i$. The EPSC$_A$ (*A*) and PPR (*B*) of the test (PF$_1$) and distant (PF$_2$) pathways are illustrated, in homozygous G-substrate knockout and wild-type mice. Asterisks represent significant differences between wild-type and homozygous mice (Mann-Whitney U-test: ** $p<0.01$, * $p<0.05$)

3.4 Discussion

The results in this chapter are largely consistent with previous data obtained in cerebellar slices. Whilst a high concentration of calcium chelator was present to inhibit calcium-dependent processes of LTD, RFS for 15s at 8-16Hz generated a long-term increase in synaptic transmission with concurrent decrease in the PPR, evidence of presynaptic potentiation. This potentiation also spread to distant PF synapses. Where a low concentration of postsynaptic calcium chelator was present, we instead observed a long-term decrease in synaptic transmission with no change in the PPR. Firstly, this study finds that diffusion of NO is responsible for heterosynaptic spread of LTP to distant synapses in PCs. Secondly, this study provides the first evidence that G-substrate is involved in cerebellar LTD.

3.4.1 The role of nitric oxide in the spread of parallel fibre plasticity.

The evidence that the NO-scavenger cPTIO created a synapse-specific LTP is vital in confirming the role of NO in the spread of plasticity. The distance NO can spread in the cerebellum has been calculated to be 182μm in one half-life of 3.3s (Schweighofer & Ferriol, 2000). Cerebellar cells have 'NO sinks', which may shorten the half-life of NO to 100ms under physiological conditions (Griffiths & Garthwaite, 2001; Griffiths *et al.*, 2002). It has been estimated that the effective diffusion distance of NO may only be 14μm (Wang *et al.*, 2000b). In their investigation of spread of LTD, they tested the AMPA-mediated response to uncaged glutamate release at various distances from the a site of PFs conjunctively activated with the CF. They found that the level of depression of glutamate responses decreases with distance from the site of PF stimulation, and is negligible at 100μm. Working on cultured snail neurons, Park et al. (1998) found that NO diffuses up to 70μm, and Hartell *et al.* (2001) found that cGMP production could be detected over 80μm from sites of PF stimulation. Mathematical modelling suggests that NO could diffuse further (Wood & Garthwaite, 1994; Philippides *et al.*, 2000). Therefore, the findings of spread of 158μm reported here might be unexpectedly great, but not impossible. As the NO-donor spermine NONOate is capable of restoring potentiation in the presence of the PKA inhibitor H-89 (Jacoby *et al.*, 2001) it can be assumed that the activity of NO is downstream of cAMP/PKA, and is capable of inducing LTP without them. It is also possible that while PKA acts presynaptically, NO may act postsynaptically, as claimed by Lev-Ram *et al.* (2002). However, the presynaptic effect of NO has been demonstrated by both a decrease in PPR and an increased frequency of miniature EPSCs (mEPSCs; Jacoby *et al.*, 2001).

What other mediators of spread of plasticity might exist? According to Wang *et al.* (2000) the decline of depression over distance was in a direct line from the site of LTD induction. This suggests that an extracellular messenger is responsible, as an intracellular messenger would have to travel through the

tortuous path of the PC dendrites. The requirement for an extracellular messenger would be likely for LTP also, unless spread of potentiation is mediated by a retrograde messenger or postsynaptically expressed. ArA can freely diffuse throughout the slice, and may affect spread of plasticity as it has been reported to activate PKC and possibly sGC (Tremblay *et al.*, 1988; Shearman *et al.*, 1989; Reynolds & Hartell, 2001). PAF has also been implicated in increasing NOS activity in the hippocampus (Catalan *et al.*, 1996; Calcerrada *et al.*, 2002). Also, postsynaptically-produced PAF has been found to act as a retrograde messenger to cause LTP in the hippocampus (Kato *et al.*, 1994). Recent work has discovered PAF also causes potentiation at PF-PC synapses (Reynolds & Hartell, 2001), thus it may be considered a potential mediator of the spread of LTP. Inhibition of PF-GC signalling has been observed through the retrograde activity of endogenous cannabinoids from PCs (Kreitzer & Regehr, 2001) which may explain spread of LTD, but not LTP. All of these signal molecules, due to their size, would have a much lower diffusion coefficient than NO, however, making them less likely candidates for the spread of plasticity.

LTP was initially believed to be exclusively presynaptic, until the recent discovery of a postsynaptic form that possibly operates through a different mechanism (Lev-Ram *et al.*, 2002). We cannot be sure whether the two forms of LTP are independent and/or exclusive or whether they involve some interaction of pre- and postsynaptic environments. While they have been elicited distinctly by different protocols (Lev-Ram *et al.*, 2002), there are some inconsistencies in existing data. Lev-Ram *et al.* (2001) claim presynaptic LTP is NO-independent. However, work both in this chapter and previously published (Jacoby *et al.*, 2001) shows potentiation at distant synapses is accompanied by a decrease in PPR, suggesting a presynaptic locus of action. Another issue to consider is the activation protocols recorded. The rates of stimulation to induce the postsynaptic and presynaptic variants of LTP (1Hz and 4-16Hz respectively) are very similar. Therefore, it may not be readily assumed that the two protocols are entirely independent. cPTIO prevents the spread of LTP, thereby implicating NO-dependence of presynaptic potentiation. This is consistent with the findings that NO can

facilitate vesicle release (Meffert *et al.*, 1994; Meffert *et al.*, 1996). If 1Hz stimulation can still induce potentiation in the presence of cPTIO, it would determine whether the NO has a postsynaptic target in the postsynaptic form of LTP.

There may be a more complex interaction of pre- and postsynaptic mechanisms. RFS with low concentration BAPTA in the PC sometimes elicited a brief potentiation before depression emerged, with PPR decreased during that potentiation and synapse specificity was observed in the four experiments that generated STP. It may be that this limited increase in synaptic strength is linked with failure to spread to the distant synapse. Under these conditions the RFS may produce insufficient NO to induce more than a transient potentiation in local synapses. Another possibility for the brief, transient potentiation is that Salin *et al.* (1996) observed an increase in the parallel fibre volley up to around ten minutes after RFS, indicating more fibres were recruited. While this would account for potentiation in the test pathway, it cannot explain the potentiation at the distant site. Nor would it satisfactorily explain why it was not observed in other experiments, or the reduction in PPR that accompanied the potentiation. It has previously been observed that PPR may return to baseline levels whereas EPSCs remain potentiated (Jacoby *et al.*, 2001). Possibly, the initial stage of LTP is primarily a presynaptic event, reliant on immediate chemical changes such as phosphorylation, maybe with later transcriptional stages (Nguyen *et al.*, 1994). The main long-term increase however may be a NO-mediated postsynaptic one.

Any diffusible messenger would also affect nearby PCs, not just other synapses on the same cell: it would be appropriate to envisage high PF activity influencing a whole area of Purkinje cells. Plasticity has been observed to spread to nearby cells in the hippocampus (Schuman & Madison, 1994a; Schuman & Madison, 1994b). As NO production is determined by presynaptic activity (Kimura *et al.*, 1998), it can be hypothesised that the distance of spread could be dependent on the number of PFs spiking, and their frequency.

3.4.2 What favours long-term depression or long-term potentiation?

While the finding that LTD can be converted to LTP in the presence of postsynaptic inhibitors that block LTD is consistent with earlier work from this laboratory (Jacoby & Hartell, 1999), Salin *et al.* (1996) observed that LTP was evident even in low concentrations of post-synaptic chelator. This discrepancy may be due to the following reason. The tendency for LTP or LTD to predominate in the hippocampus is principally determined by postsynaptic calcium (Artola & Singer, 1993). It is very difficult to maintain a voltage clamp over the extensive dendritic arborisation of the PC, so distant regions of the dendritic tree are unlikely to be fully clamped at –70mV. The stimulation strengths used here generated responses over 250pA, which equates to activation of over 30 PFs that generate a postsynaptic response (Isope & Barbour, 2002). This number of PFs activated may have caused an increase in the intracellular calcium concentration of the PC through VGCCs and/or IP_3 mobilisation that was sufficient to overwhelm the local BAPTA concentration during the train. Experiments described in chapter 5 conducted with lower $EPSC_A$ PF responses and 10mM BAPTA in the recording pipette more reliably evoked a clear LTP. In conditions where LTD was further blocked, both by the NO-scavenger cPTIO in the extracellular medium and in the absence of G-substrate, LTP was again considerably more reliable. Outright conversion between LTP and LTD can occur in visual cortex pyramidal cells (Artola *et al.*, 1990). As LTD is expressed postsynaptically, this would be unlikely in the case of presynaptic LTP without a retrograde messenger, although more likely for postsynaptic LTP.

That both LTP and LTD may be induced by high firing rates of GCs is intriguing. CF-independent LTD may act alongside conjunctive LTD, and/or as a replacement mechanism for the CF, which does not reach peripheral dendrites of the PC (Palay & Chan-Palay, 1974). This appears to occur in areas of the fish cerebellum which CFs do not innervate (Bell *et al.*, 1997). It could also be a neuroprotective response to hyperactivity at the PF-PC synapse (DeSchutter, 1995). *In vivo*, hyperpolarisation of the PC by inhibitory interneurones of the cerebellum would cause reduced ion flow through

VGCCs and thus favour potentiation (Shibuki & Okada, 1992). Picrotoxin was present in all experiments in this study, blocking $GABA_A$ receptors. However, previous work undertaken in this laboratory has shown that in the absence of picrotoxin LTP predominates (Jacoby, 2001).

3.4.3 G-substrate – an important mediator of long-term depression

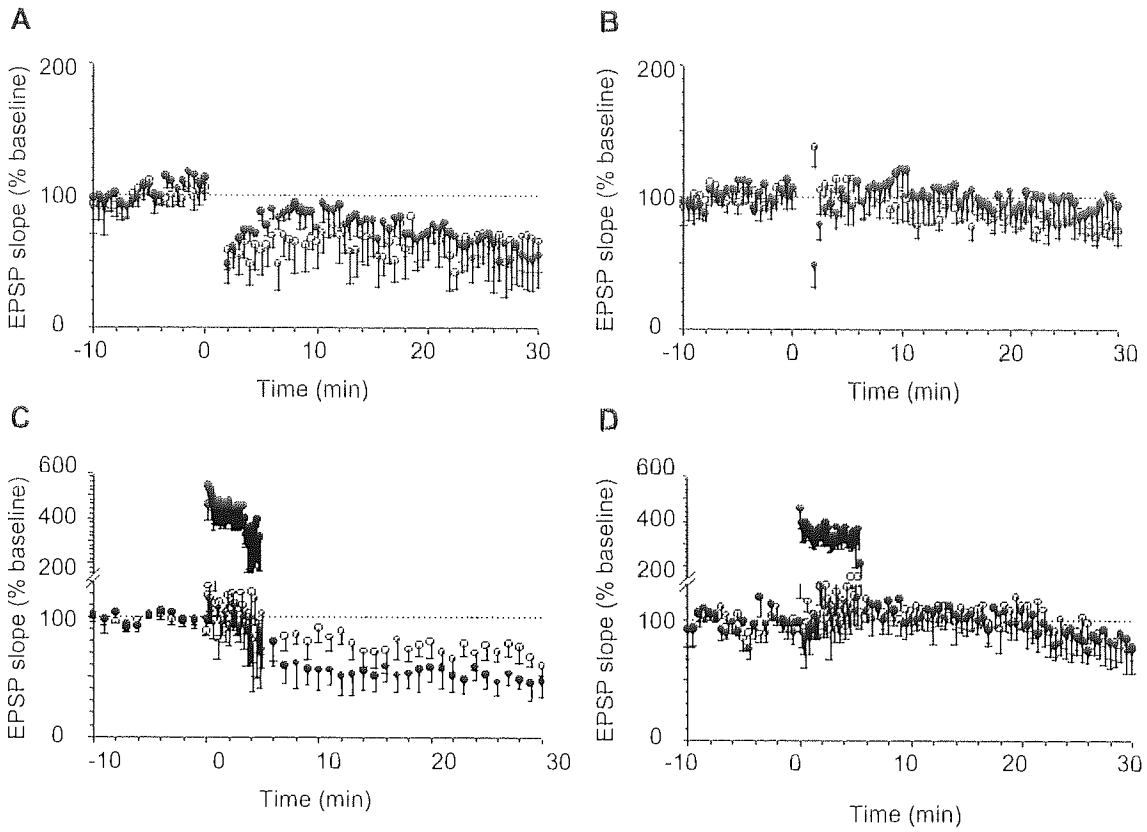

Figure 3.15 G-substrate knockout mice do not undergo LTD under a range of protocols. Experiments involved stimulation of two pathways in the molecular layer, one test (closed circles) and one distant (open circles). Conjunctive stimulation of the CF and PFs evoked LTD in the wild type mouse, *A*, but not the G-substrate knockout mouse, *B*. Raised frequency and intensity stimulation of PFs alone evoked LTD in wild type, *C*, but not G-substrate mouse, *D*. Experiments were performed by Dr. N. A. Hartell, and are presented here with permission.

Further to the work here, experiments performed in this laboratory (Hartell, unpublished data) with conjunctive stimulation of CF and PF and a CF-independent protocol (5-minute 1Hz raised frequency and intensity stimulation) did not generate LTD in the G-substrate knock-out mice (fig. 3.15). Behavioural studies of the knockout mice revealed that they displayed no ataxia, loss of motor skills, loss of eyeblink conditioning or loss of the

vestibulo-ocular reflex. However, they did show a deficit in the long-term optokinetic reflex, indicating some impairment of cerebellar learning (fig. 3.16). As is often the possibility in the case of genetic knockouts, compensatory mechanisms may have developed to counter the loss of G-substrate. A previous knockout of PKC specific to PCs has displayed poor learning ability for the vestibulo-ocular reflex, although co-ordination was largely unimpaired. (DeZeeuw *et al.*, 1998;Goossens *et al.*, 2001).

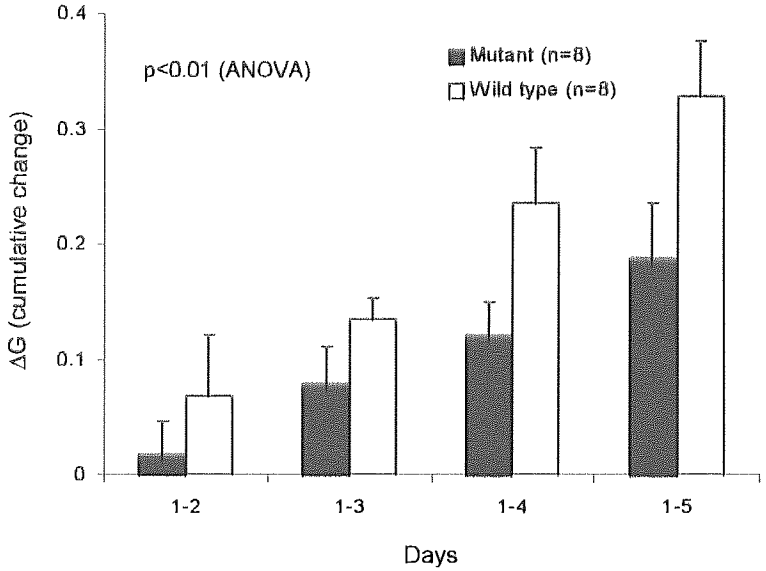

Figure 3.16 Adaptation of the optokinetic reflex in wild type and G-substrate knockout mice. Mice were trained for 1 hour per day for 5 successive days. Graph demonstrates the level of improvement each day, which is significantly deficient in mice with G-substrate knockout ($p<0.01$, ANOVA). Experiments presented here with permission of Dr. S. Endo, RIKEN, Japan.

Evidence presented in this chapter supports the view that G-substrate contributes to the induction of LTD, and in its absence high rates of GC activity produces LTP. Its role in LTD is indirect, increasing phosphorylation of AMPARs by potently inhibiting protein phosphatases. Current understanding of the NO-dependent pathway indicates that it appears to be largely independent of the PKC pathway (fig. 1.4). That there are two parallel pathways raises the question of whether both are required for LTD, or whether one or both can cause LTD independently. It may be that facilitation of PKC alone is unlikely to phosphorylate receptors sufficiently to induce internalisation, and the function of G-substrate in LTD is to ensure that the reverse process of dephosphorylation is prevented. The NO pathway of LTD

must be dependent on GC activity; to assume this as a dominant pathway would be counterintuitive in the face of conjunctive LTD for three reasons. Firstly, it partly negates the point of CF activation for the calcium dependent PKC pathway; secondly, GC activity may be relatively low compared to that needed for CF-independent LTD; and thirdly, large amounts of NO produced may cause LTP. The NO pathway is more likely to be important for CF-independent LTD, which requires considerable GC activity, and where the GC activity acts to mimic the CF. However, inhibition of the NO pathway alone will also prevent LTD (Daniel *et al.*, 1993; Hartell, 1994a; Hartell, 1994b; Lev-Ram *et al.*, 1997b), so it must also perform a vital role. There will be a dynamic equilibrium between phosphorylation/dephosphorylation at AMPARs, and basal rates of activity of kinases and phosphatases. The effects of inhibition of various factors will not just disturb their activity during LTD protocols, but also the basal rates. Therefore while LTD may appear to be blocked *in vitro*, *in vivo* basal rates of activity might provide enough phosphorylation activity (or dephosphorylation inhibition) to make LTD viable. The spread of plasticity is a possible area to evaluate the effectiveness of each pathway. However, many possible mediators of spread of plasticity exist, particularly in LTD. It cannot be assumed that NO is solely responsible, as the PKC-pathway at distant synapses could be stimulated by other diffusible messengers, such as ArA.

Chapter 4

Transmission properties of synapses formed by granule cell ascending axons and parallel fibres with Purkinje cells.

The PF has long been considered the primary source of GC transmission to PCs. Consequently the information flow in the cerebellar cortex from mossy fibres has been often hypothesised to be organised laterally. However, strong evidence exists that in fact the organisation of MF to PC signalling is vertically strong, for which the AA segment of the axon may be responsible, but weak laterally along PFs. Furthermore anatomical data suggests a physiological difference may exist between AA and PF-PC synapses, suggesting possible functional differences. This chapter will detail the electrophysiological characteristics of synapses made by the two segments of the GC with PCs.

4.1 Introduction

4.1.1 Granule cell to Purkinje cell signalling

In the cerebellar cortex MFs pass afferent excitatory signals to GCs. GCs then transmit glutamatergic, excitatory information to PCs, with an estimated 50 – 170,000 GC synapses per PC (Palay & Chan-Palay, 1974; Napper & Harvey, 1988). These synapses are formed from two segments of the GC axon: the ascending limb thrusts vertically up into the ML making several synapses on each PC before bifurcating into PFs (Mugnaini, 1972; Napper & Harvey, 1988). The PFs run for several millimetres depending upon species (ca. 5mm in rat) laterally along the cerebellar cortex, forming one synapse, or rarely two, with virtually every PC passed (Palay & Chan-Palay, 1974; Napper & Harvey, 1988; Pitchitpornchai *et al.*, 1994).

The dominant theory of cerebellar cortical function is the 'beam hypothesis', where MF signals to PCs are primarily conveyed via beams of PFs

(Braitenberg & Atwood, 1958; Eccles *et al.*, 1967; Garwicz & Andersson, 1992). This hypothesis was formed on the basis of the anatomical structure of the cerebellum, supplemented by studies which found that stimulation of the ML evoked responses along a 'beam' of PCs. (Eccles *et al.*, 1966a). However, experiments involving stimulation of the periphery evoked spatially-restricted, non-propagating patches of PC activity (Eccles *et al.*, 1972;Cody & Richardson, 1979). While initially thought to be due to complex interactions of PF-evoked inhibitory and excitatory beams, these patches of PC activity were found to correspond to the patches of activity evoked in the GL by MFs (Bower & Woolston, 1983). Experiments with voltage-sensitive dyes have demonstrated ML stimulation generates 'beam' responses (Vranesic *et al.*, 1994), whereas MF stimulation elicited only patchy activity in PCs and interneurones (Cohen & Yarom, 1998). As measured by electrophysiological methods, stimulation of the periphery recorded PC activity beyond the MF termination zone, but only in just over 50% of experiments, and the PC response frequently declined sharply beyond the MF termination zone (Garwicz & Andersson, 1992).

4.1.2 The granule cell ascending axon: an overlooked part of cerebellar studies?

There are other factors that suggest PFs are a much weaker signalling system than previously thought, contrary to the beam hypothesis. Investigation of single GC inputs to PCs found as many as 85% of PF-PC synapses were electrically silent (i.e. generated no postsynaptic response; Isope & Barbour, 2002). PC responses beyond 1.5mm downstream of the stimulation site were minimal during stimulation of the ML in rats (Heck, 1995; Vranesic *et al.*, 1994). During peripheral stimulation in cats (Garwicz & Andersson, 1992), responses were detected at distances considerably less than the full length of a PF. Average synapse density on the PF has been reported as approximately 5.2 µm in one study (Shepherd *et al.*, 2002). Another found that presynaptic density decreased further away from the GC

soma; one synapse per 4.0μm on the AA, one per 5.2μm on the PF near the bifurcation point and one per 7.4μm further along (Pitchitpornchai *et al.*, 1994). Mathematical models have introduced the possibility that action potential propagation may fail at the bifurcation point of the GC axon (Mocanu *et al.*, 2002), although this has been refuted in recent experiments (Isope & Barbour, 2002).

The vertical, as opposed to lateral, organisation of the cerebellum has been hypothesised to be due to the presence of synapses on the AA (Llinas, 1982), although the AA is absent in many descriptions of cerebellar circuitry and function. The ascending axon was initially believed to contribute to only about 3% of all GC-PC synapses (Napper & Harvey, 1988) as calculated from three aspects of GC anatomy: *i*, the number of GCs below the PC which would connect with the PC dendrites via the AA; *ii*, the average length of the AA; *iii*, the density of synapses on the GC axon. However, more accurate figures for those characteristics indicate that 7-24% of GC synapses would be a more accurate estimate (Gundappa-Sulur *et al.*, 1999). An alternative method based on the PC anatomy – the density of AA synapses on PC dendrites – provides an estimate of approximately 20% of GC-PC synapses formed by the AA (Gundappa-Sulur *et al.*, 1999): this correlates well with the calculations based on GC anatomy. If these calculations are correct, these estimates predict that AA synapses make up a considerable input to the PC. If 85% of PF synapses are electrically silent (Isope & Barbour, 2002), AA synapses could contribute the greater part of GC-PC transmission. Anatomical studies have revealed that the AA synapses are exclusively on the more distal, spiny branchlets of PC dendrites, which are prevalent in the in the deeper region of the ML. AA synapses also have a greater density of presynaptic vesicles (Gundappa-Sulur *et al.*, 1999), which has been postulated to reflect a greater probability of transmitter release (Murthy *et al.*, 1997). In PF synapses the presynaptic volume, density and number of presynaptic vesicles correlates to the postsynaptic volume and density (Harris & Stevens, 1988; Gundappa-Sulur *et al.*, 1999). This suggests that forms of activity at the pre- and postsynaptic environments of PF synapses

influence the development of both. This correlation of pre- and postsynaptic characteristics does not occur at AA synapses, thus suggesting that similar forms of interaction may not be present at these synapses. All of these anatomical observations suggest that there may be a pre- and postsynaptic heterogeneity of synapses formed between GCs and PCs.

4.1.3 Aims & Objectives

Experiments measuring PC activity following peripheral (Bower & Woolston, 1983) or MF (Cohen & Yarom, 1998) stimulation have shown a spatially limited propagation of signals along PFs. This may be explained by anatomical evidence that has revealed differences in the pre- and postsynaptic characteristics of AA- and PF-PC synapses (Gundappa-Sulur *et al.*, 1999). In particular it is suggested that PF synapses may have a lower probability of release. This chapter will describe a number of experiments designed to examine the electrophysiological properties of AA and PF synapses. Initially, possible differences in release probability were examined through measurement of PPF. Secondly, 'variance-mean' analysis was used as a more robust means of estimating the characteristics of both synapse types.

4.2 Methods

Most of the methods for the chapter are detailed in chapter 2. In brief, experiments were carried out on 14-21 day-old male, Wistar, rats, in accordance with previous work. Slices were cut initially in a sagittal orientation as per chapter 3. However, since PFs are severed in this orientation and it is not possible to distinguish synapses formed by PFs or AAs, slices cut in a coronal orientation were later used. In this orientation stimulation of the ML distant from the PC dendrites should exclusively activate PFs. Coronal slices were cut thicker (250μm) to reduce the

likelihood of PC dendrites being cut off. Thicker slices (>300μm) were found to impede visualisation excessively. 10mM BAPTA was included in the recording electrode, and slices were perfused in standard aCSF, with picrotoxin to block $GABA_A$-mediated currents. It was necessary for some experiments to obtain different transmitter release probability conditions, for which alternative aCSFs were prepared. These were based on standard aCSF but with differing calcium concentrations (1, 1.25, 2.5, 5mM $CaCl_2$, and 5mM $CaCl_2$ with DPPX). PCs were held in voltage-clamp configuration at -70mV to minimise voltage-dependent ion conductances.

Standard electrode placement was in the GL and ML as explained in chapter 2 and as demonstrated in fig. 4.1, to preferentially activate AAs and PFs respectively. In some experiments an electrode was placed in the GL, over 100μm laterally to the PC soma. This locus of stimulation was used to activate PF-PC synapses, but in a more diffuse manner across the PC dendritic tree compared to activation of a dense bundle of fibres from ML stimulation. The aims behind this lateral GL stimulation were twofold: *i*, to minimise changes in fibre excitability that might occur through potassium extrusion following activation of a dense beam of PFs; *ii*, to reduce a possible localised area of glutamate release which may lead to spillover to more distant synapses.

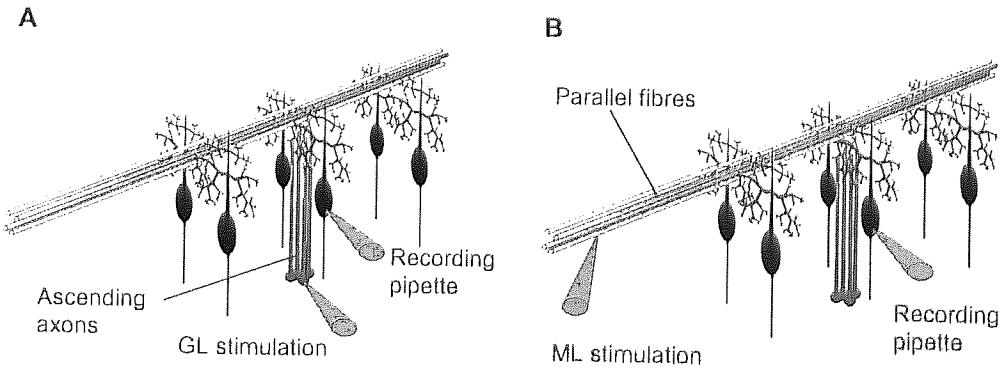

Figure 4.1 Electrode positioning for stimulation of AAs and PFs in coronal slices. *A*, Stimulation in the granule cell layer to excite AA-PC synapses; *B*, lateral stimulation of the molecular layer to excite PFs.

The basic stimulation protocol included a 100ms, 4mV hyperpolarizing pulse to monitor cell conditions. 50ms later, pairs of stimuli were applied at a separation of 50ms to each pathway, alternately at a rate of 0.2 or 0.1Hz. In some experiments the interstimulus interval or the number of pulses was altered. Experiments were initiated after at least 15 minutes had been allowed for BAPTA to perfuse the cell and after 5 minutes of stable $EPSC_A$ were acquired. As in the previous chapter I_h, R_s and R_m were monitored throughout, and cells that showed severe deterioration were discounted, as explained in chapter 2. Changes in R_s were manually adjusted for during the recording. Any response to stimulation that was smaller than the root mean square of the holding current (I_{RMS}) – as measured on the amplifier – was considered indistinguishable from noise. I_{RMS} varied between 4 and 8pA by experiment. This provided the criteria for determining failures.

For fluctuation analysis, the $EPSC_A$ responses to 50-100 sweeps were recorded in four different solutions, each generating a different release probability. These were standard aCSF containing 2.5mM calcium, 5mM calcium, 5mM calcium with 100nM DPPX (a selective A1 adenosine antagonist, to enhance calcium entry; Dittman & Regehr, 1996) and 1.25mM calcium. To ensure adequate wash-in and stability of responses with each new solution, 10 minutes were allowed to elapse before points were used for analysis. Experiments where there was a depression of P_1 responses under conditions of high release probability were discarded. For the experiments where multiple pulses were used to vary release probability, 3-10 pulses with an interstimulus interval of 50ms were applied. However, initial experiments showed that repeated, multiple pulses caused potentiation. Therefore 0.2μM H-89 (a PKA inhibitor) was added to prevent this potentiation (Salin *et al.*, 1996). Seven pulses were deemed optimal to both generate sufficient points for analysis and to prevent overstimulation of the synapse (thus depleting the presynaptic vesicle supply). In standard aCSF containing 2.5mM calcium, responses facilitated and reached a peak by the second or third response, and subsequent responses declined in amplitude. Therefore the calcium concentration in the aCSF was reduced to 1mM. The rate of alternate stimulation of AA and PF pathways was also reduced from 0.1 to 0.05Hz to

minimise the likelihood of plastic changes that might occur at higher frequencies of activation.

4.2.1 Data analysis

PPR calculated as the mean of individual PPRs (mean P_2/P_1) can be skewed to higher values. Spuriously high PPRs are correlated not with the size of the P_1 and P_2 amplitudes *per se*, but with the coefficient of variation of P_1 and P_2 amplitudes. As EPSCs become smaller, the effect of random fluctuation is more pronounced, and PPR tends to become greater. Therefore PPR was calculated where possible as mean P_1 / mean P_2 as per Kim & Alger (2001). Usually PPR is used as an indicator of the locus of synaptic plasticity (re. chapter 3). Here we used it as a simple predictor of the release probability at different synapses (Thomson, 2000).

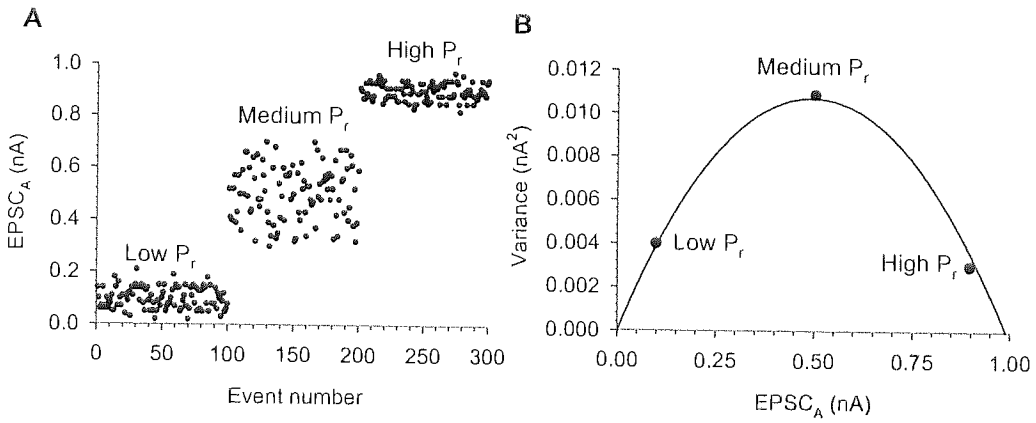

Figure 4.2 Illustration of the principles of V-M analysis. The data presented here were generated artificially by a computer. $EPSC_A$s are obtained at different release probabilities, *A*. The variance can then be plotted against the mean for each different release probability and a parabola fitted, *B*. Adapted from Clements & Silver (2000).

Variance-mean (V-M) analysis was carried out as previously published (Silver *et al.*, 1998; Clements & Silver, 2000). Responses were measured at a number of different release probabilities, with at least 50 points recorded for each. The variance of these points was then plotted against the mean, for each release probability (fig. 4.2). As the probability of transmitter release at a release site tends to 0 or 1, variance tends to 0, with peak variance

occurring when P_r = 0.5 (fig. 4.2). Thus for a constant number of release sites, over a range of different release probabilities, the relationship of the response to the variance is roughly parabolic. The equation for a parabola is:

$$y = A\,x - B\,x^2$$

In the variance-mean plot, y represents the variance of the postsynaptic current; x represents the mean of the postsynaptic current. A and B are free parameters that define the initial gradient (A) and rate of decline of the parabola (B). From A and B can be calculated the mean quantal amplitude across all release sites (Q), the minimum number of release sites (N_{min}), and the mean probability of release (P_r) that generates the given postsynaptic current, x, across all sites. For Q and P_r, the values are weighted averages, in that they are more liable to reflect larger quantal amplitudes and release probabilities.

Quantal amplitude: $Q = A / (1 + CV_I^2)$

Number of release sites: $N_{min} = 1 / B$

Probability of release: $P_r = x\,(B / A)\,(1 + CV_I^2)$

CV_I is the coefficient of variation of the postsynaptic current at a single release site. It is usually in the range of 0.2 – 0.4 (Clements & Silver, 2000), and is taken as 0.3 for the calculations in this study, as a medium value. The initial gradient of the parabola is proportional to Q, such that a greater Q will cause a steeper rise in the curve. The rate of decay of the parabola is inversely proportional to N_{min}, and a greater N_{min} will cause the parabola to decline slower. P_r is a function of the curve of the parabola, so that P_r changes do not so much affect the shape of the curve, but where on the curve a point lies.

If the probability of release in experiments is not above 0.3, then it will be difficult to fit a parabola, as the plotted points will be roughly linear. In such cases it is impossible to calculate N_{min} and P_r as no data exists for the rate of decline, but Q can be estimated by fitting the equation for the line:

$$y = A\,x$$

Data can also be represented as a graph of variance/mean against mean (V/M-M plot; Scheuss & Neher, 2001; Scheuss *et al.*, 2002). Presuming no change in Q or N, at different release probabilities this should provide a linear plot where the line's bisection of the *y*-axis is the estimate for Q, and the reciprocal of the gradient estimates the minimum number of release sites. Curve fitting was achieved by customised procedures on 'Sigmaplot' software.

4.3 Results

4.3.1 Paired-pulse facilitation at ascending axon – and parallel fibre – Purkinje cell synapses.

Following the anatomical data suggesting there may be a greater release probability in AA- than PF-PC synapses, an examination of PPR, as a simple indicator of presynaptic release probability, was carried out (Zucker, 1989; Thomson, 2000). Initially, the effects of changing stimulus intensity on PPR were tested in sagittal slices. Experiments were not started until at least 5 minutes stable baseline had been recorded, as run-up or run-down of the EPSC can be accompanied by changes in PPR. The stimulation intensity applied to one pathway was reduced to zero and then slowly increased incrementally every 10 pulses in order to examine whether stimulation intensity affected PPR. This was then repeated for the second pathway, with a minimum of 80 points sampled per pathway. Mean PPRs of responses from step-wise increases in the intensity of stimulation were grouped in bins according to $EPSC_A$. The smallest $EPSC_A$ bin (P_1 < 50pA) was not included

in regression line fitting. This was because there were generally extremely high PPRs recorded, even using the method of mean P_1 / mean P_2 (Kim & Alger, 2001). There appears to be a difference between PPRs at low intensities (fig 4.3b) in both pathways. As the postsynaptic response increased a small, gradual decrease in PPR was observed in responses from GL stimulation. Responses from ML stimulation showed a more profound decrease in PPR as intensity increases. This may be due to increasing intensities of ML stimulation in sagittal slices recruiting non-PF synapses or even activating the cell directly, especially for PCs nearer the slice surface. For each experiment over 80 traces were also recorded at constant intensity stimulation, set at an intensity that generated P_1 $EPSC_A$s of 250-350pA. PPR was higher, but not significantly so, from ML stimulation (1.71 ± 0.05) than GL stimulation (1.65 ± 0.09) in six cells (Wilcoxon signed-rank test; fig. 4.3).

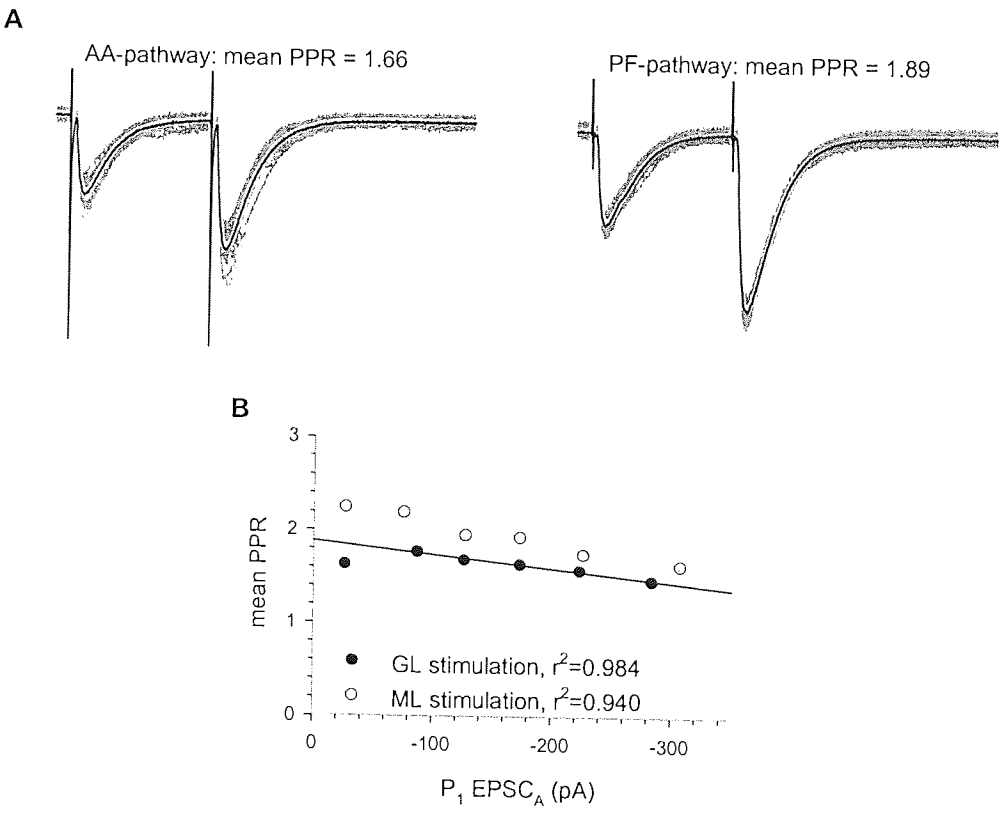

Figure 4.3 Paired-pulse ratios of PF- and AA-pathways in sagittal slices. The top figures show representative data traces obtained during constant intensity stimulation from one experiment in the AA-pathway and PF-pathway (*A*). 20 individual sweeps are shown in grey, and the black line is the average. In *B*, the mean PPR over a range of different $EPSC_A$s from both pathways from 6 cells is illustrated.

Therefore PPR was examined in coronal slices where the ML electrode can be placed far from the PC dendrites. From the anatomy of the cerebellar cortex, distant stimulation of the ML is likely to result in selective stimulation of PF synapses. However, it is recognised that ML stimulation may activate AA synapses antidromically. In view of the assumed exclusivity of each input, ML stimulation is henceforth referred to as the PF-pathway, and GL stimulation as the AA-pathway. While recording from coronal slices during stable stimulation in 2.5mM calcium and with a 50ms interstimulus interval in all experiments in this chapter, PPRs were significantly higher in the PF-pathway (1.91 ± 0.05) than the AA-pathway (1.54 ± 0.05; Wilcoxon signed rank test, $p<0.01$, $n=23$), suggesting that there is a lower probability of release at PF-PC synapses.

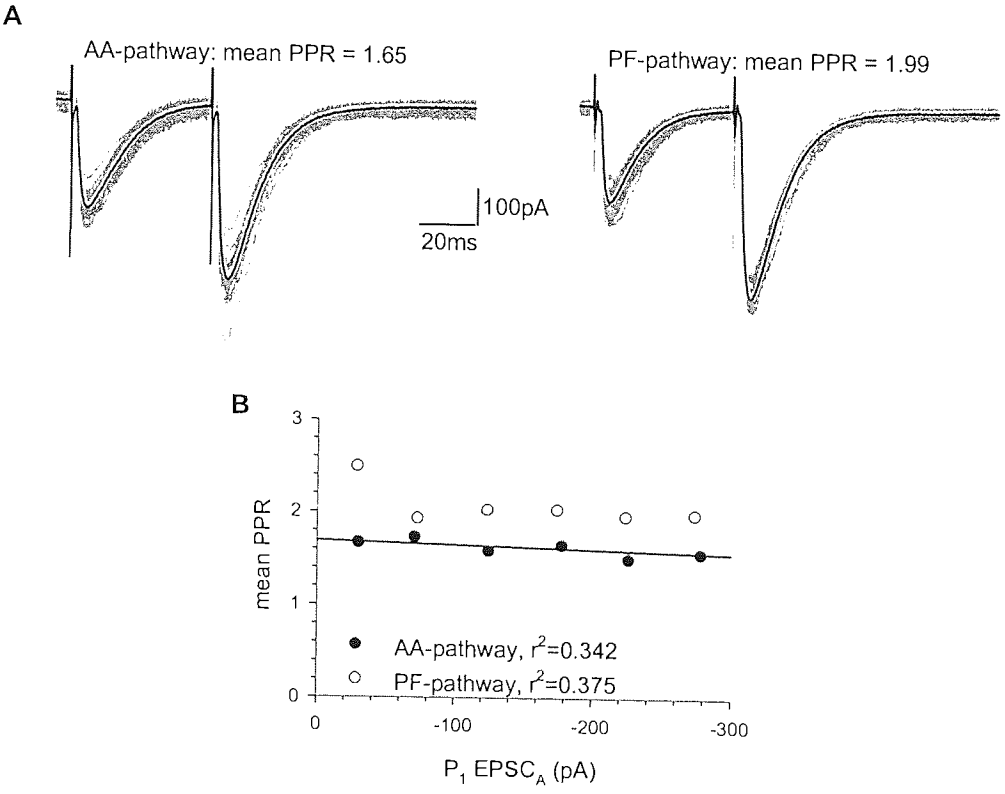

Figure 4.4 Paired-pulse ratios of PF- and AA-pathways in coronal slices. The top figures show representative data traces obtained during constant intensity stimulation from one experiment in the AA-pathway and PF-pathway (*A*). 20 individual sweeps are shown in grey, and the black line is the average. In *B*, the mean PPR over a range of different $EPSC_A$s from both pathways from 6 cells is illustrated.

The same protocol used previously in sagittal slices was repeated in six cells in coronal slices. Mean PPR during stable recording at baseline levels was

again higher in the PF-pathway (1.83 ± 0.06) than AA-pathway (1.62 ± 0.08), however here significantly so (Wilcoxon signed-rank test, $p<0.05$, $n=6$; fig. 4.4). As stimulus intensity increased there was a slight decline in PPR observed in the AA-pathway as before. Regression analysis showed that there was no relationship between stimulus intensity and PPR in either pathway (fig. 4.4b). This indicated that the size of $EPSC_A$, and thus the number of contributing synapses, did not influence the PPR. At low $EPSC_A$s, PPRs tended to be greater. This is likely due to the influence of random fluctuation or noise, even as measured by mean P_2 / mean P_1 (Kim & Alger, 2001; see methods.) In light of the high variability of responses and high PPR at low amplitudes it was attempted, where viable, to gather $EPSC_A$ responses over 50pA amplitudes in all future work.

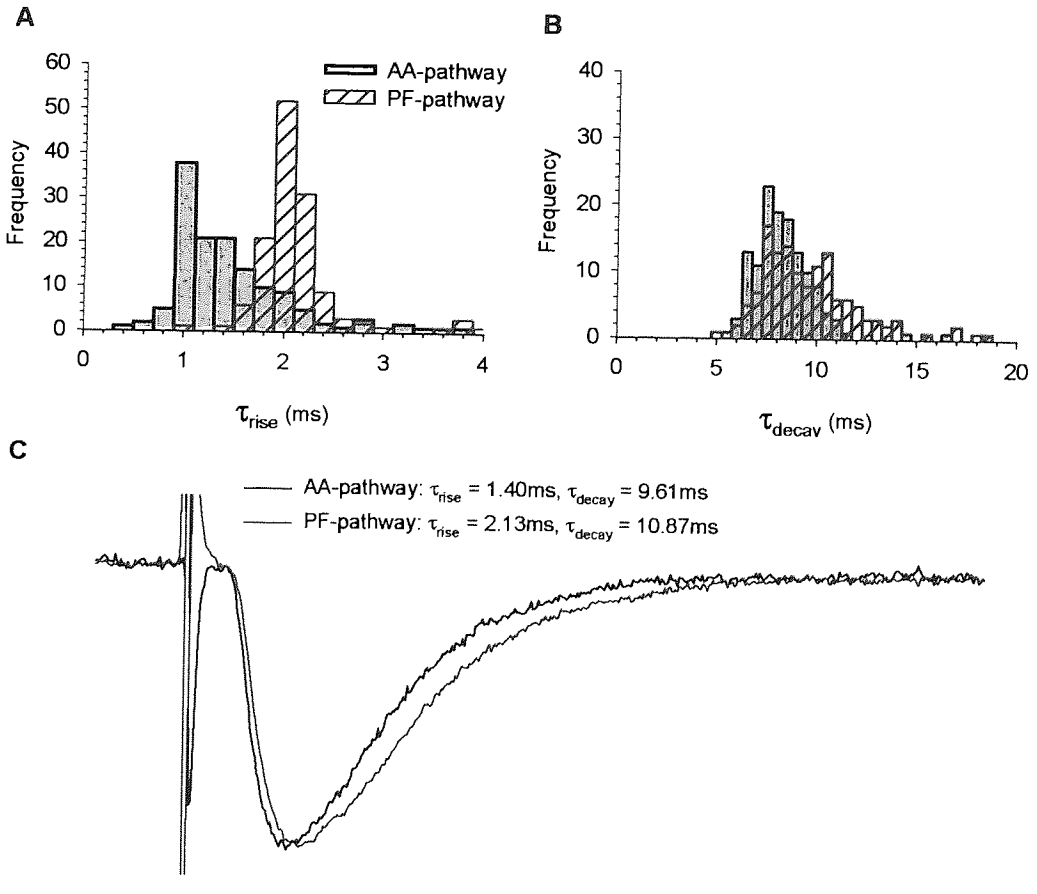

Figure 4.5 Rise and decay times of AA- and PF-pathway EPSCs in coronal slices. This figure shows histograms of rise time (*A*) and decay time (*B*) in both pathways, from 138 traces obtained from one representative cell during constant intensity stimulation. An average of 30 individual traces per pathway, normalised to equivalent amplitude, from the each pathway in the same cell are demonstrated in *C*.

There was no significant difference in the decay constants of P_1 in the two pathways in nine cells (from sections 4.3.1 and 4.3.3; AA-pathway, 9.97 ± 1.10ms; PF-pathway 10.51 ± 1.22ms), although the rise time of the PF-pathway was significantly longer than the AA pathway (1.80 ± 0.12ms and 1.56 ± 0.11ms respectively; $P<0.05$ Students T-test, two tailed, $n=9$; fig. 4.5). The P_2 EPSCs were similar to those of the P_1 in both decay times (AA-pathway, 9.90 ± 0.81ms; PF-pathway, 11.25 ± 1.02ms) and rise times (AA-pathway, 1.51 ± 0.11ms; PF-pathway, 1.83 ± 1.33ms). This suggests two things: *i*, the increased synaptic glutamate concentration from the second pulse is cleared equally quickly as from the first pulse; *ii*, if there is spillover of glutamate, it is not greater from the second pulse than the first.

Isope & Barbour (2002) found that PPR was greater when PFs were stimulated directly in the ML than when individual GCs were excited at the soma. They proposed that the greater PPR from ML stimulation is fibre recruitment due to increasing excitability of PFs, in turn resulting from extracellular potassium build-up (Kocsis *et al.*, 1983). However, extracellular recordings performed in our laboratory (Hartell, unpublished data) showed that PPF was not associated with an increase in the parallel fibre volley. PPRs of EPSCs were also recorded following lateral stimulation of the GL, over 100μm distant from the PC soma to excite PFs, alternately with regular ML stimulation. Lateral GL stimulation should reduce the likelihood that beams of tightly packed PFs are activated as might arise with direct PF stimulation, and so reduce the influence of any possible increase in excitability by factors such as build-up of extracellular potassium or glutamate spillover. During constant intensity stimulation the PPRs of lateral GL stimulation (1.91 ± 0.07) were significantly higher than those produced by PF-pathway stimulation (1.73 ± 0.03; Wilcoxon signed-rank test, $p<0.05$, $n=6$; fig. 4.6). This demonstrates that the lower PPR observed from stimulation of the AA-pathway is not an intrinsic property of stimulation in the GL. The slightly reduced PPRs observed following PF-pathway stimulation compared to lateral GL stimulation may reflect a small decrease in fibre recruitment. Double-peaked EPSCs could be could occasionally be observed from lateral

GL stimulation. This may be due to stimulation of MFs which then activated further GCs.

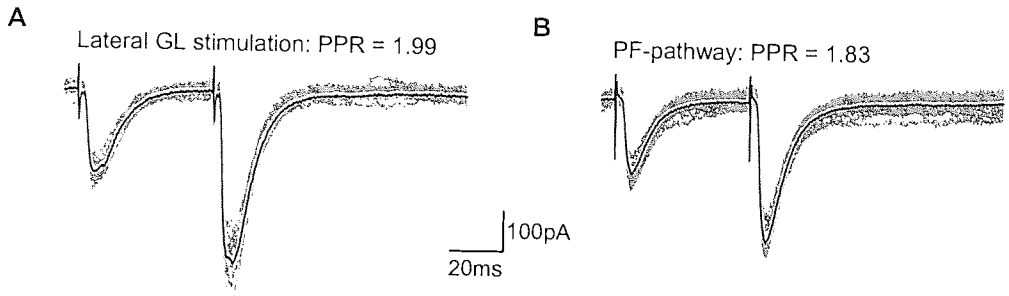

Figure 4.6 Paired-pulse ratios of PF-pathway and distant GL stimulation. This figure shows representative data traces obtained during constant intensity stimulation from one experiment in the AA-pathway (*A*) and PF-pathway (*B*). 20 individual sweeps are shown in grey, and the black line is the average.

4.3.2 Effects of changing the interpulse interval on paired-pulse facilitation

The consequence of differing interstimulus intervals in AA- and PF-pathways was investigated on coronal slices. Paired-pulses were applied alternately to each pathway, at 0.1Hz, with an initial interstimulus interval of 50ms, until the responses of both pathways were stable. Then the interval to the second pulse was reduced to 10ms, and a minimum of twenty points recorded. This process was then repeated for a range of intervals up to 500ms. At 500ms there was little or no PPF in either pathway. There was significantly greater PPR in the PF-pathway at 50-200ms intervals, at all intervals in that range tested except 150ms (Wilcoxon signed-rank test, $p<0.05$, $n=6$; fig. 4.7). This would indicate that GCs firing action potentials at less than 20Hz transmit information more reliably through AA synapses than PF synapses. Rapid spiking at frequencies greater than 20Hz may raise the probability of release at PF synapses in later pulses to similar levels as those at AA synapses. This may not be the case if PF-pathway stimulation also has a greater PPR at interstimulus intervals under 50ms. However, as the second pulse is applied before the cell has fully recovered from the first EPSC, it is difficult to measure.

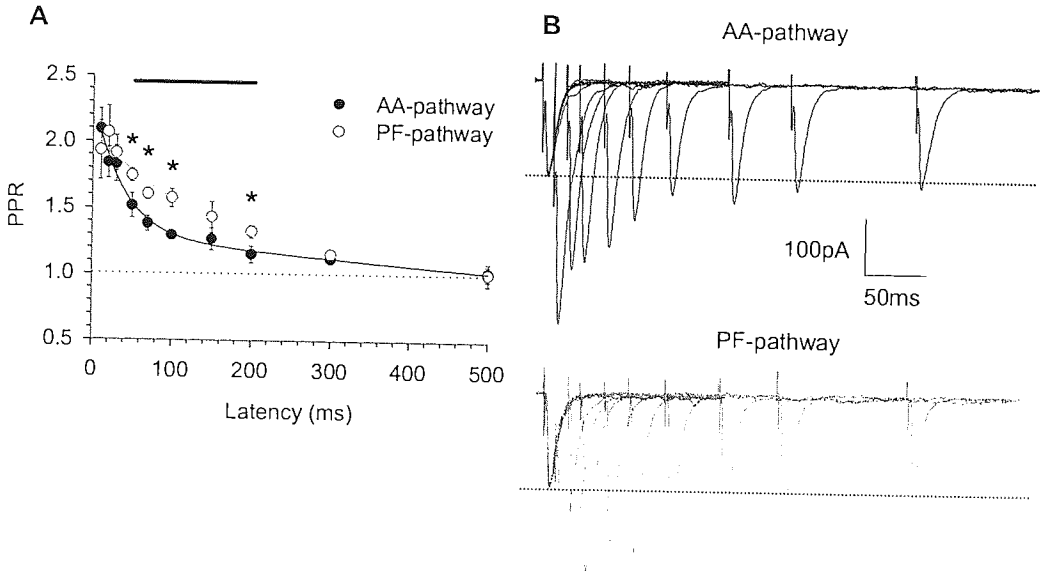

Figure 4.7 Paired-pulse facilitation with different interstimulus intervals in AA- and PF-pathways. *A*, A graph of PPR at interstimulus intervals from 10 to 500ms. The black bar represents the interstimulus interval where PPRs are different between AA- and PF-pathways. The asterisks statistical significance (Wilcoxon signed-rank test, $p<0.05$, $n=6$.) *R*epresentative traces for both AA- and PF-pathways of P_2 EPSCs in relation to P_1 are shown in *B*.

4.3.3 Near-threshold stimulation in the granule cell and molecular layers.

The response of the AA- and PF-pathways and lateral GL stimulation to near-threshold stimulation also differed greatly. The stimulation intensity was reduced to sub-threshold values, and then increased by small increments every 20 pulses. Failures were counted as anything that was below the noise of the experiment, as measured by the amplifier (I_{RMS}). In the AA-pathway there was a sharp transition between failure and success of responses at minimal stimulation intensities (fig. 4.8). As stimulation strength increased to threshold levels and beyond, $EPSC_A$ increased in a 'stepwise' manner: several stimulus increments would have no additional effect on $EPSC_A$, but the next increment would result in a large increase in $EPSC_A$. In three cells, there were a total of nine stepwise $EPSC_A$ increases. The mean, stepwise increase was -44.3 ± 7.7pA (range -10.9pA to -82.0pA.) In both the PF-pathway (6 cells; fig. 4.9) and with lateral GL stimulation pathways (3 cells;

fig. 4.10), however, there was no clear division between successes and failures, and the $EPSC_A$ increased steadily from the threshold in smaller (<10pA) amounts, with rare larger increases of 10-20pA.

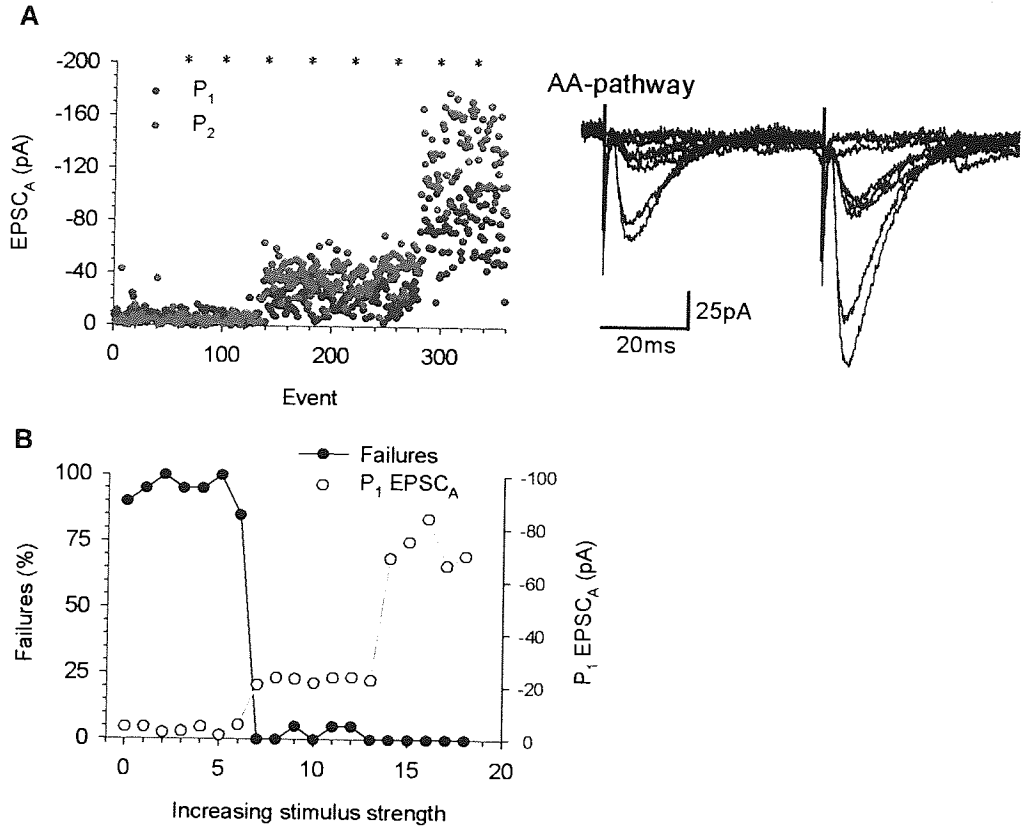

Figure 4.8 Representative example of graded increases in stimulation from sub-threshold values of the AA-pathway. Stimulation strength was increased every 20 pulses from zero volts. The $EPSC_A$ responses through the course of stimulation are illustrated in *A*. The asterisks denote the points where the representative traces shown are taken from. The relationship of average $EPSC_A$ and number of failures at each successive stimulation strength (where 0 is zero stimulation) is shown in *B*.

The results obtained from AA-pathway stimulation are consistent with the successive recruitment of GCs, with synapses to PCs that are both powerful and reliable. Occasional supra-threshold failures would be likely caused by failure to generate an action potential. On the other hand distant stimulation evokes $EPSC_A$s from PFs. The small increases in $EPSC_A$ are consistent with gradual recruitment from a large number of fibres with just one or two, possibly weak, synapses.

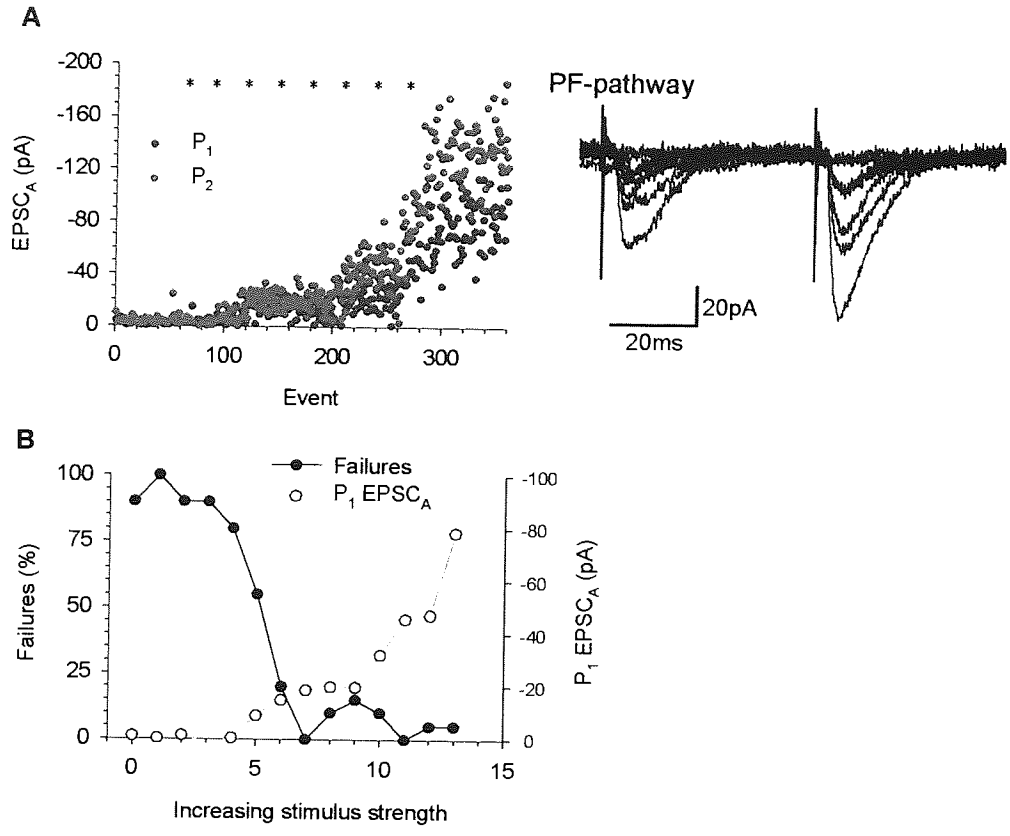

Figure 4.9 Representative example of graded increases in stimulation from sub-threshold values of the PF-pathway. Stimulation strength was increased every 20 pulses from zero volts. The $EPSC_A$ responses through the course of stimulation are illustrated in *A*. The asterisks denote the points where the representative traces shown are taken from. The relationship of average $EPSC_A$ and number of failures at each successive stimulation strength (where 0 is zero stimulation) is shown in *B*.

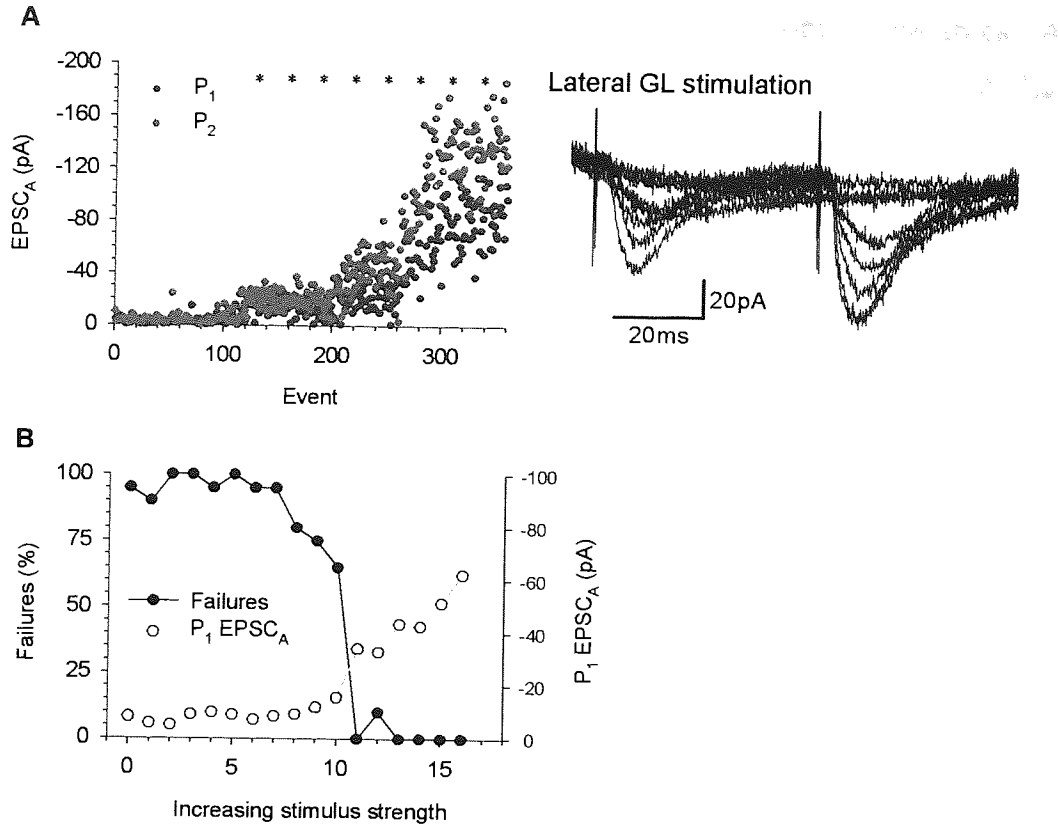

Figure 4.10 Representative example of graded increases in stimulation from sub-threshold values laterally in the GL. Stimulation strength was increased every 20 pulses from zero volts. The $EPSC_A$ responses through the course of stimulation are illustrated in *A*. The asterisks denote the points where the representative traces shown are taken from. The relationship of average $EPSC_A$ and number of failures at each successive stimulation strength (where 0 is zero stimulation) is shown in *B*.

4.3.4 Non-stationary fluctuation analysis of ascending axon and parallel fibre synapses with Purkinje cells

Having found evidence for a difference in probability of release by examination of PPR, a more robust method, variance-mean analysis, was employed to investigate the synaptic characteristics of AA- and PF-pathways. Each of the four different external solutions (see methods) caused PFstimulation to generate EPSCs with differing mean peak amplitudes and variances. Background variance was calculated as the variance of the difference in current amplitude of a 1ms period while the cell was unstimulated from the holding current. After background variance was subtracted, the EPSC variance was then plotted against the mean amplitude

response for each release probability, and fitted with a parabola. A representative example is shown in fig 4.11. The values for Q, P_r and N_{min} from the first pulse in five different cells are shown in table 4.1.

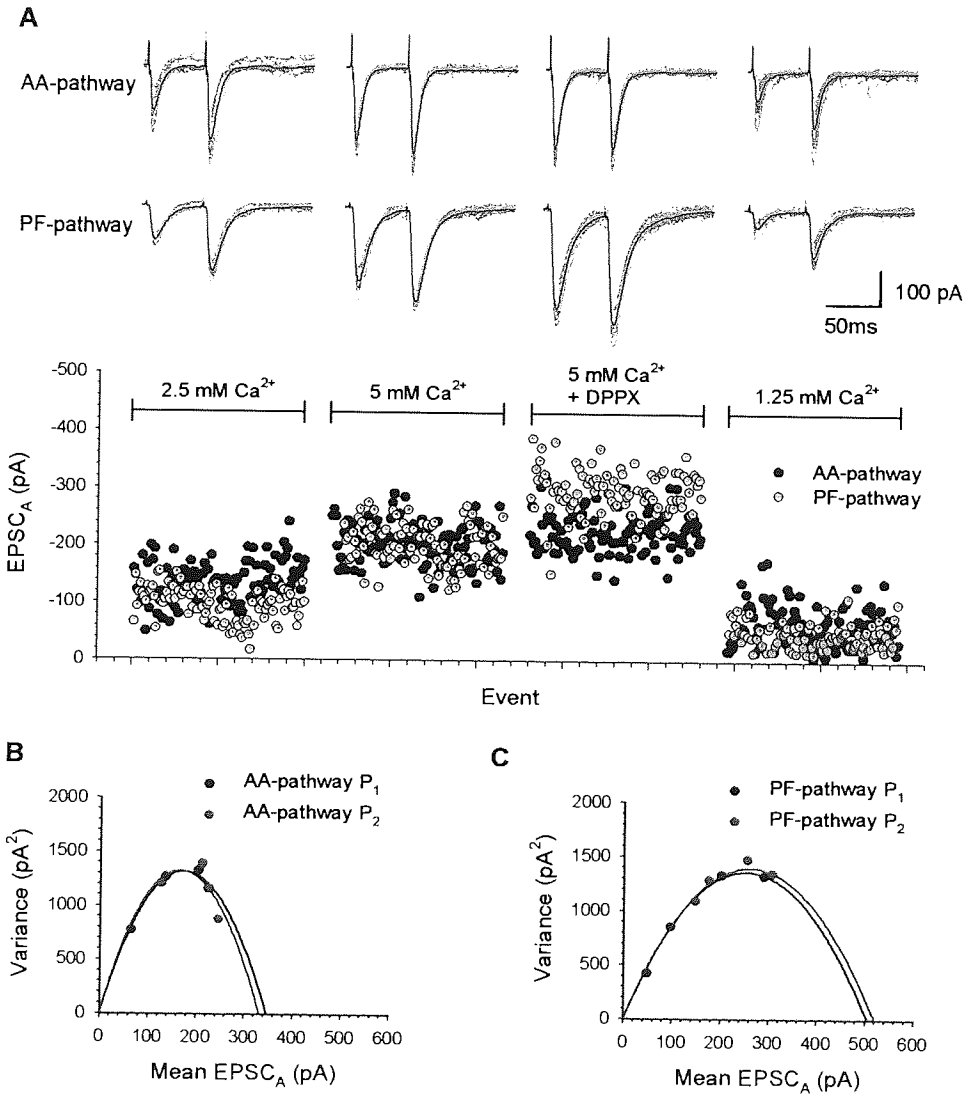

Figure 4.11 Representative example of variance-mean analysis of AA- and PF-pathway P_1 responses at four different release probabilities. The distribution of ~100 P_1 events per release probability, with raw data traces plotted above (the black trace represents the average) in AA- and PF-pathway are shown in *A*; A plotted parabola of P_1 and P_2 results are shown for the AA-pathway (*B*) and the PF-pathway (*C*).

Data from five cells were pooled, by averaging the constants A and B (that define the parabola) for each experiment. These were used to form a parabola for the pooled data (fig. 4.12a). The results revealed a higher

release probability in the AA-pathway compared to the PF-pathway (P_r: AA, 0.39; PF 0.26). This adds weight to the lower PPR in the AA-pathway being the result of a higher release probability. In addition, the initial slopes of the parabolae were different. Values for Q were 10.4pA for the AA pathway and 7.7pA for the PF-pathway. Fewer release sites were required in the AA-pathway to generate a similarly sized response (N_{min}: AA, 31.5; PF, 56.7; Mean $EPSC_A$ at 2.5mM Ca^{2+}: AA, -128.6 ± 9.2pA; PF, -111.5 ± 7.8pA). This data was also analysed using V/M-M plots (Fig. 4.12b). This gathered slightly higher estimates for Q in both pathways (AA, 13.7pA; PF, 9.0pA) and lower estimates for N_{min} (AA, 20.9; PF, 48.3).

Cell	AA-pathway			PF-pathway		
	Q (pA)	P_r	N_{min}	Q (pA)	P_r	N_{min}
1	10.1	0.45	29.4	6.6	0.35	42.3
2	10.2	0.35	34.8	7.4	0.26	55.9
3	6.7	0.29	51.0	4.5	0.23	114.4
4	8.6	0.34	50.4	11.9	0.21	39.1
5	16.4	0.47	17.7	7.9	0.21	80.8

Table 4.1 **V-M analysis of 5 cells.** Data was taken at four different release probabilities, showing quantal amplitude (Q), Probability of release at 2.5mM calcium (P_r) and minimum number of release sites (N_{min}).

The second pulse data was harder to interpret in isolation, as in 3 of 5 cells it was not possible to fit parabolae to the data, as high calcium concentrations sometimes produced a large paired-pulse depression. In those cases where a parabola could be fitted, the points lay closely upon the same curve as formed from the first pulse data (fig. 4.11b). These data are in accordance with the suggestion that PPF at this synapse reflects an increase in the probability of transmitter release, and not an increase in quantal amplitude or number of release sites.

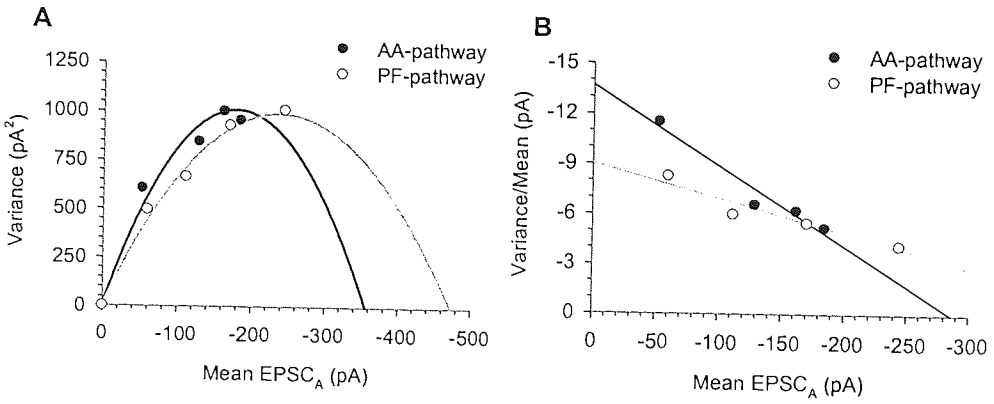

Figure 4.12 Variance-mean analysis of data from 5 pooled cells under four different conditions of release probability. Analysis for P_1 values for AA- and PF-pathways were constructed using: *A*, a V-M plot with fitted parabola; *B*, a V/M-M plot with linear fit.

In the V-M analysis using differing calcium concentrations, increases in the peak amplitude of the second EPSC appeared to be due to an increase in P_r. Therefore it was reasoned that multiple pulses might provide sufficient EPSCs at different release probabilities to construct parabolae. We initially used an interstimulus interval of 50ms and aCSF containing 2.5mM calcium. 3-10 pulses per run were tested. It was observed that these repeated stimulus trains induced a notable potentiation over the course of several minutes, particularly in the PF-pathway (fig. 4.13). Subsequently 0.2μM H-89, a PKA inhibitor, was added to the aCSF to prevent LTP. Furthermore the rate of basic alternate stimulation was slowed to 0.05Hz in order to further reduce the likelihood of LTP generation by trains applied too frequently. 7 pulses were deemed suitable to generate sufficient points to construct a parabola. With 2.5mM external calcium, $EPSC_A$ in the AA-pathway peaked by the second or third pulse and parabolic functions could not be formed. As the release probability for the initial pulse would have been around 0.2-0.4, it was also deemed likely that there was too much of an error to obtain an accurate value for Q by trying to fit a line to the initial slope. Furthermore, later pulses (P_{3-7}) in both pathways showed a decline in $EPSC_A$, which may be attributable to vesicle depletion. The AA-pathway tended to show a much greater decrease in $EPSC_A$ than the PF-pathway. A representative example of this decline in later pulses is shown in fig. 4.14. Therefore later lower external calcium concentration was used to lower the release probability and

hence increase the chances of obtaining sufficient points to calculate Q, P_r and N_{min}.

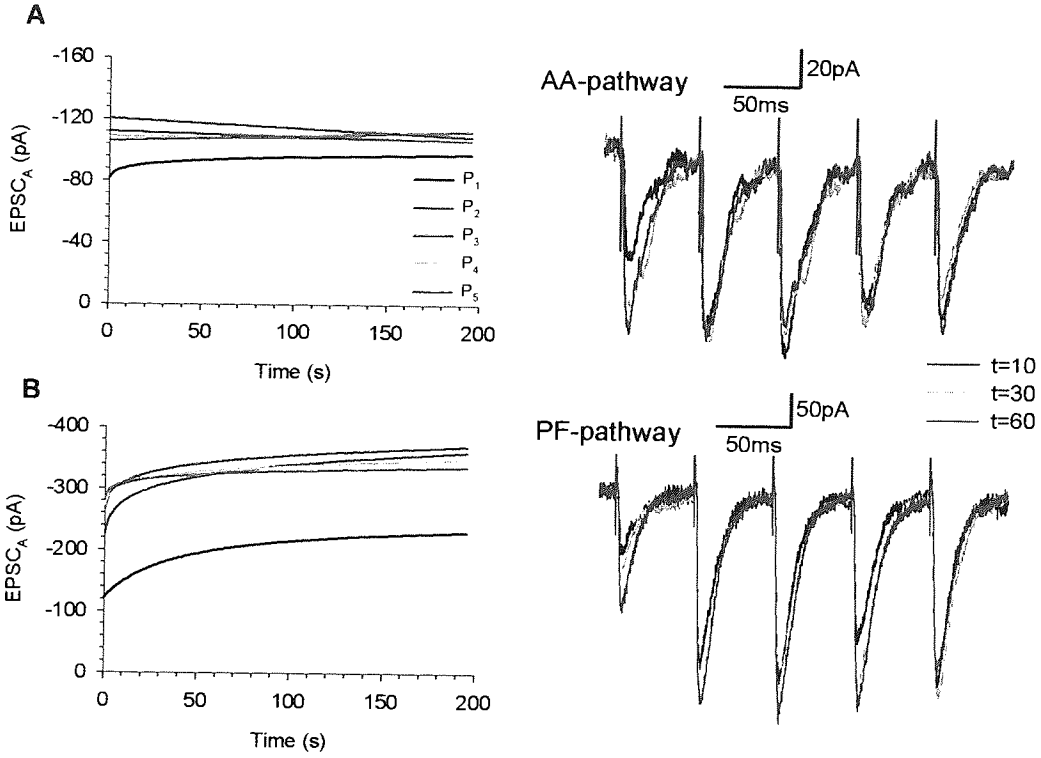

Figure 4.13 Repeated trains of stimuli induce LTP in the absence of H-89. Data from a representative single cell showing the trends in $EPSC_A$ for a 5-pulse train is illustrated for the AA-pathway (*A*) and PF pathway (*B*). To the right are raw data traces of P_1-P_5 taken at 10, 30 and 60 seconds after multiple pulse stimulation was initiated for each pathway. The trends are illustrated rather than individual points because the variation and closeness of the $EPSC_A$s of later pulses makes the individual points difficult to distinguish.

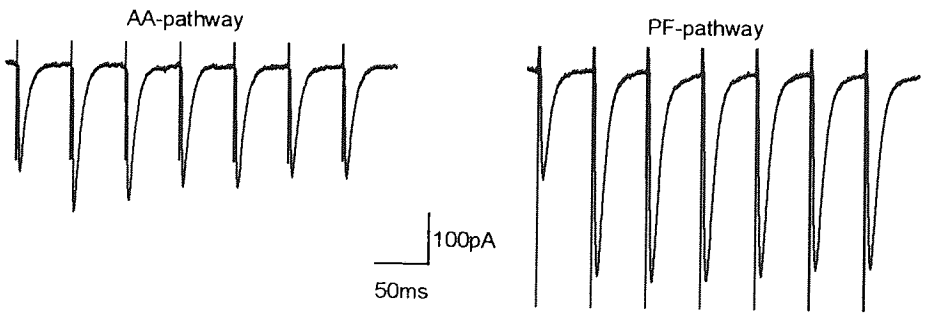

Figure 4.14 $EPSC_A$ declines in later pulses of train stimulation during train stimuli in 2.5mM calcium. This figure shows averaged values of ten sweeps from a single representative cell, illustrating a decline in $EPSC_A$ in the AA-pathway in later pulses, and a small decline in the PF-pathway.

From the V-M analysis conducted with different external calcium concentrations to generate different release probabilities, 1.25mM external

calcium generated low P_r values (AA-pathway, 0.16; PF-pathway 0.13). In order to improve results from V-M analysis of multiple stimuli, aCSF with 1mM calcium concentration was thought likely to produce sufficiently low release probabilities at early pulses, and allow an increase over successive pulses. However, it was still not possible to fit parabolae to the plots in most experiments. Possibly this was due to saturation of the calcium signal before high enough release probability was obtained. Possibly P_r may have continued to rise, but vesicle depletion prevented further facilitation. Therefore, the initial slope of the first 2 data points was used to estimate Q in both pathways (fig. 4.15). These values were approximately 20% lower than the previously generated data in both pathways, although consistent in that the values for the AA-pathway were again greater (AA-pathway, -8.2 ± 1.73pA; PF-pathway -6.3 ± 0.65pA; n=5). It was not possible to fit accurate V/M-M plots to these experiments. The lower values than those from the differing aCSF solutions may be explained by the fact that a linear fit is more likely to underestimate the quantal amplitude than a parabola.

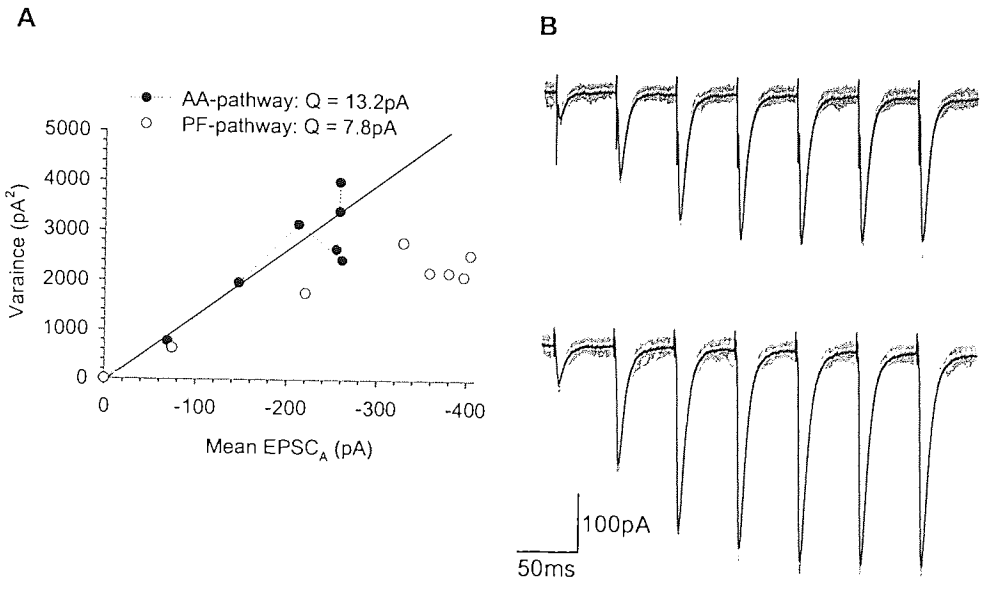

Figure 4.15 Variance-mean analysis of a 7-pulse train in the presence of 1mM calcium and H-89. This figure demonstrates data from a single representative cell. The V-M analysis by linear fit to the first two points is illustrated in *A*. Data traces from the same cell are shown in *B*. 12 individual traces are shown in grey, and the average is the black trace.

4.3.5 Examination of the postsynaptic receptor populations.

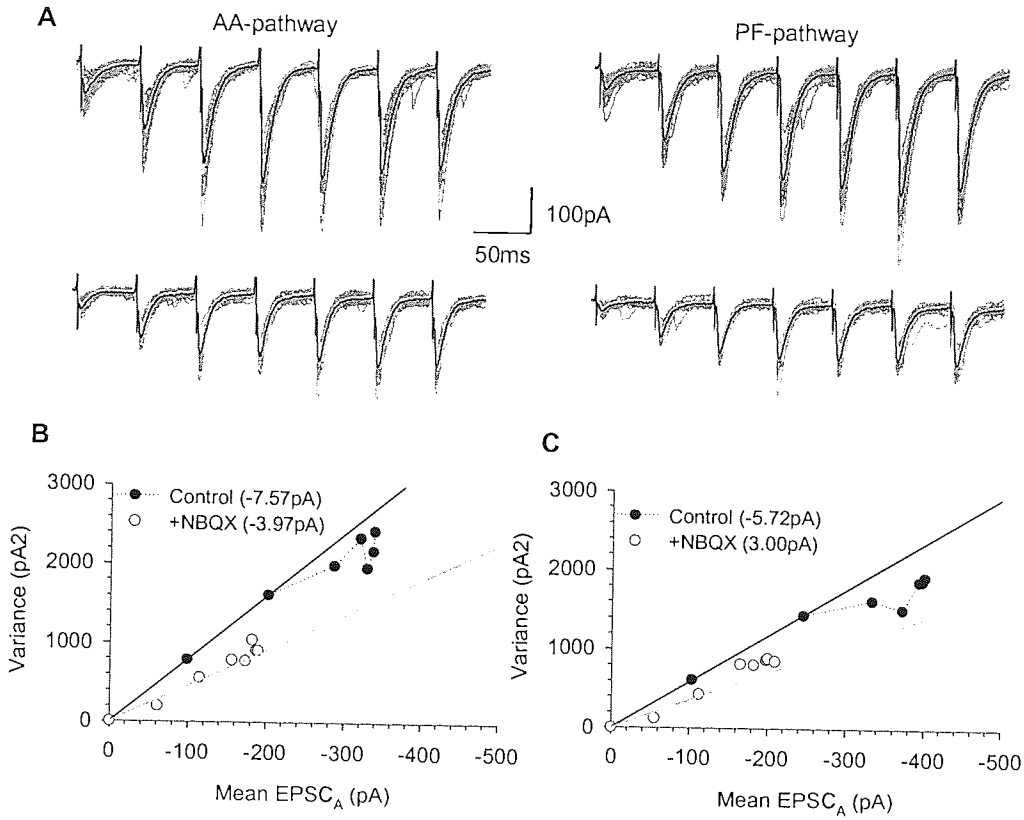

Figure 4.16 Variance-mean analysis of 7-pulse train in the presence and absence of NBQX. This figure shows data from a representative cell from a single cell showing raw data traces for the AA- and PF-pathways in the absence (top) and presence (bottom) of NBQX (*A*). In each diagram, the grey traces represent 12 individual traces, and the black line the average. In *B*, the V-M analysis of the same cell in the absence of NBQX is shown, by fitting a linear plot to the first two points. *C* represents the same, but in the presence of NBQX.

Fast EPSCs at the PF-PC synapse are known to be mediated by AMPARs (Konnerth *et al.*, 1990). Could the difference in quantal amplitude be due to different a different type of receptor at the AA synapses? To examine this, the same protocol (7 pulses, 50ms pulse interval) was applied in 1mM calcium in the absence and presence of 75nM NBQX, a selective AMPA/kainate receptor inhibitor. This concentration was chosen to reduce $EPSC_A$s by approximately 50% of baseline (fig 4.16). The absolute reduction in $EPSC_A$ in the AA-pathway was 44%, and the reduction in Q of 51% (from -8.6 ± 1.7pA to -4.2 ± 1.4pA; n=5). In the PF pathway, $EPSC_A$ was decreased by 50%, and Q decreased by 46% (from -7.4 ± 0.6pA to -3.8 ± 0.7pA, n=5.)

Once again, the greater quantal response at the AA-pathway was maintained. Also, the similar decrease in $EPSC_A$ and Q in the presence of the AMPA inhibitor suggests that the difference in quantal amplitude between the synapse types is unlikely to be the result of different types of postsynaptic receptor. It is possible that the density of AMPARs at each synapse is different.

4.4 Discussion

In this chapter several differences in the characteristics of GC-PC synapses made by AAs and PFs have been described, along with the first detailed examination of the properties of AA synapses. In summary, consistent with previous anatomical findings (Gundappa-Sulur *et al.*, 1999), AA synapses appear to have a 50% greater mean probability of release than PF synapses. Also, postsynaptic responses to a quantal event were on average 30% greater in the AA-pathway than in the PF-pathway. This means that a single AA synapse has approximately twice the synaptic strength of a single PF synapse. This would lend weight to the theory that there is a strong 'vertical' component to GC-PC signalling in the cerebellar cortex, as opposed to lateral projection along PFs. The presence of qualitatively different synaptic contacts formed by the same axon to the same cell type has been previously recognised and this may be an important part of accurate dissemination of information in the central nervous system (Markram *et al.*, 1998). In chapter 6, experiments are presented which suggest that the various forms of plasticity described between GCs and PCs may contribute to these qualitative differences.

4.4.1 Probability of transmitter release at ascending axon – and parallel fibre – Purkinje cell synapses.

The probability of release at synapses varies very widely in published data, although the PF-PC synapse is generally considered a low probability

synapse. A P_r under 0.05 has been claimed for an individual release site (Dittman *et al.*, 2000). On the other hand, although the number of inactive PF-PC connections is reported to be in the order of 85%, those that do exhibit a detectable response in PCs do so with a reliability of 0.9 (Isope & Barbour, 2002). It is important to note that these values are not equivalent; the first represents probability of release at a single site and the second the probability of a single GC will generate a postsynaptic response through the PF segment. These two values could be explained by assuming a single PF forms several release sites, at possibly more than one synapse, with PCs. It is well established anatomically that PFs form one synapse (occasionally two) with PCs (Palay & Chan-Palay, 1974; Pitchitpornchai *et al.*, 1994). 7-8 docked vesicles per synapse are reported at PF-PC synapses, although some of these may not be release-ready (Xu-Friedman *et al.*, 2001). Certainly the number of vesicles that are released at the PF-PC synapse is unclear. Taking this into account, it is still not possible to explain the disparity in these studies. It is worth noting that in Dittman *et al.'s* (2000) study, the rats were 9-14 day-old and 1.5mM extracellular calcium used, and Isope & Barbour (2002) used 2mM calcium and 2-3 month-old rats. Lower calcium concentration decreases release probability, and synapse reliability may increase with development. The finding of P_r = 0.26 in this study would appear to be a credible value, and in accordance with the results of Isope & Barbour (2002). Whilst the mean release probability is low at the release site, where there are many vesicles ready for release, the probability of a single successful synaptic transmission will be considerably higher. Fig. 4.17 illustrates the probability of at least one vesicle being released and the average strength for a PF synapse over a number of release sites, assuming P_r = 0.26 and Q = 7.7pA for all release sites. To achieve a 90% probability that at least one vesicle would be released would require the presence of 7-8 release sites. There is a strong relationship between PPR and estimated release probability observed in this chapter and the studies of Dittman *et al.* (2000) and Isope & Barbour (2002): where PPR is higher, estimated release probability is lower. Differences in PPR and release probability between the studies may be the result of experimental conditions.

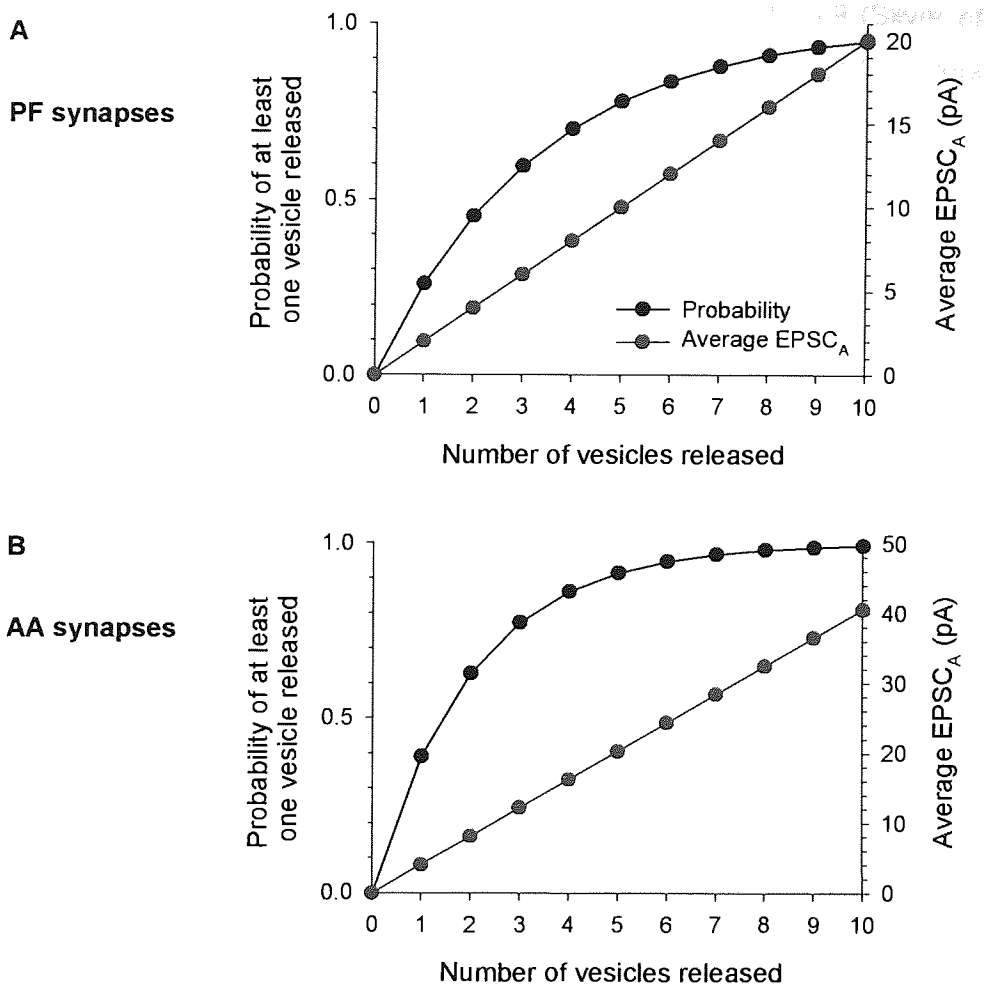

Figure 4.17 Simple model of AA and PF synapse characteristics. This figure shows the probability of at least one vesicle being released and the average postsynaptic response ($EPSC_A$), depending on the number of release sites, when a PF (*A*) or AA (*B*) synapse is activated. It assumes uniform Q and P_r (PF: 7.7pA and 0.26 respectively; AA: 10.4pA and 0.39 respectively; as derived from this chapter) and a single quantum released at each release site.

In the AA segment, the estimated 50% higher probability of release than PFs may be due to a number of factors. PPF was primarily observed at low probability synapses whereas PPD is usually observed at synapses with high probability such as the CF (Thomson, 2000). It has been theorised that release probability is connected with the number of docked vesicles (Bower & Haberly, 1986; Harris & Sultan, 1995; Murthy *et al.*, 1997; Schikorski & Stevens, 1997; Schikorski & Stevens, 2001). However while CF-PC synapses have very similar presynaptic characteristics to PF-PC synapses (Xu-Friedman *et al.*, 2001) from an anatomical perspective, the probability of

release at a CF release site actually is much higher, up to 0.9 (Silver *et al.*, 1998). Therefore anatomical features alone may not be enough to accurately predict the release behaviour of a synapse. Xu-Friedman *et al.* (2001) suggest reasons such as differences in the state of presynaptic phosphorylation (Sudhof, 1995), calcium influx and buffering, or vesicle release machinery may influence release probability. Similar, as yet unidentified factors may be responsible for the disparity observed between AA- and PF-PC synapses.

4.4.2 Quantal amplitude at ascending axon- and parallel fibre-Purkinje cell synapses.

Our values for PF quantal amplitude are comparable with published data on the PF-PC synapse. A mean average (± standard deviation) of 8.4 ± 7.1pA has been found for PF-PC connections, with distribution skewed to higher values (Isope & Barbour, 2002). This is very similar to the value for Q found in this study. Referring again to fig. 4.17 this may indicate around 4-5 vesicle docking sites per PF-PC connection are release-ready. A high degree of variability of quantal amplitudes may occur, due to the variability of postsynaptic AMPAR density (Tempia *et al.*, 1996; Hausser & Roth, 1997). Considering the variation observed in Isope & Barbour's study (2002), we must be cautious about drawing such a direct relationship between the value for the PF-PC connection they report, and the value of Q found here.

Increasing stimulation intensity from threshold levels within the GL near the PC soma, as opposed to laterally distant in the ML or GL, generated stepwise increases in $EPSC_A$ of up to 82.0pA, with a mean value of 44.3pA. This is similar to values of 50-60pA found by stimulation of individual GCs (Barbour, 1993; Isope & Barbour, 2002). The former study did not record the location of the GCs stimulated, although the latter study found EPSC amplitudes of that magnitude only from GCs near to the PC soma. These proximal GCs had negligible rates of failure in generating a postsynaptic response, and other proximal cells that generated lesser amplitude EPSCs

had a much higher connection rate with the PC compared to distant GCs. Fig. 4.17 illustrates the probability of a postsynaptic response being recorded and average postsynaptic response for an AA synapses depending on the number of release sites. Assuming that AA synapses have a similar number of docked vesicles (8-10) as PF- and CF-PC synapses, of which some would not be release-ready (Xu-Friedman *et al.*, 2001), single GC-PF connections of over 40pA could only be explained by multi-synaptic connections.

Q varied by experiment and analysis method from around 8.2 – 13.7pA for AA synapses, and 6.3 – 9.0pA for PF synapses. The average Q at AA synapses was consistently greater than PF synapses, and in all but one analysis by approximately 30%. Whether the greater Q at AA synapses is due to a greater amount of glutamate in presynaptic vesicles or to a greater density of postsynaptic receptors is unclear from this study. Dendritic filtering may cause an underestimation of Q, but synaptic location has been reckoned to lead to little decrease in EPSP amplitudes in PCs (Roth & Hausser, 2001). Further to this, as AAs are thought to be located on more distal spiny branchlets (Gundappa-Sulur *et al.*, 1999), we might expect this to lead to a greater underestimate of AA quantal amplitude than PF quantal amplitude. Another possible influencing factor could be glutamate spillover to distant synapses (Barbour, 2001; Barbour & Hausser, 1997; DiGregorio *et al.*, 2002), although this is an unstudied characteristic at GC-PC synapses. The effect of spillover may be a negligible proportion of the EPSC (Barbour, 2001). If this is the case it could not account for the size of differences in Q or PPR. A narrow beam of parallel fibres might be expected to cause a greater localised glutamate concentration than a limited number of ascending axons whose synapses are spread throughout the dendritic tree. If this were the case, it would be likely to cause a greater Q in PF synapses, so could not explain AA synapses having higher Q. At CF-PC synapses, the high probability of release means a large concentration of glutamate is released into the synaptic cleft. This not only makes spillover more likely, but also limits paired-pulse depression, as the glutamate cannot be cleared from the synapses quickly enough (Harrison & Jahr, 2003). As both PF and AA release sites have a markedly lower probability of release than CFs, we

might expect that fewer vesicles, and therefore lesser quantities of glutamate, will be released into the synaptic cleft. Consequently, glutamate will be less likely to excite distant receptors, or remain in the synaptic cleft in large quantities on the second pulse. The decay times of the AA- and PF-pathway were similar, as were the decay times of P_2 pulses in relation to P_1 in both pathways, which suggests there is no significant difference in spillover under these conditions of activation.

4.4.3 Number of release sites at ascending axon- and parallel fibre-Purkinje cell synapses.

The minimum number of release sites is difficult to interpret, as it will partly dependent on the number of fibres recruited, in either pathway. The number of synapses activated has not been evaluated here, thus it is not possible to confirm the average number of release sites at the synapse. It is still debated as to precisely what a 'release site' (N) represents in fluctuation analysis. It is reported to represent variously the number of vesicle docking sites, the number of vesicles ready to be released at docking sites, or the number of active zones of docked vesicles (Oleskevich *et al.*, 2000; Redman, 1990; Korn *et al.*, 1982). With the former two, presynaptic vesicle depletion may be considered a decrease in N_{min}, and with the latter, a decrease in P_r.

4.4.4 The kinetics of ascending axon pathway and parallel fibre pathway stimulation

The difference in rise time kinetics is intriguing as the postsynaptic receptor type is presumed to be identical. It is feasible that this may be due to dendritic filtering effects (Roth & Hausser, 2001). As the AA mostly forms synapses in the deepest third of the ML, this may be the reason they have faster rise times, although faster decay times would also be expected. Another possibility is that PFs are reported to have conduction velocities that are faster the deeper (i.e. closer to the PC layer) they are in the ML (Vranesic

et al., 1994). ML stimulation could result in activation of fibres with very different conduction velocities, which could mean reduced synchronicity in the PF-pathway, and therefore a greater spread of time over which synapses are activated. While this could be more evident in the brief rise time (1-2ms), the difference may be less noticeable in the relatively long (ca. 8ms) decay time.

4.4.5 Other considerations for variance-mean analysis

There are a number of other factors that may affect our V-M analysis. Q and P_r as determined by VM-analysis are weighted means, and favour higher values for both from the population (Clements & Silver, 2000). Other issues to contend with may be variation due to non-synaptic causes. When an afferent fibre is stimulated, failure to record a postsynaptic effect has been attributed to four likely causes: *i*, fluctuation of axon thresholds; *ii*, failure of conduction of action potential; *iii*, unreliability due to temperatures below those *in vivo*; *iv*, failure of vesicle release at the synapse (Allen & Stevens, 1994). Although working on Schaffer collaterals to CA1 in the hippocampus, unreliability through reasons *i-iii* is reported to be minimal (Allen & Stevens, 1994). In the past it has been believed that only one vesicle is released at a single release site, but more recently evidence has arisen for multi-vesicular release which may increase the level of variation (Conti & Lisman, 2003). Also, V-M analysis is based upon the assumption of a linear relationship between quanta released and the postsynaptic response. This may not be the case as the more vesicles that are released at the synapse, and the nearer the postsynaptic receptors get to saturation. The likely result of this may be an underestimate of quantal amplitude. Additionally, there are newly discovered forms of synaptic release, termed 'kiss and run' and 'kiss and stay', where there is partial fusing and release of transmitter (Gandhi & Stevens, 2003; Aravanis *et al.*, 2003). This can cause only partial transmitter release, and thus would create a degree of non-quantal release. However, there is no evidence to assume this should affect AA- or PF- synapses more. The risk of vesicle depletion may distort the data by a reduction in N_{min} or

maybe P_r. It is possible that the large reduction in the second pulse in some experiments with high extracellular calcium could be the result of an inability to replace vesicles after the multiple release in the presynaptic termini during P_1.

One explanation as to why it was not possible to fit parabolae to V-M data using seven pulses may be vesicle depletion. This would also explain the difficulty in achieving linear V/M-M graphs. The greater level of depletion in the AA-pathway is very interesting. Possibly, it may be evidence that due to increased release probability more vesicles are released per action potential and the calcium-dependent recovery of vesicle readiness (Dittman *et al.*, 2000) is not sufficient over this time period to replace them. No decrease in $EPSC_A$ in later pulses was observed in low calcium (fig. 4.12), although increased release probability in later pulses may mask depletion. The same calcium transient that causes facilitation at the PF synapses also causes a phenomenon known as 'delayed release', albeit by a different mechanism (Atluri & Regehr, 1998). There is a period where the quantal release rate is enhanced that lasts for hundreds of milliseconds; as this is greatly magnified by successive pulses, this may add to the increased $EPSC_A$ in later pulses. The interplay of facilitation and calcium-dependent recovery of the response at PF-PC synapses has been demonstrated to be maximal at 20Hz stimulation, which equates to a 50ms pulse interval (Dittman *et al.*, 2000). However, AA synapses may not be able to operate so efficiently at such high frequencies.

Chapter 5

Plasticity at synapses formed between the ascending and parallel fibre segments with the Purkinje cell.

Several characterised forms of synaptic plasticity have been identified at the PF-PC synapse, including LTP and LTD. In the previous chapter it was shown that synapses made by the AA segment with the PC have a greater probability of release and quantal amplitude than those made by the PF segment. In this chapter, the possibility that these differences underlie a differential susceptibility of AAs to forms of plasticity, or that plasticity may provide the means whereby these differences arise, is addressed. The various protocols known to produce LTP or LTD were applied to each pathway in turn and the degree of susceptibility and cross-talk between pathways is assessed.

5.1 Introduction

5.1.1 Long-term depression at granule cell – Purkinje cell synapses.

The mechanisms that underlie cerebellar LTD are discussed fully in chapters 1 and 3. Depression is the result of a downregulation of AMPARs at the PF synapses. Desensitisation of AMPARs has been suggested (Hemart *et al.*, 1994), although this is disputed (Linden, 2001). More likely is declustering (Matsuda *et al.*, 2000; Hirai, 2001) and internalisation (Wang & Linden, 2000) at the synapse. Anatomical evidence indicates that AAs form synapses on more distal regions of the PC dendrites (Gundappa-Sulur *et al.*, 1999). The CF however innervates the soma and proximal dendrites of the PC (Palay & Chan-Palay, 1974). This means it is possible that the calcium influx evoked by CF stimulation may not reach some or all of the AA synapses. Therefore AA synapses could have a diminished capability to undergo LTD with conjunctive stimulation of the CF, compared to PFs. There is greater mean quantal amplitude at AA-PC synapses compared to PF-PC synapses. If LTD

is expressed as a downregulation or declustering of AMPARs, and if LTD is less likely at AA synapses, this could account for the difference in Q.

5.1.2 Long-term potentiation in granule cell – Purkinje cell synapses.

Cerebellar LTP is fully detailed in chapter 3. LTP is best observed in the presence of high concentrations of calcium chelators that block LTD (Shibuki & Okada, 1992; Salin *et al.*, 1996; Lev-Ram *et al.*, 2002). Two forms of LTP at PF-PC synapses are thought to exist. RFS of PFs for 15s at 4-16Hz causes a presynaptically located LTP in PFs, dependent on the AC-cAMP-PKA pathway (Salin *et al.*, 1996; Jacoby *et al.*, 2001; Lev-Ram *et al.*, 2002). While it is also reported as being dependent on NO (Jacoby *et al.*, 2001), this is disputed (Lev-Ram *et al.*, 2002). This form of LTP has been found to spread to distant PFs via a NO-dependent process (Jacoby *et al.*, 2001; chapter 3). Presynaptic LTP at PF-PC synapses is characterised by a concurrent decrease in PPR, thought to represent an increase in the probability of transmitter release. Work from chapter 4 found that AA synapse release sites have a greater P_r than PF synapse release sites. Experiments in chapter 4 also revealed that potentiation were observed in both AA and PF synapses when a brief train of high frequency stimuli was applied (fig. 4.13). This potentiation was blocked by the presence of the PKA inhibitor H-89, which has previously been demonstrated to block LTP (Salin *et al.*, 1996; Jacoby *et al.*, 2001). The potentiation was more marked at PF synapses. This led to speculation that PF-PC synapses undergo LTP either more readily or to a greater extent than AA-PC synapses. It may be possible that AAs are already in a state of presynaptic potentiation.

The second form of LTP is thought to be postsynaptic and NO-dependent, and can be generated in PF-PC synapses by 300 stimuli delivered at 1Hz (Lev-Ram *et al.*, 2002). In that study the authors suggested that this form of potentiation may be a means of restoring AMPARs to the membrane, and thus capable of reversing LTD. AA synapses have greater quantal amplitude than PF synapses (chapter 4). Therefore, it can be postulated that AA

synapses may be similar to PF synapses, but already in a state of postsynaptic potentiation and so less likely to undergo further LTP.

During their work on the anatomy of GC-PC synapses, Gundappa-Sulur *et al.* (1999) found that PF synapses have various correlations between pre- and postsynaptic anatomy that are absent in AA synapses. Following their assumption that AA synapses are formed on areas of PC dendrites not affected by the calcium influx from the CF, they suggest that this may be due to there being no LTD expression at the synapse, as it is suggested that LTD may involve molecular interaction of the pre- and postsynaptic termini. If LTP were also to similarly modify both the pre- and postsynaptic environments, this lack of correlation at AA synapses may suggest they are not susceptible to LTP either.

5.1.3 Aims and objectives

Anatomical studies have found distinct differences in synaptic morphology between AA and PF synapses that suggested there might be a greater probability of transmitter release at AA synapses (Gundappa-Sulur et *al.*, 1999). In chapter 4, this was confirmed by electrophysiological means, together with the observation that there is also greater mean quantal amplitude at AA synapses than PF synapses. Further to this, the studies of Gundappa-Sulur *et al.* (1999) also revealed AA synapses are formed on the distal, spiny branchlets of PC dendrites, which the calcium influx from the CF might not reach. This would mean they may not undergo LTD from conjunctive activation of CFs and PFs. Secondly, they also showed that that there was a lack of correlation between presynaptic and postsynaptic morphology at AA synapses that was evident at PF synapses, which they suggested may indicate a reduced susceptibility to synaptic plasticity. In light of the findings in chapter 4 of different probability of transmitter release and quantal amplitude at AA and PF synapses, it was theorised that synaptic plasticity may cause these synaptic differences. Consequently, in this chapter protocols that induced synaptic plasticity were applied to both AA-

and PF-pathways to discern any possible differences. The forms of synaptic plasticity examined were conjunctive LTD, pairing CF and PFs, presynaptic LTD, and postsynaptic LTD.

5.2 Methods

The methods used in this chapter are detailed more fully in chapter 2. Briefly, experiments in this chapter were conducted on cerebellar slices from 14-21 day old, male, Wistar rats in accordance with previous work (Jacoby *et al.*, 2001; chapters 3 & 4). Slices were cut in a coronal orientation to facilitate selective activation of AA and PF synapses, and perfused with standard aCSF with 20μm picrotoxin. When stated, 10μM forskolin was added to the aCSF.

Cells were held in voltage clamp configuration at –70mV. 10mM BAPTA was present in the recording pipette when postsynaptic calcium-dependent processes were to be inhibited. For studies of LTD, which require increases in postsynaptic calcium, 0.5mM BAPTA was present in the recording pipette. Stimulating electrodes were positioned in the ML and GL to preferentially activate PFs and AAs respectively, as per chapter 4. Baseline stimulation was a 100ms, 4mV hyperpolarizing command pulse to monitor cell conditions, followed 50ms later by paired pulses (stimulus width 100μs, 50ms interstimulus interval) to one pathway. Pathways were stimulated by this protocol alternately at 0.2Hz. When postsynaptic LTP was examined, baseline stimulation was applied to each pathway alternately at 0.1Hz, to help avoid possible run-up of response (Lev-Ram *et al.*, 2002). Six individual sweeps were averaged for each data point, and data were normalised to baseline values. R_m, R_s and I_h were monitored throughout experiments, and fluctuations in R_s adjusted for manually. Experiments in which R_m or I_h either dropped below 40MΩ or -1000pA respectively, or changed considerably (>10%) and abruptly, were discounted, as the cell was considered unhealthy.

At least 10 minutes stable baseline was collected before any of these protocols were initiated. Each pathway was termed 'AA-pathway' and 'PF-pathway' to denote the synapses that were preferentially activated. The protocol to generate presynaptic LTP was a 15s, 16Hz RFS to one (AA- or PF-) pathway while the other was not stimulated, then baseline stimulation was resumed in both pathways. The protocol to generate postsynaptic LTP was 300 pulses at 1Hz stimulation applied to one pathway (Lev-Ram *et al.*, 2002). The protocol to generate conjunctive LTD was carried out in current-clamp mode so voltage-dependent calcium influx was not hindered. Current was supplied to the PC to keep the unstimulated PC membrane potential at -70 ± 3mV. Stimulation of the PC in current-clamp mode was as follows. Initially, a 100ms, -100pA hyperpolarizing command pulse was applied to ensure that the amplifier was correctly balanced and to assess the health of the cell and the recording conditions. After 40ms, five pulses were applied at 100Hz to one GC pathway, followed by stimulation of the climbing fibre 100ms later (fig 2.6). The other pathway was not stimulated during this period. Data for $EPSC_A$ and PPR are expressed as a percentage of the baseline period. The paired-pulse ratio was calculated as mean P_2 / mean P_1 for each data point.

Coefficient of variation (CV) analysis is a form of fluctuation analysis, and is carried out in accordance with Bekkers & Stevens (1990). It was used to analyse data to assess changes in synaptic characteristics where it was not practical to create multiple release probability conditions. Quantal theory suggests that changes in release probability and number of release sites is a presynaptic, and changes in Q are postsynaptic. Fluctuation analysis assumes that postsynaptic changes in response will not affect CV, whereas presynaptic changes do. Hence CV is related to the probability of transmitter release and number of release sites such that (Korn & Faber, 1991):

$$CV^2 = (1 - P_r) / (N \,.\, P_r)$$

The CV of EPSCs is calculated as:

$$CV^2 = (\text{Standard deviation} / \text{mean})^2$$

For this form of CV analysis, for each experiment a minimum of 20 P_1 responses were taken at halfway through the baseline period and 20 or 30 minutes after and protocols had been initiated. These were then normalised to baseline values. For each group of points, normalised CV^{-2} was plotted against normalised mean $EPSC_A$ (fig. 5.1; adapted from Bekkers & Stevens 1990). Where responses at 20 or 30 minutes moved left or right parallel with the x-axis compared to baseline values indicates a change in Q. If they moved along a diagonal with a gradient of 1, it indicates a change in N. Deviation from these may indicate changes in P_r, whose relationship with CV^{-2} is less clear.

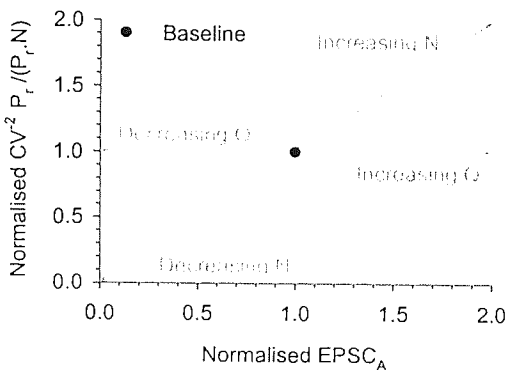

Figure 5.1 **CV-based quantal analysis.** This graph demonstrates the principles behind CV analysis. Individual EPSCs are selected from the baseline and after plasticity is induced. Mean $EPSC_A$ and CV^{-2} are normalised against baseline levels for both sets of data and plotted. If the plotted points vary along the directions illustrated, they represent changes in Q or N.

5.3 Results

Initially control data was acquired with 10mM BAPTA in the recording pipette (termed hereafter as 'constant 0.2Hz stimulation'). The AA- and PF-pathways were stimulated alternately at 0.2Hz for over 40 minutes after a 10-minute stable baseline was established. In these experiments 20 minutes after

baseline, the $EPSC_A$ of the AA-pathway was 102.8 ± 7.7%, and of the PF-pathway 97.4 ± 6.4%. 20 minutes after baseline, PPR was 101.5 ± 5.6% in the AA-pathway, and 102.1 ± 3.4% in the PF-pathway, (n=6; fig. 5.2). 30 minutes after baseline, $EPSC_A$ was 97.0 ± 6.6% in the AA-pathway, and 93.8 ± 4.5% in the PF-pathway, whilst PPR was 105.5 ± 6.6% in the AA-pathway, and 106.6 ± 4.5% PF-pathway.

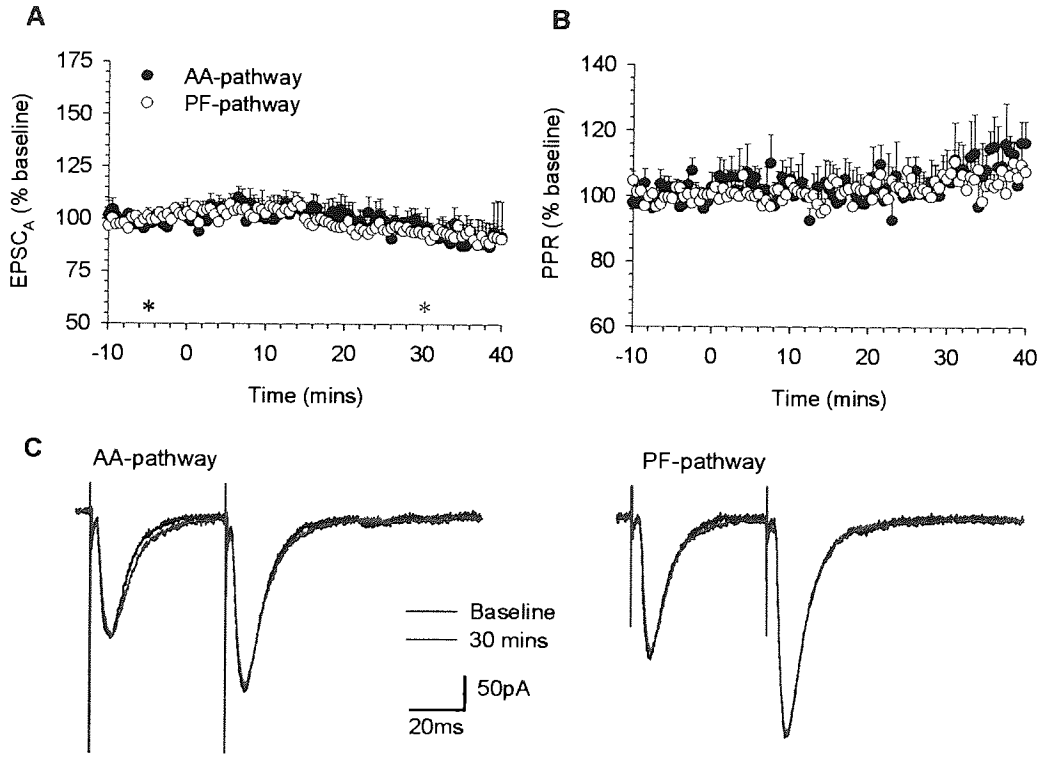

Figure 5.2 The effects of 0.2Hz alternate stimulation of AA- and PF-pathways with 10mM $BAPTA_i$. Two stimulating electrodes were placed in the molecular layer, and both pathways were stimulated alternately at 0.2 Hz. The mean values for $EPSC_A$ (*A*) and PPR (*B*) from 6 cells are illustrated. Representative traces of EPSCs at baseline and 30 minutes in the AA- and PF- pathways are shown in *C*. The traces are averages of 6 sweeps comprising the single time point, and asterisks denote the time points where the traces were sampled.

5.3.1 Comparing conjunctive long-term depression at ascending axon and parallel fibre pathways

The long-term response of both pathways, in turn, to repetitive stimulation associated with the CF was examined with 0.5mM BAPTA in the recording pipette. This was done to see whether, as postulated, the AA synapses were

partially or wholly immune to conjunctive LTD. First we applied the LTD induction protocol to the PF-pathway (fig. 5.3). There was an immediate decrease in $EPSC_A$ that continued to decline over the course of the experiment in the PF-pathway. 30 minutes after baseline, $EPSC_A$ was significantly lower in the PF-pathway (72.1 ± 4.5%) compared to constant 0.2Hz stimulation at a similar time, whereas PPR remained similar (106.7 ± 3.5%; Mann-Whitney U test, $p<0.05$, n = 8 test vs. 6 control). The AA-pathway, however, was similar to constant 0.2Hz stimulation in terms of both $EPSC_A$ (100.3 ± 10.7%) and PPR (102.6 ± 4.6%) assessed 30 minutes after baseline. The two pathways were significantly different from each other (Wilcoxon signed-rank test, n=8). This significant decrease in $EPSC_A$ shows that conjunctive PF and CF stimulation evokes LTD. Depression however did not spread to the AA-pathway, which may indicate that that synapse is not susceptible to LTD.

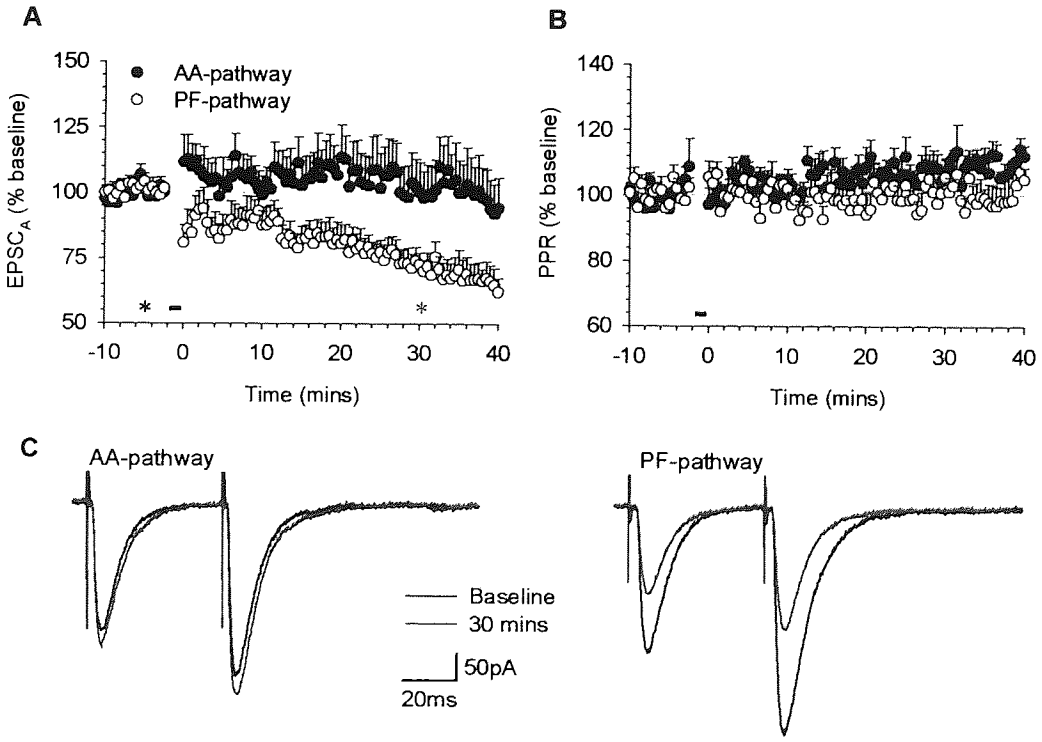

Figure 5.3 The effect of conjunctive stimulation of the CF and PF-pathway. All experiments were performed with 0.5mM $BAPTA_i$. The figure shows the mean values for EPSC (*A*) and PPR (*B*) in eight cells. The black bar represents the period of LTD induction. Representative traces of EPSCs at baseline and 30 minutes in the AA- and PF- pathways are shown in *C*. The traces are averages of 6 sweeps comprising the single time point, and asterisks denote the time points where the traces were sampled.

To ensure that the depression was not caused by the higher frequency stimulation of PFs alone during LTD induction, the LTD protocol was applied to the PF-pathway as normal, but with no stimulation of the CF (fig. 5.4). In five cells after 30 minutes, $EPSC_A$ and PPR were not significantly different from constant 0.2Hz stimulation in the PF-pathway ($EPSC_A$, 113.7 ± 8.1%; PPR, 105.9 ± 6.1%) or AA-pathway ($EPSC_A$, 92.0 ± 4.7%; PPR, 103.7 ± 5.5%; Mann-Whitney U test, $p<0.05$, n = 5 test vs. 6 control). PF-pathway $EPSC_A$ was significantly greater than that measured with conjunctive stimulation of the CF (Mann-Whitney U-test, $p<0.05$, n = 5 –CF vs. 8 +CF). Hence depression due to increased PF stimulation alone can be discounted, and in fact this pattern of PF stimulation may cause a small potentiation.

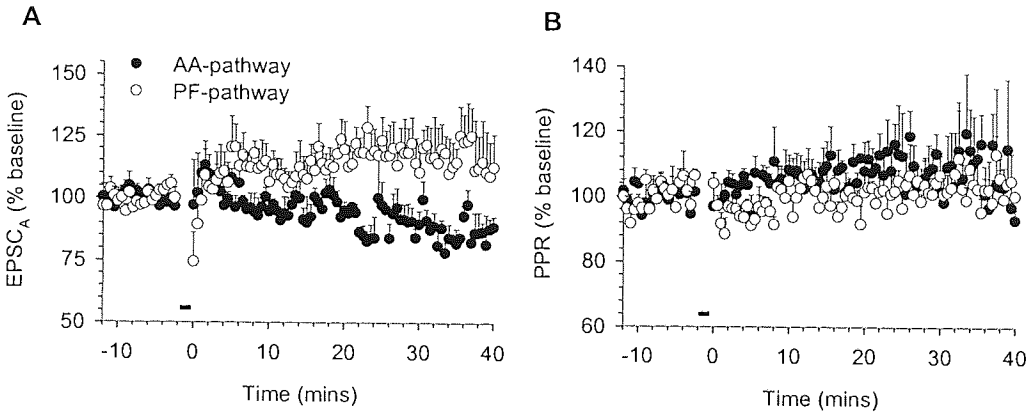

Figure 5.4 LTD-induction protocol applied to the PF-pathway without conjunctive CF stimulation. All experiments were performed with 0.5mM $BAPTA_i$. The figure shows the mean values for EPSC (*A*) and PPR (*B*) in five cells. The black bar represents the period of LTD induction.

Next, the AA-pathway instead of the PF-pathway was conjunctively stimulated with the CF (fig. 5.5). 30 minutes after the LTD induction protocol, the AA-pathway did not display a significantly altered $EPSC_A$ (90.0 ± 4.3%) or PPR (107.3 ± 3.1%) when compared to constant 0.2Hz stimulation at a similar time (Mann-Whitney U-test, n = 7 test vs. 6 control). The PF-pathway showed a small decline in $EPSC_A$ that was not significant (85.3 ± 14.6%), and PPR remained unchanged (104.6 ± 6.2%). Both pathways were not significantly different when compared to each other (Wilcoxon signed-rank test, n=7). These data reveal that AA synapses do not undergo the characteristic LTD that can be observed at PF synapses when conjunctively

stimulated with the CF (fig. 5.6). However, the slight overall decline in the PF-pathway might indicate that some depression occurred at that distant pathway.

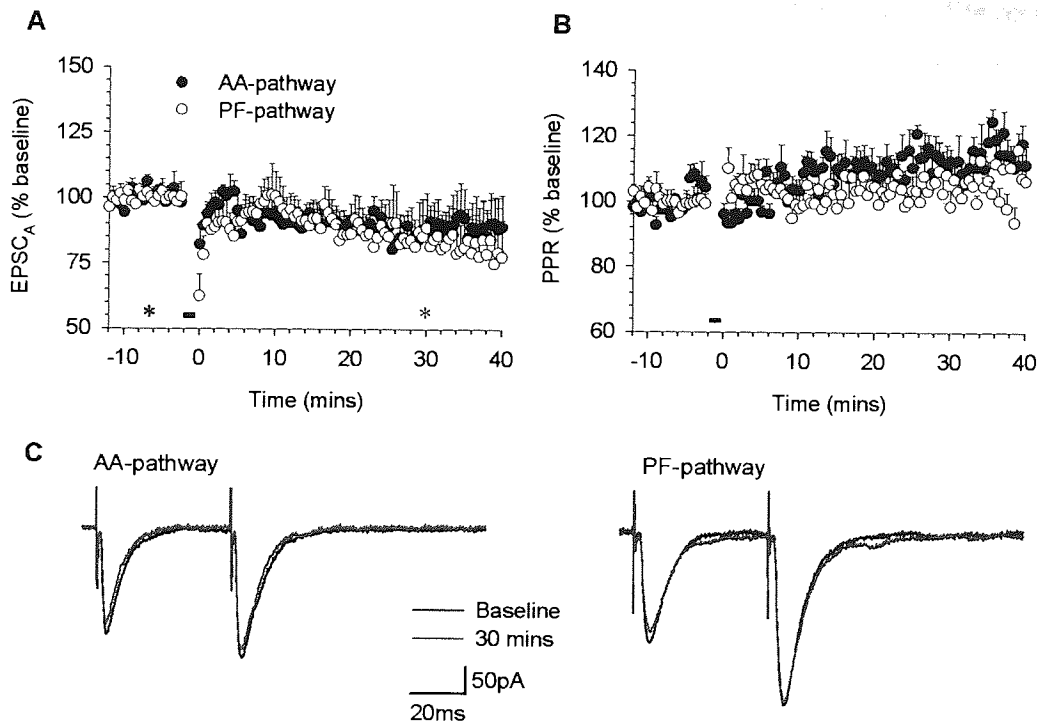

Figure 5.5 The effect of conjunctive stimulation of the CF and AA-pathway. All experiments were performed with 0.5mM BAPTA$_i$. The figure shows the mean values for EPSC (*A*) and PPR (*B*) in seven cells. The black bar represents the period of LTD induction protocol. The EPSCs in both pathways at baseline and after 30 minutes are illustrated in *C*. The traces are averages of 6 sweeps comprising the single time point, and asterisks denote the time points where the traces were sampled.

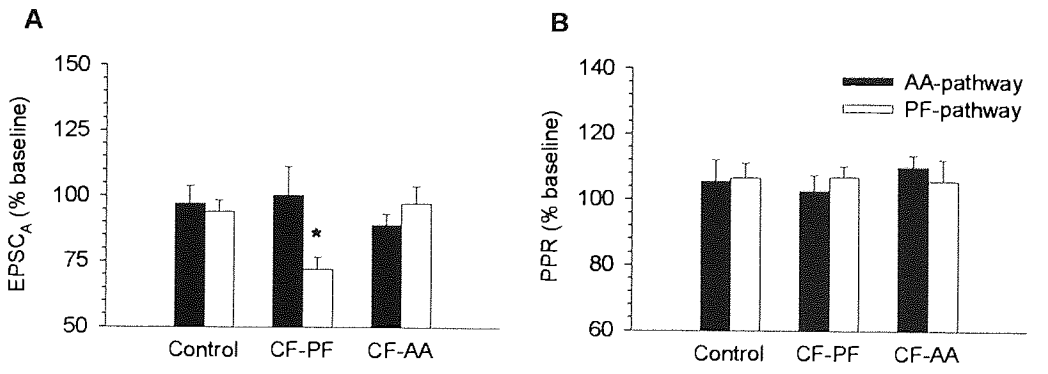

Figure 5.6 Conjunctive stimulation of CF and GC inputs only causes depression at PF synapses. All points were taken 30 minutes after baseline, and compared to the constant 0.2Hz stimulation (n=6). The EPSC$_A$ (*A*) and PPR (*B*) of the AA- (n=7) and PF- (n=8) pathways are illustrated when the conjunctive LTD protocol was applied to each. Asterisks represent significance (Mann-Whitney U-test, $p<0.05$.)

LTD is thought to result in a decrease in the sensitivity of postsynaptic AMPARs, which should be manifest as a decrease in Q. It was not possible to use a V-M or V/M-M analysis to accurately measure Q using only a single extracellular calcium concentration of 2.5mM (see chapter 4.3.4.) Consequently an analysis based on CV was used (Bekkers & Stevens, 1990). At least 20 individual P_1 values were taken around 5 minutes before, and 30 minutes after the LTD-induction protocol, and both $EPSC_A$ and CV^{-2} were normalised to the baseline values for each experiment. In constant 0.2Hz stimulation experiments, while $EPSC_A$ remained unchanged, normalised CV^{-2} values actually decreased by about 15% in both pathways, 30 minutes after baseline (AA-pathway, 0.87 ± 0.02; PF-pathway, 0.85 ± 0.04; fig. 5.7a).

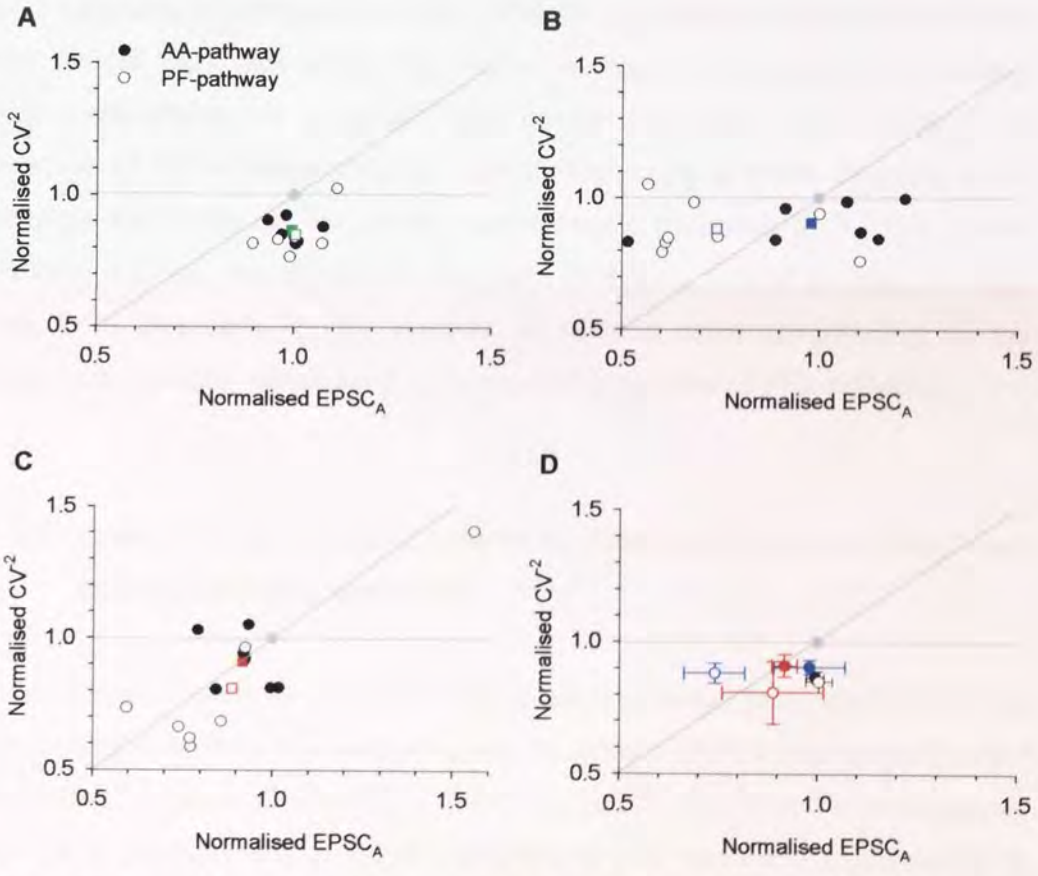

Figure 5.7 CV analysis of experiments with LTD induction protocol. Normalised CV^{-2} was plotted against normalised $EPSC_A$ at baseline and 30 minutes later, with values normalised to baseline values (grey circles). These were plotted for each individual experiment in the constant 0.2Hz stimulation (*n*=6; *A*), with conjunctive CF-PF activation (*n*=8; *B*), and conjunctive CF-AA activation (*n*=7; *C*). In each graph, filled symbols represent AA-pathway, and open symbols PF-pathway, the differently coloured square dots represent average values. The average values (± s.e.m.) for controls (black circles), CF-PF activation (blue circles) and CF-AA activation (red circles) are illustrated in *D*.

When the PF-pathway was conjunctively activated with the CF, after 30 minutes normalised CV^{-2} values had declined by similar amounts below baseline levels as compared to the constant 0.2Hz stimulation experiments (AA-pathway, 0.90 ± 0.03; PF-pathway, 0.88 ± 0.04), although $EPSC_A$ was notably lower in the PF-pathway values. When compared to constant 0.2Hz stimulation experiments at 30 minutes, the PF-pathway demonstrated a leftward shift along the x-axis consistent with a decrease in Q (fig. 5.7b). When the AA-pathway was conjunctively activated with the CF, after 30 minutes normalised CV^{-2} declined similarly to the constant 0.2Hz stimulation experiments in the AA-pathway (0.91 ± 0.04). In the PF-pathway normalised CV^{-2} had declined slightly more (0.81 ± 0.12; fig. 5.7c) and was accompanied by a decrease in normalised $EPSC_A$. The AA-pathway average at 30 minutes had shifted very little along the x-axis or diagonal compared to constant 0.2Hz stimulation at a similar time period (fig. 5.7d). The PF-pathway average at 30 minutes however had shifted along a more diagonal trend towards the origin on the graph, suggesting a decrease in N. This would indicate that the non-significant decrease in $EPSC_A$ in that pathway is likely due to a decrease in the number of release sites contributing to the response, possibly because of a decrease the number of PFs activated.

5.3.2 Comparing presynaptic long-term potentiation at ascending axon and parallel fibre pathways

To investigate whether AA- and PF-pathways undergo presynaptic LTP, the 16Hz RFS paradigm was used (chapter 3). 10mM BAPTA was present in the recording pipette to prevent concurrent expression of LTD in the postsynaptic cell. It is possible that the low reliability of LTP induction experienced in chapter 3 may have been due to the size of baseline $EPSC_A$s generated. These may have been sufficiently great to facilitate calcium entry into the PC that the local BAPTA concentration may not have effectively chelated. Consequently, initial baseline $EPSC_A$s were kept lower than in chapter 3, at under 200pA. LTP generation was observed to be much more reliable. When 16Hz RFS was applied to the PF-pathway, LTP was generated in 6 out of 8

cells, in contrast to 6 out 17 in chapter 3. 20 minutes after RFS $EPSC_A$ in the PF-pathway had increased (135.7 ± 12.1%) with a concurrent decrease in PPR (93.3 ± 5.2%; fig. 5.8). $EPSC_A$ had increased slightly from baseline in the AA-pathway (115.0 ± 13.1%), although there was little change in PPR (101.8 ± 6.3%) 20 minutes after RFS. According to the Mann-Whitney U-test, only the $EPSC_A$ in the PF-pathway was significantly different from constant 0.2Hz stimulation at a similar time ($p<0.05$, n = 6 test vs. 6 control). Neither $ESPC_A$ nor PPR in the AA-pathway were significantly different from constant 0.2Hz stimulation at a similar time point. However, neither $EPSC_A$ nor PPR was significantly different between the two pathways (Wilcoxon signed-rank test, $p<0.05$, n=6). This might be evidence of a limited spread of potentiation to the AA-pathway from the PF-pathway.

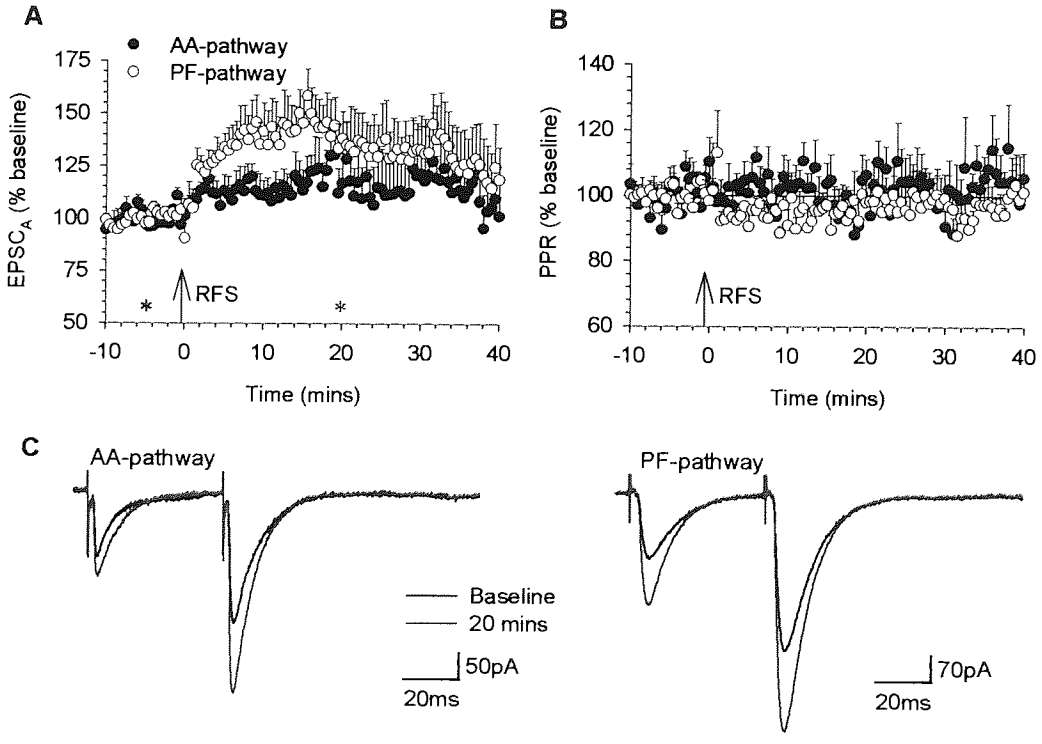

Figure 5.8 15s 16Hz RFS applied to the PF-pathway with 10mM $BAPTA_i$. The figure shows the mean values for EPSC (*A*) and PPR (*B*) in six cells. The EPSCs in both pathways at baseline and after 20 minutes are illustrated in *C*. The traces are averages of 6 sweeps comprising the single time point, and asterisks denote the time points where the traces were sampled.

15s 16Hz RFS was then applied to the AA-pathway in 6 cells (fig. 5.9). After 20 minutes, there was little sign of potentiation in the AA-pathway ($EPSC_A$,

104.1 ± 8.5%; PPR, 98.4.0 ± 3.1%) or PF-pathway ($EPSC_A$, 96.9 ± 6.0%; PPR, 103.3 ± 5.3%). Neither pathway was significantly different from constant 0.2Hz stimulation data (Mann-Whitney U-test, n = 6 test vs. 6 control), and neither $EPSC_A$ nor PPR were significantly different between pathways (Wilcoxon signed rank test, n=6.) This indicates that presynaptic LTP was not elicited by 16Hz RFS in the AA-pathway, nor was enough mediator produced that could evoke potentiation in the distant the PF-pathway.

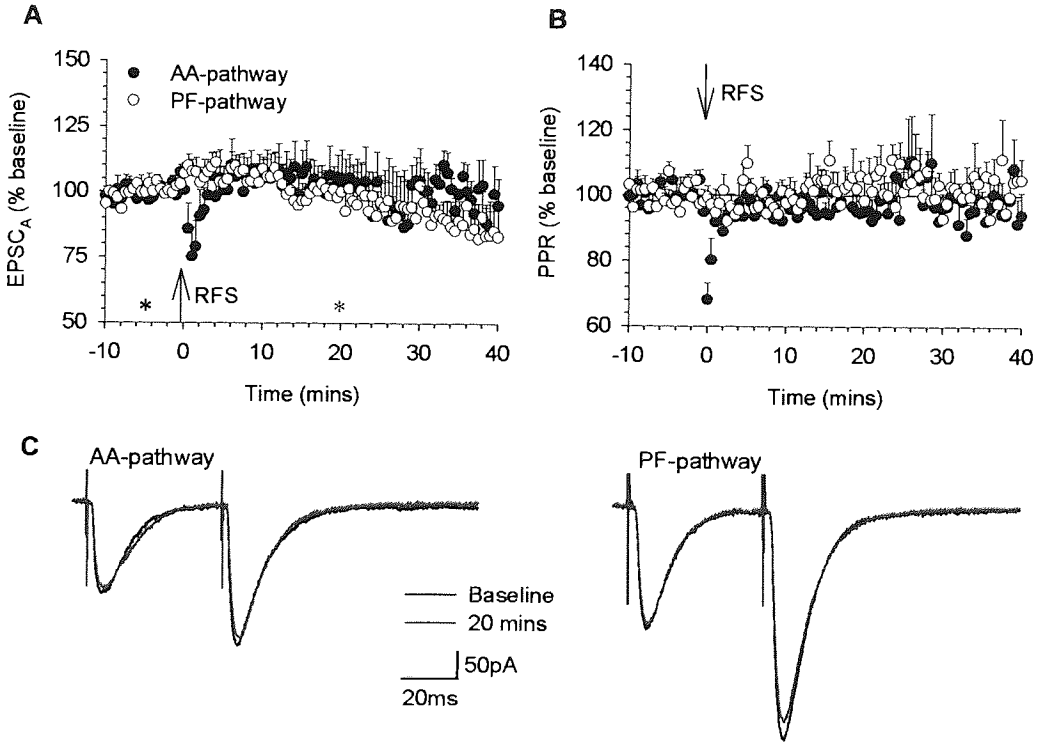

Figure 5.9 15s 16Hz RFS applied to the AA-pathway with 10mM $BAPTA_i$. The figure shows the mean values for EPSC (*A*) and PPR (*B*) in seven cells. The EPSCs in both pathways at baseline and after 20 minutes are illustrated in *C*. The traces are averages of 6 sweeps comprising the single time point, and asterisks denote the time points where the traces were sampled.

These experiments were also subjected to CV analysis. 20 minutes after baseline, the normalised CV^{-2} values of constant 0.2Hz stimulation experiments were about 90% of baseline values in both pathways (AA-pathway, 0.91 ± 0.06; PF-pathway, 0.91 ± 0.04; fig. 5.10a). 20 minutes after 16Hz RFS was applied to the PF-pathway, both pathways had potentiated, the PF-pathway to a greater degree than the AA-pathway. In the PF-pathway, the average normalised CV^{-2} value was greater than that of

constant 0.2Hz stimulation (1.16 ± 0.12). When compared to constant 0.2Hz experiments, the mean point for PF-pathway stimulation had moved more along the diagonal away from the origin. This indicates that the potentiation was likely due to an increase in N or P_r than Q in the PF-pathway. After 16Hz RFS to the PF-pathway, the mean normalised CV^{-2} value was similar to that of constant 0.2Hz stimulation in the AA-pathway at a similar time (0.94 ± 0.04; fig 5.10b). When compared to constant 0.2Hz experiments, the mean point for PF-pathway stimulation had moved more along the x-axis away from the origin, indicating a likely increase in Q in the AA-pathway.

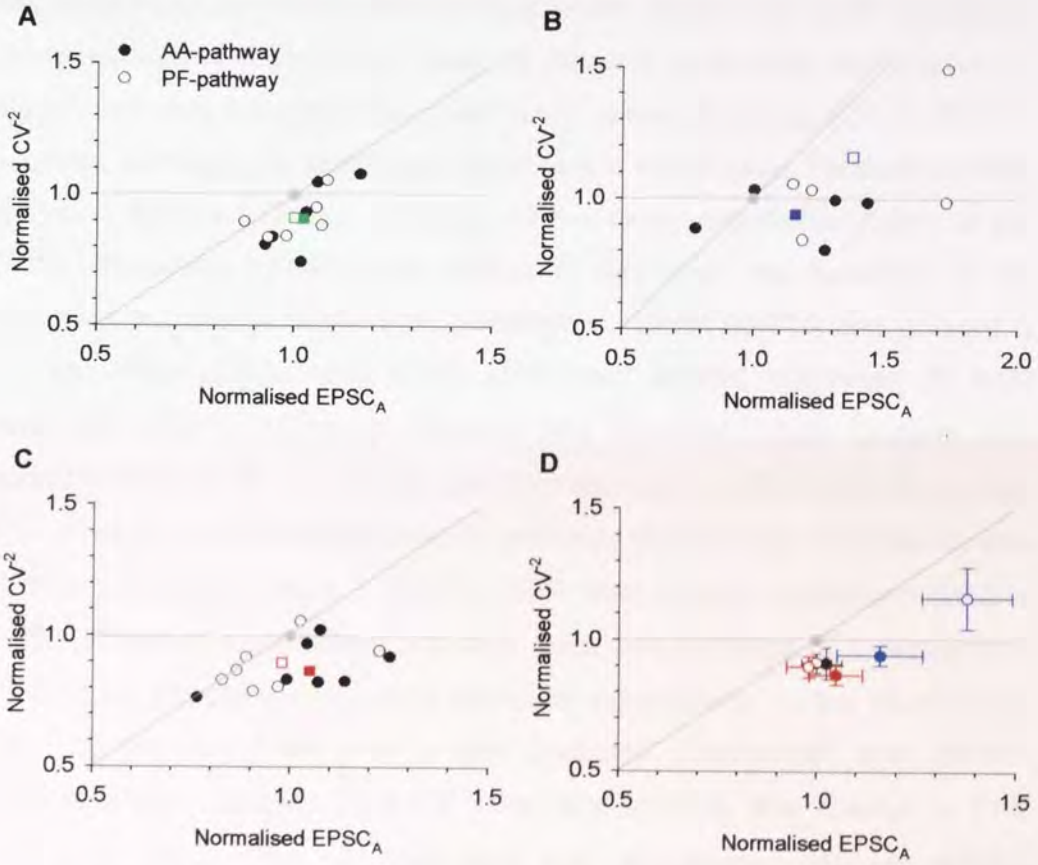

Figure 5.10 CV analysis of experiments with 15s 16Hz RFS. Normalised CV^{-2} was plotted against normalised $EPSC_A$ at baseline and 20 minutes later, with values normalised to baseline values (grey circles). These were plotted for each individual experiment in the constant 0.2Hz stimulation (n=6; *A*), with 16Hz RFS to the PF-pathway (n=6; *B*), and 16Hz RFS to the AA-pathway (n=7; *C*). In each graph, filled symbols represent AA-pathway, and open symbols PF-pathway, the differently coloured square dots represent average values. The average values (± s.e.m.) for constant 0.2Hz stimulation (black circles), 16Hz RFS to the PF-pathway (blue circles) and 16Hz RFS to the AA-pathway (red circles) are illustrated in *D*.

When 16Hz RFS was applied to the AA-pathway, neither pathway had potentiated. After 20 minutes mean normalised CV^{-2} values were 85-90% of

baseline values in both pathways (AA-pathway, 0.86 ± 0.04; PF-pathway, 0.90 ± 0.04; fig. 5.10c) and thus similar to constant 0.2Hz stimulation at a similar time in both normalised CV^{-2} and $EPSC_A$. The increase in the AA-pathway however appears to have been more due to an increase in Q. Neither $EPSC_A$ nor normalised CV^{-2} was much different from control experiments when 16Hz was applied to the AA-pathway (fig. 5.10d).

The previous experiments with 15s 16Hz RFS demonstrated that potentiation may exist at AA synapses, although to a lesser degree than at PF synapses. There was some potentiation observed not only when RFS was applied to the AA-pathway, but also when potentiation spread following RFS at the PF-pathway, although not statistically significant in either case. Forskolin, a PKA activator, mimics LTP and occludes RFS-evoked potentiation (Salin *et al.*, 1996). Therefore forskolin was added to determine the capability of AA synapses to undergo presynaptic potentiation. 10mM BAPTA was present in the recording pipette, and 0.2Hz stimulation applied alternately to both pathways. After a 10-minute baseline was acquired, 10μM forskolin was added to the bath for 10 minutes, and then washed out (fig. 5.11). 20 minutes after forskolin was first applied the PF-pathway was strongly potentiated, with $EPSC_A$ increased (156.4 ± 25.3%). PPR was largely unchanged (99.5 ± 4.9%) across all experiments, although there was evidence of a decrease in PPR of the PF-pathway in some individual experiments. In the AA-pathway after 20 minutes there was a less profound potentiation, with $EPSC_A$ increased from baseline (118.3 ± 9.6%) and similarly little change in PPR (100.1 ± 4.2%). The two pathways had significantly different $EPSC_A$ (Wilcoxon signed-rank test, $p< 0.05$, $n=7$). The $EPSC_A$ was significantly greater in both the AA-pathway ($p<0.05$) and PF-pathway ($p<0.01$) than control data, whereas PPR was not significantly different (Mann-Whitney U test, n = 7 test vs. 6 control). The potentiation observed in both pathways from forskolin was however only a short-term potentiation. From all cells, the mean $EPSC_A$ of the AA-pathway had returned to baseline levels by 30 minutes, and the PF-pathway had declined from peak to only about 20% above baseline at 40 minutes.

These experiments would suggest that AA synapses have the capacity to undergo LTP, although whether that potentiation is pre- or postsynaptic is unclear. Forskolin has previous been shown to decrease PPR when applied to cerebellar slices (Salin *et al.*, 1996), and in that study and others (Jacoby *et al.*, 2001; Lev-Ram *et al.*, 2002) the potentiation was also long-term. In 5 out of 7 cells, $EPSC_A$ was greater at 20 minutes after forskolin application than during the baseline in the AA-pathway. This compares with a greater $EPSC_A$ in the PF-pathway 20 minutes after forskolin application, than during baseline in all 7 cells. Further to this, normalised $EPSC_A$ at 20 minutes after forskolin application was smaller in the AA-pathway than the PF-pathway in all seven cells. This would suggest that AA synapses have not only a more limited ability to undergo PKA-dependent potentiation, but also that some synapses will not undergo this form of potentiation. The results for 16Hz RFS and forskolin are summarised in fig. 5.12.

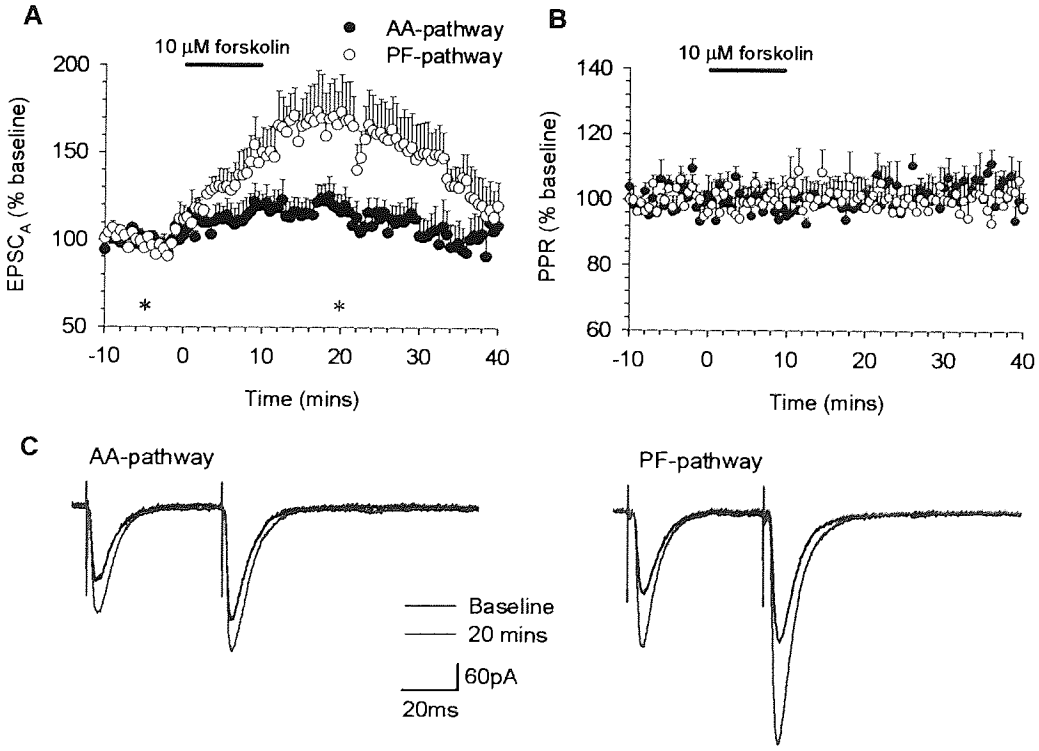

Figure 5.11 The effect of forskolin application on the AA- and PF-pathways. All experiments were performed with 10mM $BAPTA_i$. The figure shows the mean values for EPSC (*A*) and PPR (*B*) in seven cells. The black bar represents the period of forskolin application. The EPSCs in both pathways at baseline and after 20 minutes are illustrated in *C*. The traces are averages of 6 sweeps comprising the single time point, and asterisks denote the time points where the traces were sampled.

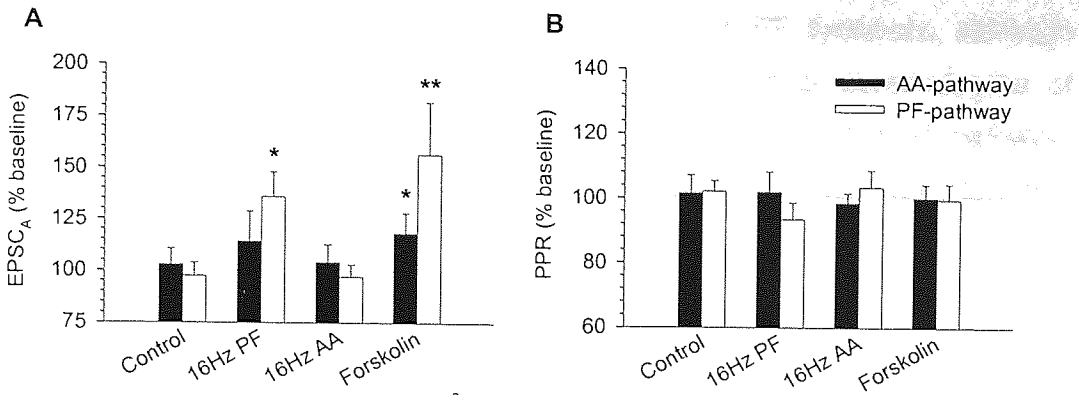

Figure 5.12 Presynaptic LTP is limited in the AA-pathway compared to the PF-pathway. All points were taken 20 minutes after baseline, and analysed in comparison to constant 0.2Hz stimulation as the control (n=6). The $EPSC_A$ (*A*) and PPR (*B*) of the AA- and PF- pathways are illustrated for 16Hz RFS to the PF-pathway (n=6) and AA-pathway (n=7), and for forskolin application (n=7). Asterisks represent significance, Mann-Whitney U-test, * $p<0.05$, ** $p<0.01$.

5.3.3 Comparing postsynaptic long-term potentiation in ascending axon and parallel fibre pathways.

It has been suggested that postsynaptic LTP may be the means for LTD to be reversed, as presynaptic LTP is unlikely to restore AMPARs to the postsynaptic cell membrane (Lev-Ram *et al.*, 2002). If this is true, postsynaptic LTP may not occur at AA synapses as they do not undergo conjunctive LTD. The effects of this newly discovered form of LTP were tested in both pathways, again with 10mM BAPTA in the recording pipette. A 5-minute, 1Hz stimulation of one pathway was applied after 10 minutes stable baseline had been obtained. When the 1Hz RFS was applied to the PF-pathway, potentiation was observed in the PF-pathway in 6 cells out of 7. This is similar to the 80% likelihood of LTP reported previously (Lev-Ram *et al.*, 2002). In the six cells where the PF-pathway potentiated (fig. 5.13), after 20 minutes $EPSC_A$s were significantly higher than control (constant 0.2Hz stimulation) values in the PF-pathway (136.5 ± 7.4%) but not in the AA-pathway (103.1 ± 12.9%; Mann-Whitney U-test, $p<0.05$, n = 6 test vs. 6 control). While PPR in the PF-pathway was transiently lower after the 1Hz stimulation, this gradually returned to baseline within 10 minutes. 20 minutes

after 1Hz RFS, PPR was similar to control data in both the PF-pathway (100.2 ± 1.8%) and AA-pathway (108.5 ± 5.3%). Therefore it can be concluded that 1Hz RFS can cause potentiation in PF synapses, although considering the brief decrease in PPR it may suggest some degree of presynaptic involvement. The plasticity did not spread to the AA-pathway, thus we may assume that postsynaptic potentiation is either synapse specific, or the AA synapses are not susceptible to it.

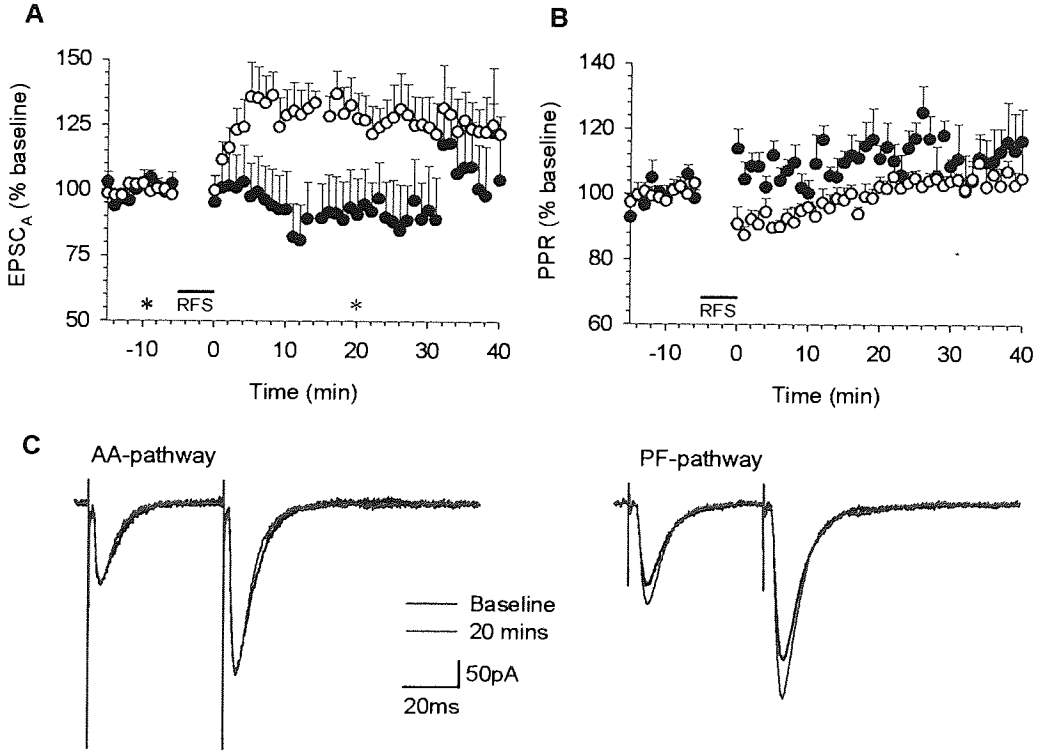

Figure 5.13 1Hz 300-pulse RFS applied to the PF-pathway with 10mM BAPTA$_i$. The figure shows the mean values for EPSC (*A*) and PPR (*B*) in seven cells. The EPSCs in both pathways at baseline and after 20 minutes are illustrated in *C*. The traces are averages of 6 sweeps comprising the single time point, and asterisks denote the time points where the traces were sampled.

Next the 1Hz RFS was applied to the AA-pathway (fig. 5.14). The AA-pathway showed no potentiation, with neither EPSC$_A$ (96.7 ± 9.6%) nor PPR (109.7 ± 4.0%) significantly different from control data after 20 minutes. The PF-pathway however was markedly lower than the baseline period in 5 out of 7 cells, with a decreased EPSC$_A$ apparent immediately after RFS. Some recovery towards baseline EPSC$_A$ values was observed in these 5 cells. At 20 minutes after RFS, neither EPSC$_A$ (79.3 ± 9.8%) nor PPR (111.5 ± 7.4%)

was significantly different from control data (Mann-Whitney U test, n = 7 test vs. 6 control). Thus it can be concluded that the AA-pathway will not undergo postsynaptic LTP, whereas the PF-pathway can (fig. 5.15).

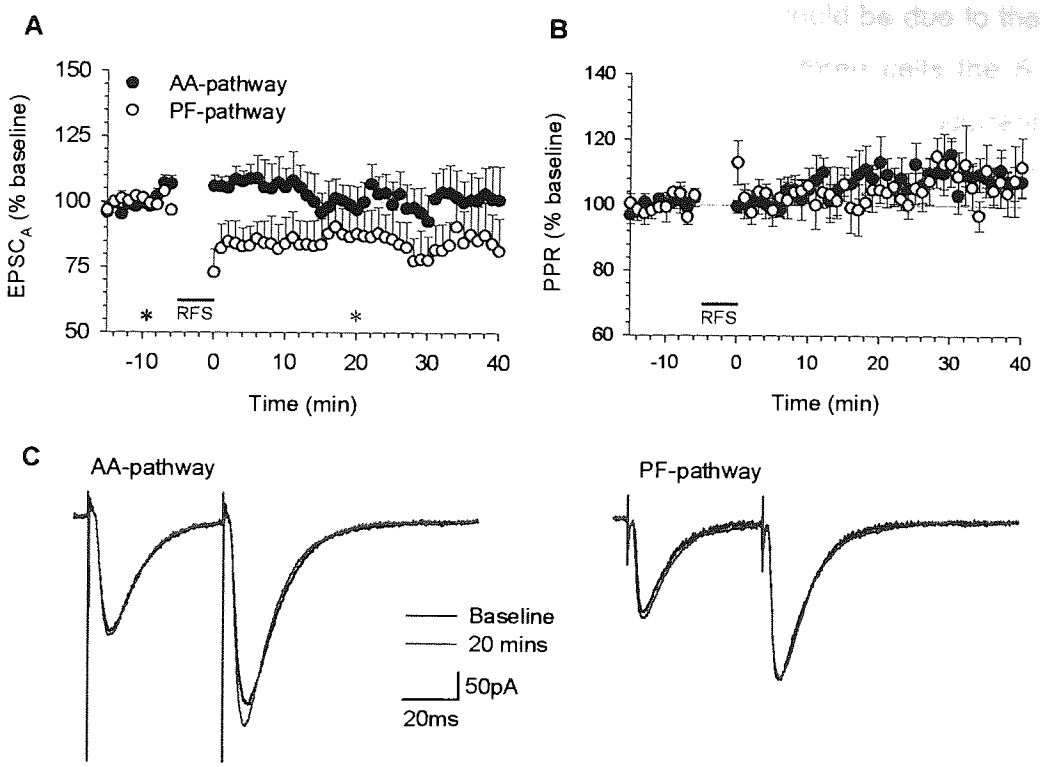

Figure 5.14 1Hz 300-pulse RFS applied to the AA-pathway with 10mM BAPTA$_i$. The figure shows the mean values for EPSC (*A*) and PPR (*B*) in seven cells. The EPSCs in both pathways at baseline and after 20 minutes are illustrated in *C*. The traces are averages of 6 sweeps comprising the single time point, and asterisks denote the time points where the traces were sampled.

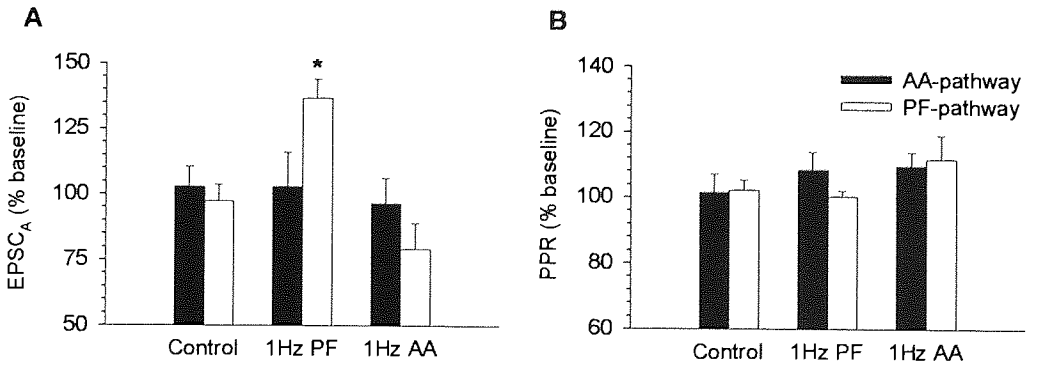

Figure 5.15 Postsynaptic LTP only occurs in the PF-pathway. All points were taken 20 minutes after baseline, and analysed in comparison to constant 0.2Hz stimulation as the control (n=6). The EPSC$_A$ (*A*) and PPR (*B*) of the AA- and PF- pathways are illustrated for 1Hz RFS to the PF-pathway (n=7) and AA-pathway (n=7). Asterisks represent significance, Mann-Whitney U-test, * $p<0.05$.

What caused the decrease in $EPSC_A$ in the PF pathway when the AA-pathway received the 1Hz RFS? It was either due to the 1Hz RFS in the AA-pathway inducing a form of LTD to the PF-pathway, or it could be due to the inactivity of the PF-pathway for 5 minutes. Therefore in three cells the 5-minute 1Hz RFS to the AA-pathway was accompanied by concurrent stimulation of the PF-pathway at the baseline rate of 0.1Hz (fig. 5.16). As before, the AA-pathway did not undergo potentiation but remained steady 20 minutes after RFS ($EPSC_A$, 103.4 ± 28.4%; PPR, 106.9 ± 4.8%). There was, however, no evidence of a decrease in $EPSC_A$ in the PF-pathway either immediately or after 20 minutes (EPSC amplitude, 104.2 ± 9.3%; PPR, 102.7 ± 11.8%.) in any of the three cells. Hence the cessation of 0.1Hz stimulation for the 5-minute period was likely to be responsible for the decrease in $EPSC_A$ in the PF-pathway in the previous data.

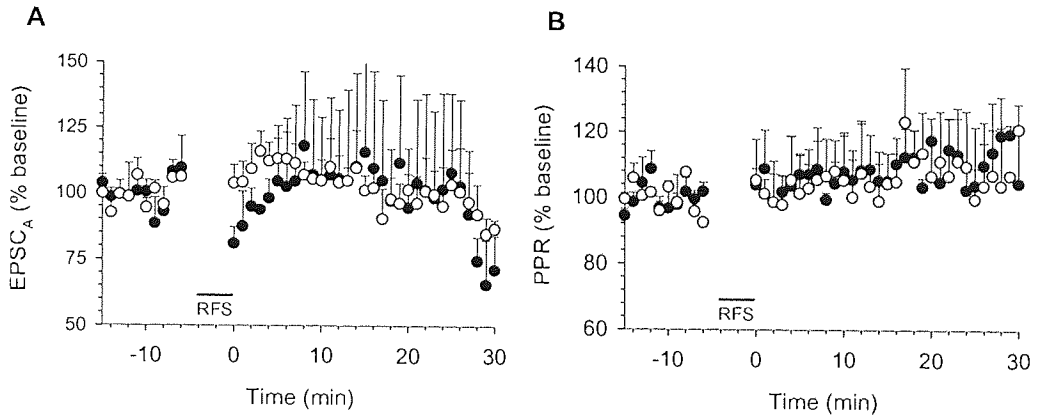

Figure 5.16 0.1Hz stimulation of the PF-pathway during 1Hz 300-pulse RFS applied to the AA-pathway with 10mM $BAPTA_i$. The figure shows the mean values for EPSC (*A*) and PPR (*B*) in three cells. The EPSCs in both pathways at baseline and after 20 minutes are illustrated in *C*.

The results for postsynaptic LTP generation were also examined by CV analysis. 20 minutes after 1Hz RFS was applied to the PF-pathway, the increase in $EPSC_A$ in the PF-pathway was accompanied by a decrease in normalised CV^{-2} to 0.91 ± 0.05). CV^{-2} in the AA-pathway also decreased, to 0.84 ± 0.05 (fig. 5.17b). 20 minutes after 1Hz RFS to the AA-pathway, while normalised CV^{-2} the AA-pathway decreased from baseline levels to 0.86 ± 0.04, The PF-pathway decreased both in $EPSC_A$, and in normalised CV^{-2} to

0.75 ± 0.02. Compared to control data at 20 minutes, it is suggested that the increase in PF-pathway $EPSC_A$ from 1Hz RFS to that same pathway is due to an increase in Q. The decrease in $EPSC_A$ from 1Hz RFS to the AA-pathway is likely the result of a decrease in N, and thus a decrease in either the number of PFs activated or a reduction in the number of contributing release sites.

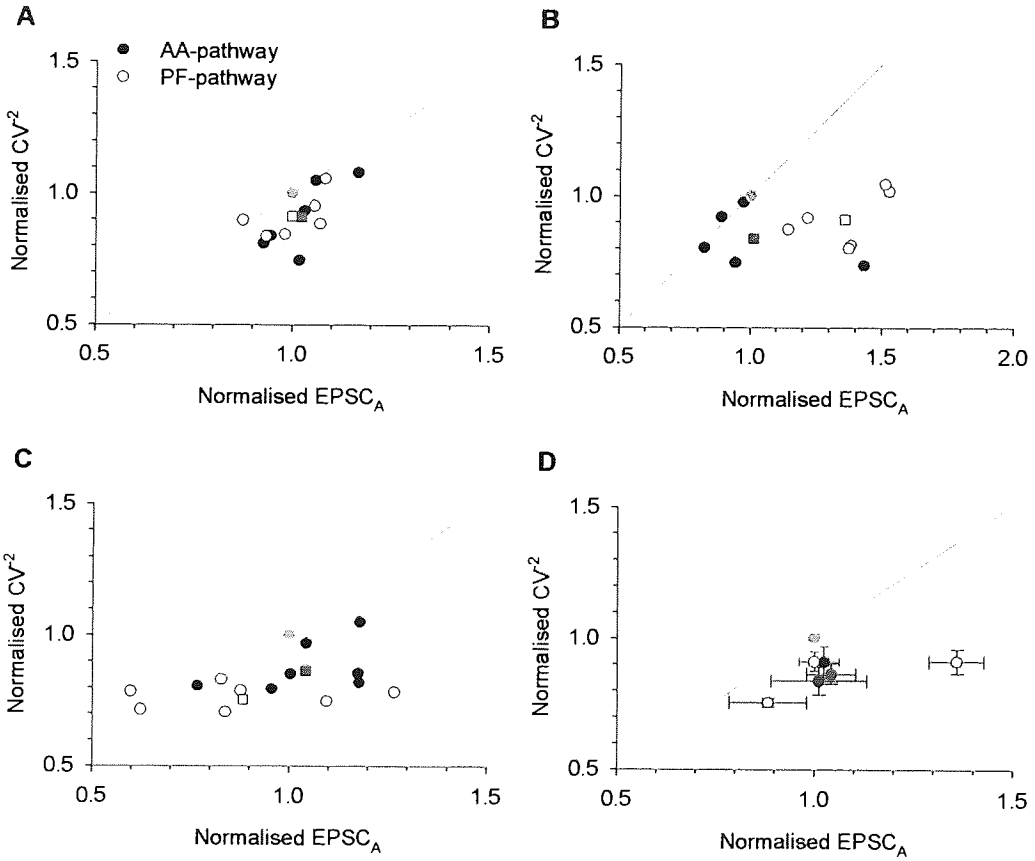

Figure 5.17 CV analysis of experiments with 300-pulse 1Hz RFS. Normalised CV^{-2} was plotted against normalised $EPSC_A$ at baseline and 20 minutes later, with values normalised to baseline values (grey circles). These were plotted for each individual experiment in the constant 0.2Hz stimulation (n=6; *A*), with 1Hz RFS to the PF-pathway (n=7; *B*), and 1Hz RFS to the AA-pathway (n=7; *C*). In each graph, filled symbols represent AA-pathway, and open symbols PF-pathway, the differently coloured square dots represent average values. The average values (± s.e.m.) for constant 0.2Hz stimulation (black circles), 1Hz RFS to the PF-pathway (blue circles) and 1Hz RFS to the AA-pathway (red circles) are illustrated in *D*.

5.4 Discussion

The data in the chapter have revealed that AA synapses are largely resistant to the forms of plasticity previously identified at PF synapses. They underwent neither conjunctive CF-LTD nor postsynaptic LTP, nor did plasticity spread to AA synapses when it was induced in the PF-pathway. When potentiation appeared to spread from the PF-pathway following application of 16Hz RFS, it was less profound than that at the PF-pathway. That this was a genuine potentiation is possible, considering the response of AA synapses to forskolin, which varied from no potentiation in under a third of cells to a lesser degree of potentiation than that observed at PF synapses in the rest. Therefore it can be postulated that MF signals via the AA synapses supply a steady excitatory input to PCs that is relatively resistant to synaptic plasticity, ensuring faithful transmission to PCs directly above the MF termination zone. MF signalling via PFs is however highly plastic. Therefore, MF signals carried outside the MF termination zone by PFs may be readily modulated to ensure the appropriate strength of transmission.

5.4.1 Long-term depression at granule cell – Purkinje cell synapses.

Conjunctive pairing of CF and PF inputs to PCs generated LTD consistent with previous studies (e.g. Ito & Kano, 1982; Reynolds & Hartell, 2000; Wang *et al.*, 2000a). Furthermore the CV analysis verified that the likely cause of LTD at the PF-pathway was due to a decrease in postsynaptic response. On the other hand the AA synapses did not undergo LTD with the same protocol. This would fit with the anatomical suggestion that they are influenced to a lesser extent by the calcium influx caused by the CF, due to their distal location on the PC dendrites (Gundappa-Sulur *et al.*, 1999). Thus we may assume that all PCs should be excited by a MF if they are above that MFs termination zone, as the CF cannot selectively depress them. Isope & Barbour (2002) have estimated that only several hundred PF synapses are needed to bring a PC to action potential threshold, assuming PFs generate a response of 10pA and that PCs have a –60mV resting membrane threshold.

As AAs supply about 20% of the 150,000 GC-PC synapses, MFs should be expected to readily cause action potentials in PCs directly above their termination point. This could account for the 'patchy', vertical response following studies stimulation of MFs (Bower & Woolston, 1983; Cohen & Yarom, 1998). However, it will be interesting to examine the susceptibility of AA synapses to CF-independent LTD. CF-independent LTD has been theorised to replace the CF in synapses on distal dendrites, or where CFs are absent in some species (Palay & Chan-Palay, 1974; Bell *et al.*, 1997). As AA synapses have greater quantal amplitude than PF synapses, they are more likely to induce local calcium influx and thus LTD through strong stimulation, without the CF.

The principal theory of cerebellar function is that it adapts motor commands from the cortex, which involves a learning element (Marr, 1969; Albus, 1971; Ito, 1989). It predicts only a portion of the ~150,000 PF synapses are important for controlling PC activity. The CF acts as an 'error signal' that causes the selective weakening of inappropriate PF-PC signals, and LTD forms the mechanism by which it does so. Under this theory the AA synapse will have no role in cerebellar learning, as it cannot undergo conjunctive LTD. Also suggested is that both conjunctive LTD and PF-LTD weaken GC-PC synapses to prevent overstimulation of the PC (DeSchutter, 1995). In this case it may be that AAs are designed to be the main excitatory GC input to the PC, and the PFs are secondary inputs, suitable to be reduced for neuroprotective reasons.

5.4.2 Long-term potentiation at granule cell – Purkinje cell synapses.

The results in this chapter are largely consistent with previous work. 16Hz RFS induced a potentiation in PF synapses as has been previously observed (Salin *et al.*, 1996; Jacoby *et al.*, 2001; Lev-Ram *et al.*, 2002). However, while a decrease in PPR was noted in the PF-pathway, surprisingly it was not significant at 20 minutes as previously observed (chapter 3). Therefore there may be some doubt regarding a presynaptic location. PPR has been

observed to return to baseline while EPSCs are still potentiated (Jacoby *et al.*, 2001), and this may have occurred here, but at an earlier time point. It is possible that postsynaptic LTP may have been evoked in these experiments, although the two different stimulation protocols were reported to discriminate between the two (Lev-Ram *et al.*, 2002). It may be further evidence of a two-phase LTP, where an early presynaptic element gives way to a later postsynaptic one. 10μM Forskolin caused potentiation in both pathways, although surprisingly, across all cells it failed to reduce PPR in either pathway. This contrasts with previous data showing the PKA-dependence of presynaptic LTP and decreased PPR with forskolin (Salin *et al.*, 1996; Jacoby *et al.*, 2001; Lev-Ram *et al.*, 2002). Thus the issue of presynaptic and postsynaptic expression of LTP remains unclear from the data obtained in this study.

It has been revealed that AA synapses can undergo potentiation under some circumstances, as demonstrated by the spread from the PF pathway or forskolin application, although the latter was only short-term. The lack of potentiation arising from 16Hz RFS to the AA-pathway seems contradictory, however. A possible explanation might be that were AA synapses to lack NOS, the potentiation from forskolin in the AA-pathway could be the result of NO generated at the PF pathway, assuming that PKA causes NO production as previously found (Jacoby *et al.*, 2001).

300 pulses at 1Hz evoked LTP, consistent with previous findings (Lev-Ram *et al.*, 2002). There was a brief decrease in PPR (<10 minutes) in the PF-pathway after RFS, which may indicate a presynaptic STP. However, while the decrease in PPR was only transient, the potentiation in $EPSC_A$ continued for over 30 minutes, suggesting potentiation was postsynaptic in the long term. There was little evidence of potentiation spreading from the PF-pathway to the AA-pathway. As with the 16Hz RFS, no LTP was observed when 1Hz RFS was applied to the AA-pathway, nor was spread to the PF-pathway observed.

The CV analysis seemed to bear out the predicted sites of action of LTP. LTP following 16Hz RFS was accompanied by increased normalised CV^{-2} compared to control, which would suggest a presynaptic locus involving N or P_r. 1Hz RFS however caused no change in normalised CV^{-2} compared to control, thus suggesting the change in $EPSC_A$ was due to an increase in Q. As the increase in Q observed during the spread of potentiation from 16Hz RFS to the PF-pathway lay more to the line representing Q than that representing N, this would appear to agree with the lack of change in PPR and favour a postsynaptic LTP.

5.4.3 The spread of synaptic plasticity between ascending axon and parallel fibre synapses

A spread of plasticity from activated pathway to non-activated pathway was rarely observed in the data in this chapter. This is in contrast to experiments performed with two PF pathways activated (chapter 3; Reynolds & Hartell, 2000; Jacoby *et al.*, 2001), where spread of plasticity was a common occurrence. There did appear to be a spread of potentiation from the test PF-pathway to distant AA-pathway after 16Hz RFS, although the potentiation was not significant in the AA-pathway. Whilst 16Hz RFS should evoke the presynaptic form of LTP, as PPR was not depressed in the long term, this may mean it was postsynaptic LTP. Although not a spread of potentiation, the PF-pathway was slightly reduced during LTD induction in the AA-pathway (fig. 5.5). This may have been the result of a 2-minute period of inactivity similar to that observed by the 5-minute inactivity during postsynaptic LTP induction. The finding that there was a possible reduction in N rather in Q from the CV analysis would suggest that this was due to a reduction in the number of PFs or release sites activated.

What reasons could there be for the failure of potentiation to be evident at distant synapses? Failure of plasticity to spread to the AA-pathway may be explained by the general lack of plasticity observed at that synapse. It might be expected that NO or other mediators of plasticity could be produced by

RFS of AA synapses, and diffuse to potentiate or depress PF synapses. However, failure for plasticity to be expressed in the PF-pathway when protocols were applied to the AA-pathway might indicate inadequate production of the mediators to spread plasticity at those synapses.

16Hz RFS to the AA-pathway might have been expected to spread potentiation to PF synapses. NO is the likely cause of spread of plasticity, and should be capable of spreading LTP to distant synapses as demonstrated in chapter 3. An explanation might be that there is no, or very little, NOS in the presynaptic termini of AA synapses. This would explain not only the lack of spread of potentiation, but also the failure for 1 or 16Hz RFS to the AA-pathway to generate LTP in that same pathway.

There may have been insufficient generation of NO (or other potential mediators for the spread of plasticity) through reasons other than lack of NOS. In this chapter, lower baseline $EPSC_A$s were elicited, and thus fewer fibres were stimulated, compared to chapter 3. As fewer fibres were activated, NO production would have been reduced, which may have contributed to the failure of spread of plasticity. Failure of spread when 1Hz RFS was applied may be explained by the lower amount of NO that would be produced, as NO production is dependent upon the intensity and frequency of stimulation (Wood & Garthwaite, 1994; Kimura *et al.*, 1998; Philippides *et al.*, 2000). 1Hz RFS to the PF-pathway could increase NO production enough for NO to cross from the pre- to postsynaptic environment, but not enough to spread between synapses. Finally, the distance between AA and PF synapses may have been an influencing factor. It was not possible to work out how far apart the PF and AA synapses were in experiments on coronal orientation slices. However, considering the placement of electrodes in the slice, the synapse separations are likely to have been within the 150-170μm that plasticity has previously been observed to spread (Jacoby *et al.* 2001). It would be interesting to observe the responses of AA and PF synapses to addition of a NO donor, such as spermine NONOate. If AA synapses are potentiated, it would provide evidence that NO does not seem to be produced at the presynaptic termini of AA synapses.

Chapter 6

General Discussion

This study has continued the investigation of the role of NO in the spread of synaptic plasticity started by Jacoby *et al.* (2001). Prevention of NO diffusing through the extracellular environment with the scavenger cPTIO prevented the spread of LTP evoked by 15s 16Hz RFS to distant synapses. It was confirmed that NO is vital in the spread of potentiation in cerebellar slices. Potentiation spread to, and occasionally beyond, distances that have been frequently observed in both the spread of LTD (Hartell, 1996; Finch & Augustine, 1998; Wang *et al.*, 2000b), and that NO has been found to diffuse in biological preparations *in vitro* (Park *et al.*, 1998). It has already been established that the NO-sGC-cGMP-PKG pathway influences LTD. This study also finds that G-substrate, activated by PKG, is involved in cerebellar LTD, but not LTP.

Secondly, this study has revealed important differences in the characteristics of synapses made by the two segments of the GC axon, the AA and PFs, previously only hinted at by anatomical evidence (Gundappa-Sulur *et al.*, 1999). AA synapses were found to have a greater quantal amplitude and probability of release than PF synapses. When tested for synaptic plasticity, AA synapses were found to not undergo conjunctive LTD, nor did LTD spread to AA synapses from conjunctive CF-PF stimulation. AA synapses had only limited capability to undergo LTP, and did not potentiate as greatly as PF synapses when the PKA activator forskolin was applied. While LTP in the AA-pathway was only generated by spread from the PF-pathway from a protocol thought to generate the presynaptic variant, it is unclear whether the potentiation was expressed pre- or postsynaptically.

6.1 Long-term potentiation – presynaptic or postsynaptic?

LTP in the cerebellum was initially thought to be exclusively a presynaptic phenomenon evoked by a short duration RFS at 4-16Hz (Shibuki & Okada, 1992; Salin *et al.*, 1996; Jacoby *et al.*, 2001; Lev-Ram *et al.*, 2002), although postsynaptic LTP has been predicted from research mapping MF and CF receptive fields from stimulation of the periphery (Jorntell & Ekerot, 2002). The first finding of an apparent postsynaptic potentiation at a cellular level, evoked by a RFS over 300 pulses at 1Hz, was published recently (Lev-Ram *et al.*, 2002). The postsynaptic potentiation is independent of both PKA- and sGC-pathways, which are involved in presynaptic LTP and LTD respectively. It was also proposed in that study that postsynaptic LTP might be a means of reversing LTD by restoring AMPARs to the postsynaptic termini. The CV analysis (figs. 5.10, 5.17) would seem to add some weight to this theory. While postsynaptic LTP seemed to be caused more by an increase in Q, presynaptic LTP demonstrated an increase more in N or P.

It was not clear whether presynaptic or postsynaptic LTP was predominant during several experiments in this study. Presynaptic cerebellar LTP is generally accompanied by a decrease in PPR (Salin *et al.*, 1996; Jacoby *et al.*, 2001; Lev-Ram *et al.*, 2002), as decreased PPR is a possible indicator for increased probability of transmitter release (Zucker, 1989; Thomson, 2000). While PPR was significantly reduced as expected in chapter 3, in chapter 5 this was not so reliably observed. When 16Hz RFS was applied to the PF-pathway, 20 minutes after RFS PPR was not significantly decreased in the PF-pathway from pooled data from all cells. However, several individual cells did show a long-term decrease in PPR, and all showed evidence of a transient decrease in PPR. Previous results have also shown a recovery of PPR after 16Hz RFS (Jacoby *et al.* 2001). During the application of forskolin, a PKA activator, or in the spread of 16Hz-induced potentiation to the AA-pathway, a transient decrease of PPR was observed only in some cases of either. The lack of decrease in PPR after forskolin application is surprising, as PKA is strongly implicated in presynaptic LTP, and has previously been observed to decrease PPR (Salin *et al.*, 1996) and increase the frequency of

mEPSCs (Jacoby *et al.*, 2001). LTP from 16Hz RFS that spread to the distant PF synapses in chapter 3 was accompanied by a decrease in PPR, suggesting it is presynaptic. The potentiation that spread to AA synapses in chapter 5 was not accompanied by a decrease in PPR, which could be explained by the LTP in AA synapses being postsynaptic. This is reasonable, as NO has been implicated both in presynaptic (Jacoby *et al.*, 2001) and postsynaptic (Lev-Ram *et al.*, 2002) LTP, and so NO could spread either or both.

Considering the separate stimulation protocols, together with the PKA-independence of postsynaptic LTP, there may be an indication that the presynaptic and postsynaptic mechanisms are unlinked. PPR was decreased but gradually returned towards baseline levels after 1Hz RFS to the PF-pathway and a recovery was also seen in Jacoby *et al.* (2001), albeit after 20 minutes. In both cases, potentiation continued beyond the point where PPR recovered to baseline. PPR was also decreased when STP was generated, although potentiation returned to baseline with PPR. Therefore, it is possible that a dual phase of LTP might exist. Presynaptic LTP may be a short-lived effect (10-20 minutes), and it may be the postsynaptic form that persists over longer periods. While both forskolin and an NO donor increased the mEPSC frequency in PCs, both also caused a smaller increase in mEPSC amplitude (Jacoby *et al.*, 2001). This also could be evidence of the coexistence of both forms of plasticity. This does not, however, answer whether the two mechanisms are dependent in some fashion. Nor is it clear regarding the role of NO. No mechanism has been identified for postsynaptic LTP, and the means of action of NO in presynaptic LTP is not clear. A link between PKA and NO is contentious, with evidence for (Inada *et al.*, 1998;Inada *et al.*, 1999) and against (Brune & Lapetina, 1991). NO has been demonstrated to directly increase presynaptic vesicle release (Meffert *et al.*, 1994; Meffert *et al.*, 1996), and a NO donor increased the frequency of mEPSCs recorded in PCs (Jacoby *et al.*, 2001). As an NO donor can cause lasting potentiation while PKA is inhibited (Jacoby *et al.*, 2001), it might be assumed NO is downstream of PKA, unless there is some form of mutual interaction. Further investigation of cerebellar LTP is vital to elucidate these issues. Lev-Ram *et*

al. (2002) used 0.1Hz baseline stimulation to prevent a run-up of the EPSC response observed at higher frequencies, even 0.2Hz, Run-up was also frequently noted in this study before baselines were acquired. It is possible that there is a use-dependent increase in synaptic transmission at GC-PC synapses, of which postsynaptic LTP may be the principal mechanism. At frequencies over 4Hz, however, the presynaptic form of LTP may predominate, possibly through some additional effect such as LTP of NOS activity (Kimura *et al.*, 1998).

An important consideration must be the physiological firing rate of GCs, which is currently unknown, although a modelling study has found that 5Hz is the optimal rate for learning (Schweighofer *et al.*, 2001). The decrease in $EPSC_A$ in later pulses that occurred when fibres were stimulated by seven pulses at 20Hz in 2.5mM external calcium (fig. 4.14) suggests that GCs are not capable of maintaining that rate of activity for long bursts. Although a previous study that suggested that PF synapses could operate at up to 20Hz without a decline in later pulses, a lower external calcium concentration of 1.5mM was used (Dittman *et al.*, 2000). That study suggested that the determining factors for EPSC sizes in a train of stimuli are calcium-dependent facilitation of vesicle release, and calcium-dependent recovery of release site readiness (CDR). It is possible that AA synapses have a more limited capacity for CDR as well being less capable of facilitation. However, both Dittman *et al.* (2000) and Schweighofer *et al.* (2001) would seem to indicate that physiological GC firing rates could manage frequencies great enough to cause presynaptic LTP.

6.2 The spread of cerebellar plasticity.

Evidence for the spread of plasticity is growing, although it is controversial, particularly in the case of conjunctive LTD. The theories of Marr (1969) and Albus (1971) have underpinned the understanding of cerebellar motor learning. The CF is proposed to act as an 'error' signal to depress PF inputs that are associatively activated with it. Consequently, spread of LTD is

contrary to Marr-Albus-based theories. Conjunctive LTD has been observed to spread up to 100μm (Reynolds & Hartell, 1998). If this LTD at the distant site were mediated by the diffusion of NO acting via the sGC-pathway alone, it would mean not only many synapses on the same cell being depressed, but also synapses on all the cells around. Spread of potentiation was recorded over 150μm in this study, as was found in Jacoby *et al.* (2001). However, few results of spread over 100μm were recorded. Spread of plasticity to this sort of distance may be unusual, particularly considering endogenous NO scavengers and NO 'sinks' that may be present *in vivo* (Griffiths & Garthwaite, 2001; Griffiths *et al.*, 2002). Spread of plasticity up to 100μm is well within the distances that have been measured for NO to diffuse in several biological systems and modelling work (for instance Park *et al.*, 1998; Schweighofer & Ferriol, 2000; Philippides *et al.*, 2000).

Plasticity in this study was observed to spread from PF synapses to distant PF synapses in the case of CF-independent LTD and presynaptic LTP. The possibility that plasticity spreading was the result of some change in cell conditions such as health is unlikely. Deterioration of the cell would be likely to cause a decrease in $EPSC_A$, but not an increase that could explain LTP. Where CF-independent LTD spread, cells remained similarly healthy to control experiments, where $EPSC_A$ and PPR remained constant over time. The possibility of an overlap of stimulation fields in sagittal slices is also improbable. The stimulation strengths and distances between electrodes used in this study are similar to those used by Jacoby *et al.* (2001), where no overlap was measured based on a protocol according to Hartell (1996). Reynolds & Hartell (2000) observed overlap when the electrodes were placed 5.6μm apart, but not 22μm apart, similar to the minimum distance used in this study.

Heterosynaptic plasticity (i.e. plasticity spreading from one GC synapse to another) would have the benefit of mutual reinforcement between synapses. In the case of conjunctive LTD, *in vitro* it is derived by repetitive, associative stimulation of PFs and CFs, where the CF can be activated from 750ms

before to 250ms after the PF (Ekerot & Kano, 1989; Chen & Thompson, 1995; Karachot *et al.*, 1995; Schreurs *et al.*, 1996; Wang *et al.*, 2000a). However, LTD only developed at distant synapses that were activated within 20 minutes after LTD induction (Reynolds & Hartell, 2000). Hence it has been theorised that PF inputs which are weakly temporally coincidental with the CF may be less likely to be depressed, and so would retain a degree of input specificity (Ito, 2001). In both forms of LTD, the spread of plasticity via NO to distant synapses would probably only activate the NO-dependent dephosphorylation-inhibiting pathway, which would limit indiscriminate synapse depression. Furthermore, the level of depression has been found to lessen over distance, with depression half-maximal at 50μm, and unlikely beyond 100μm (Wang *et al.*, 2000b). If potentiation is spread by the same mediator as depression, it might be expected this would be true also of LTP. As the memory functioning of the cerebellum is based upon the theories of LTD, input specificity may not be a necessary feature of LTP, as LTD may still selectively depress required GC inputs. It is unknown whether PF synapses on a PC from the same MF terminal will be spatially close. PC dendrites may extend over a hundred micrometres from the soma in each direction (Rapp *et al.*, 1994). Thus if some form of reinforcement were to occur, plasticity may need to be able to spread a long distance. This would increase the likelihood that any selectivity of plasticity in the cerebellar cortex would need to be caused by timing of AA, PF and CF activity.

The other consideration must be spread to other cells, which is observed in the hippocampus (Schuman & Madison, 1994a). A system has been postulated there where memory is stored in groups of cells rather than individual synapses (Montague & Sejnowski, 1994). The microzone system in the cerebellum (Ito, 1984) could also benefit from a similar system of 'volume learning'. In this case were the spread of plasticity would support synapses undergoing plasticity across an entire region. As microzones are estimated at 0.3 – 1mm in length spread of plasticity under 100μm would only have limited influence on adjacent microzones. Dual recordings from two adjacent PCs with independent PF inputs (i.e. where each PF beam

activates only one PC) should be able to ascertain whether plasticity is able to spread between cells. 16Hz RFS to one pathway may be able to induce plasticity in the independent pathway.

6.3 Raised frequency stimulation can induce long-term potentiation and depression.

Work in this study and previously reported (Jacoby & Hartell, 1999) has revealed that LTP and LTD can both be induced by a 15s, 8-16Hz RFS. LTD induced by this protocol also spread to the distant synapses. There is some evidence of potentiation being evoked with this LTD (fig. 3.10), although LTD predominated. As PPR was only transiently decreased, potentiation may have been only short term. Alternatively the potentiation may have been long term, but involving only a brief presynaptic effect. The deciding factor for whether potentiation or depression predominates would appear to be the postsynaptic calcium levels. Where an increase in postsynaptic calcium levels is reduced, it might be expected for LTP to be dominant as LTD is calcium dependent. This has been demonstrated by *in vitro* interventions, such as hyperpolarisation of the PC (Jacoby, 2001), or a high concentration of calcium chelator, used in this study. A physiologically likely factor would be $GABA_A$-mediated inhibitory currents in the PC from interneurones. The absence of picrotoxin has blocked LTD from both conjunctive CF-PF stimulation (Schreurs & Alkon, 1993) and RFS of PFs (Jacoby, 2001). Inhibitory signals would hyperpolarize the cell and thus reduce calcium influx through VGCCs. The CF may also be vital in this regard. High frequency PF activation would cause LTP along a beam of PCs where inhibitory signals restrict postsynaptic calcium entry. The CF could, however, depolarise a PC along this beam to facilitate calcium entry. Thus while this cell underwent LTD, its neighbours would undergo LTP.

The interneurones of the ML, basket and stellate cells, are also activated by PFs. However, while PFs activate 'on-beam' PCs as they pass them, the interneurones inhibit PCs off-beam, to either side of the activated PFs. The

high frequency GC activity to PCs may offset any off-beam signals along the microzone, whereas outside the microzone there would be limited GC-PC activity, limiting LTP.

LTD and LTP may be important in regulating the strength of PF synapses to prevent over- or underexcitation of PCs. LTD has previously been postulated as a means of preventing PC overexcitability (DeSchutter, 1995). LTP however would be the means by which synapses are strengthened. A theory could be proposed where high frequency PF activity will cause LTP. Once these potentiated synapses generate a sufficiently high postsynaptic response, they may begin to cause sufficient localised depolarisation to induce LTD at those synapses. However, unless LTP does in some way reverse the internalisation of AMPARs – as yet unproven – it is improbable that the two act as opposite sides of the same process. This is because LTP could not, ultimately, restore activity to a synapse. If a synapse is rendered 'mute' (i.e. silent because there are no postsynaptic receptors) then no amount of presynaptic increase in transmitter release will generate a response at that synapse. Another reason LTP and LTD may not be regulatory is their long time-courses, which would make it difficult for either to respond to short-term changes in GC activity.

6.4 Functional relevance of differentiated ascending axon and parallel fibre synapses

AA segments are a relatively overlooked part of the cerebellar cortex. GC axon inputs are often treated as synonymous with PFs, and AAs are marginalized or ignored in many models of cerebellar cortical function (for instance Eccles *et al.*, 1967; Gabbiani *et al.*, 1994; Braitenberg *et al.*, 1997). This study has revealed that the AA must now be considered an important part of the cerebellar cortex in its own right.

AA synapses have both greater quantal amplitude and probability of release than PF synapses, and do not appear to be susceptible to conjunctive LTD.

Also important is that AAs form numerous synapses per PC, whereas PFs usually form just one, and an estimated 85% of PF synapses are silent (Isope & Barbour, 2002). Consequently, MF stimulation is expected to evoke a large signal in PCs directly above its termination zone. However, any MF-PC signals conducted beyond the termination zone by PFs, will be transmitted by synapses that are less reliable and less numerous per PC. The AA signal will be relatively temporally discrete as well as strong, as AA synapses are located on PC dendrites nearer the PCL (Gundappa-Sulur *et al.*, 1999). On the other hand, PFs conduct action potentials with slower velocity the nearer they are to the pial surface (Vranesic *et al.*, 1994). This delay would be further increased by the extra time taken for action potentials to travel up the AA to the bifurcation point if it is nearer the pial surface. If GC axons activated by the same MF signal from bifurcate at varying depths in the ML, MF transmission via PFs may become more temporally diffuse, which could be increasingly accentuated with distance from the MF termination point. This diffuse PF activity could be part of the reason that voltage sensitive dyes failed to recognise PC responses along PF beams (Cohen & Yarom, 1998). As measured by electrical signals, responses in PCs have been recorded up to and, rarely, above 1.5mm from the MF terminal (Garwicz & Andersson, 1992). However, the strength of transmission declined from the centre of the MF terminal area. PFs are considerably longer than a microzone, which also makes it unlikely that they are used to pass signals to a single microzone. Possibly, the AA is responsible for the signal from MFs to their microzones, whilst the PFs, however, carry MF signals beyond the microzone. This PF-mediated signal could act to co-ordinate the activity of microzones, where plasticity plays an important role determining the strength of transmission necessary to achieve accurate co-ordination.

6.5 Future work

There are a number of questions posed by this thesis. Firstly, the question of whether AA synapses can undergo LTD needs to be further addressed.

While it has been shown here that AA synapses are not affected by conjunctive pairing of CF and PF inputs, they may still be capable of undergoing LTD. In order to test this, the AA synapses could be activated by conjunction with PC depolarisation, although this is less reliable than CF-PF conjunction (Reynolds & Hartell, 1998). Secondly, a protocol to generate CF-independent LTD could be applied, which may be the means that LTD occurs in PF synapses that are not affected by the CF in fish cerebella (Bell *et al.*, 1997). Calcium imaging experiments should also be able to reveal the relative abilities of PF and AA synapses to mobilise calcium or activate mGluRs. This could also provide valuable additional evidence about the location and number of AA synapses, which have been reported as prevalent only on PC dendrites in the bottom third of the ML (Gundappa-Sulur *et al.*, 1999). Due to the planar nature of PC dendrites, imaging experiments would need to be done in sagittal slices in order to achieve visualisation of the whole PC.

The effect of spread of plasticity must also be examined on neighbouring PCs by recording from multiple PCs. Two PF inputs, where at least one is specific to one PC and within 100μm of each other, could be stimulated. If RFS can be applied to a PC-specific PF input, it would be possible to observe whether LTP or LTD could spread to the other pathway in the second cell. By varying the concentration of calcium chelator in each recording electrode, it would also be possible to observe whether LTD could be evoked in test pathway, yet LTP manifested in the other cell, and vice versa. Addition of a NO scavenger would also be able to determine whether NO spreads both forms of plasticity to the distant cell. Similarly, two PCs could be recorded from along the same beam of PFs. Using high frequency stimulation of PFs to both cells and applying a CF input to one cell, it would also be possible to see whether LTD were evoked in the cell with conjunctive stimulation and LTP in the other. These experiments would not only involve electrophysiology, but fluorescence imaging of substances such as cGMP could also help determine the effects of NO spreading to distant cells. Also of interest is the spatial distribution of PF inputs from GCs, as if synapses are to mutually support plasticity in each other, it may be advantageous for them to

be close together. Using imaging techniques, stimulation of the GL to activate PCs via PFs may be able to determine whether groups of adjacent GCs have PFs that are closely packed in the ML.

There is still work that needs to be done on the role of NO in plasticity, particularly to identify the targets of NO in both forms of LTP as NO appears to be associated with both forms (Jacoby *et al.*, 2001; Lev-Ram *et al.*, 2002). A 1Hz RFS to generate the postsynaptic form of LTP could be applied in the presence of a NO scavenger, which should be able to determine whether NO needs to diffuse transcellularly for postsynaptic LTP. From the results in this thesis, it is not clear the induction protocols for both forms of LTP generate a purely pre- or postsynaptic effect. While a PKA inhibitor inhibits the presynaptic form, if a NO scavenger can prevent postsynaptic LTP, it will allow the two to be separated more conclusively. It would also be worth examining two separate inputs in postsynaptic LTP to see whether plasticity spreads, which might be expected if it is NO-dependent.

Reference List

Ahn, S., Ginty, D. D., & Linden, D. J. (1999). A late phase of cerebellar long-term depression requires activation of CaMKIV and CREB. *Neuron* **23**, 559-568.

Akaike, T., Yoshida, M., Miyamoto, Y., Sato, K., Kohno, M., Sasamoto, K., Miyazaki, K., Ueda, S., & Maeda, H. (1993). Antagonistic action of imidazolineoxyl N-oxides against endothelium-derived relaxing factor/.NO through a radical reaction. *Biochemistry* **32**, 827-832.

Albus, J. S. (1971). A theory of cerebellar function. *Mathematical Bioscience* **28**, 167-171.

Allen, C. & Stevens, C. F. (1994). An evaluation of causes for unreliability of synaptic transmission. *Proceedings Of The National Academy Of Sciences Of The United States Of America* **91**, 10380-10383.

Anderson, W. W. & Collingridge, G. L. (1999). A data acquisition program for on-line analysis of long-term potentiation and long-term depression. *Society Of Neuroscience Abstracts* **23**, 665.

Aramori, I. & Nakanishi, S. (1992). Coupling of two endothelin receptor subtypes to differing signal transduction in transfected Chinese hamster ovary cells. *Journal Of Biological Chemistry* **267**, 12468-12474.

Arancio, O., Kiebler, M., Lee, C. J., LevRam, V., Tsien, R. Y., Kandel, E. R., & Hawkins, R. D. (1996). Nitric-oxide acts directly in the presynaptic neuron to produce long- term potentiation in cultured hippocampal-neurons. *Cell* **87**, 1025-1035.

Aravanis, A. M., Pyle, J. L., & Tsien, R. W. (2003). Single synaptic vesicles fusing transiently and successively without loss of identity. *Nature* **423**, 643-647.

Ariano, M. A., Lewicki, J. A., Brandwein, H. J., & Murad, F. (1982). Immunohistochemical localization of guanylate cyclase within neurons of rat brain. *Proceedings Of The National Academy Of Sciences Of The United States Of America* **79**, 1316-1320.

Artola, A., Brocher, S., & Singer, W. (1990). Different voltage-dependent thresholds for inducing long-term depression and long-term potentiation in slices of rat visual cortex. *Nature* **347**, 369-372.

Artola, A. & Singer, W. (1993). Long-term depression of excitatory synaptic transmission and its relation to long-term potentiation. *Trends In Neurosciences* **16**, 480-487.

Aswad, D. W. & Greengard, P. (1981a). A specific substrate from rabbit cerebellum for guanosine 3':5'-monophosphate-dependent protein kinase. I. Purification and characterization. *Journal Of Biological Chemistry* **256**, 3487-3493.

Aswad, D. W. & Greengard, P. (1981b). A specific substrate from rabbit cerebellum for guanosine 3':5'-monophosphate-dependent protein kinase. II. Kinetic studies on its phosphorylation by guanosine 3':5'-monophosphate-dependent and adenosine 3':5'-monophosphate-dependent protein kinases. *Journal Of Biological Chemistry* **256**, 3494-3500.

Atluri, P. P. & Regehr, W. G. (1998). Delayed release of neurotransmitter from cerebellar granule cells. *Journal Of Neuroscience* **18**, 8214-8227.

Barbour, B. (1993). Synaptic currents evoked in Purkinje cells by stimulating individual granule cells. *Neuron* **11**, 759-769.

Barbour, B. (2001). An evaluation of synapse independence. *Journal Of Neuroscience* **21**, 7969-7984.

Barbour, B. & Hausser, M. (1997). Intersynaptic diffusion of neurotransmitter. *Trends In Neurosciences* **20**, 377-384.

Barbour, B., Keller, B. U., Llano, I., & Marty, A. (1994). Prolonged presence of glutamate during excitatory synaptic transmission to cerebellar Purkinje cells. *Neuron* **12**, 1331-1343.

Barria, A., Derkach, V., & Soderling, T. (1997). Identification of the Ca2+/calmodulin-dependent protein kinase II regulatory phosphorylation site in the alpha-amino-3-hydroxyl-5-methyl- 4-isoxazole-propionate-type glutamate receptor. *Journal Of Biological Chemistry* **272**, 32727-32730.

Batchelor, A. M., Madge, D. J., & Garthwaite, J. (1994). Synaptic activation of metabotropic glutamate receptors in the parallel fibre-Purkinje cell pathway in rat cerebellar slices. *Neuroscience* **63**, 911-915.

Bekkers, J. M. & Stevens, C. F. (1990). Presynaptic mechanism for long-term potentiation in the hippocampus. *Nature* **346**, 724-729.

Bell, C. C., Han, V. Z., Sugawara, Y., & Grant, K. (1997). Synaptic plasticity in a cerebellum-like structure depends on temporal order. *Nature* **387**, 278-281.

Bi, X., Standley, S., & Baudry, M. (1998). Post-translational regulation of ionotropic glutamate receptors and synaptic plasticity. *International Review of Neurobiology* **42**, 227-284.

Blond, O., Daniel, H., Otani, S., Jaillard, D., & Crepel, F. (1997). Presynaptic and postsynaptic effects of nitric oxide donors at synapses between parallel fibres and Purkinje cells: Involvement in cerebellar long-term depression. *Neuroscience* **77**, 945-954.

Bower, J. M. & Haberly, L. B. (1986). Facilitating and non-facilitating synapses on pyramidal cells - a correlation between physiology and morphology. *Proceedings Of The National Academy Of Sciences Of The United States Of America* **83**, 1115-1119.

Bower, J. M. & Woolston, D. C. (1983). Congruence of spatial organization of tactile projections to granule cell and Purkinje cell layers of cerebellar hemispheres of the albino rat: vertical organization of cerebellar cortex. *Journal Of Neurophysiology* **49**, 745-766.

Boxall, A. R. & Garthwaite, J. (1996). Long-term depression in rat cerebellum requires both NO synthase and NO-sensitive guanylyl cyclase. *European Journal Of Neuroscience* **8**, 2209-2212.

Boxall, A. R., Lancaster, B., & Garthwaite, J. (1996). Tyrosine kinase is required for long-term depression in the cerebellum. *Neuron* **16**, 805-813.

Braitenberg, V. & Atwood, R. P. (1958). Morphological observations on the cerebellar cortex. *Journal Of Comparative Neurology* **109**, 1-33.

Braitenberg, V., Heck, D., & Sultan, F. (1997). The detection and generation of sequences as a key to cerebellar function: experiments and theory. *Behavioural Brain Science* **20**, 229-245.

Bredt, D. S., Ferris, C. D., & Snyder, S. H. (1992). Nitric-oxide synthase regulatory sites - phosphorylation by cyclic amp-dependent protein-kinase, protein-kinase-c, and calcium calmodulin protein-kinase - identification of

flavin and calmodulin binding-sites. *Journal Of Biological Chemistry* **267**, 10976-10981.

Bredt, D. S., Hwang, P. M., & Snyder, S. H. (1990). Localization of nitric oxide synthase indicating a neural role for nitric oxide. *Nature* **347**, 3768-3770.

Brune, B. & Lapetina, E. G. (1991). Phosphorylation of nitric oxide synthase by protein kinase A. *Biochemical & Biophysical Research Communications* **181**, 921-926.

Calcerrada, M. C., Catalan, R. E., & Martinez, A. M. (2002). PAF-stimulated protein tyrosine phosphorylation in hippocampus: involvement of NO synthase. *Neurochemical Research* **27**, 313-318.

Catalan, R. E., Martinez, A. M., Hernandez, F., Perez, M. J., & Calcerrada, M. C. (1996). Nitric oxide mediates the PAF-stimulated cyclic GMP production in hippocampal slices. *Biochemical & Biophysical Research Communications* **226**, 27-31.

Chabot, C., Gagne, J., Giguerre, C., Bernard, J., & Baudry, M. (1998). Bidirectional modulation of AMPA receptor properties by exogenous Phospholipase A_2 in the hippocampus. *Hippocampus* **8**, 299-309.

Chen, C., Kano, M., Abeliovich, A., Chen, L., Bao, S. W., Kim, J. J., Hashimoto, K., Thompson, R. F., & Tonegawa, S. (1995). Impaired motor coordination correlates with persistent multiple climbing fiber innervation in PKCg mutant mice. *Cell* **83**, 1233-1242.

Chen, C. & Thompson, R. F. (1995). Temporal specificity of long-term depression in parallel fiber-Purkinje synapses in rat cerebellar slice. *Learning and Memory* **2**, 185-198.

Chung, H. J., Xia, J., Scannevin, R. H., Zhang, X., & Huganir, R. L. (2000). Phosphorylation of the AMPA receptor subunit GluR2 differentially regulates its interaction with PDZ domain-containing proteins. *Journal Of Neuroscience* **20**, 7258-7267.

Clements, J. D. & Silver, R. A. (2000). Unveiling synaptic plasticity: a new graphical and analytical approach. *Trends In Neurosciences* **23**, 105-113.

Cody, F. W. & Richardson, H. C. (1979). Mossy and climbing fibre mediated responses evoked in the cerebellar cortex of the cat by trigeminal afferent stimulation . *Journal Of Physiology-London* **287**, 1-14.

Cohen, D. & Yarom, Y. (1998). Patches of synchronized activity in the cerebellar cortex evoked by mossy-fiber stimulation: questioning the role of parallel fibers. *Proceedings Of The National Academy Of Sciences Of The United States Of America* **95**, 15032-15036.

Conquet, F., Bashir, Z. I., Davies, C. H., Daniel, H., Ferraguti, F., Bordi, F., Franz-Bacon, K., Reggiani, A., Matarese, V., Conde, F., Collingridge, G. L., & Crepel, F. (1994). Motor deficit and impairment of synaptic plasticity in mice lacking mGluR1. *Nature* **372**, 237-243.

Conti, R. & Lisman, J. (2003). The high variance of AMPA receptor- and NMDA receptor-mediated responses at single hippocampal synapses: Evidence for multiquantal release. *Proceedings Of The National Academy Of Sciences Of The United States Of America* **100**, 4885-4890.

Crepel, F., Audinat, E., Daniel, H., Hemart, N., Jaillard, D., Rossier, J., & Lambolez, B. (1994). Cellular locus of the nitric oxide-synthase involved in cerebellar long-term depression induced by high external potassium concentration. *Neuropharmacology* **33**, 1399-1405.

Crepel, F. & Jaillard, D. (1990). Protein kinases, nitric oxide and long-term depression of synapses in the cerebellum. *NeuroReport* **1**, 133-136.

Crepel, F. & Jaillard, D. (1991). Pairing of pre-and postsynaptic responses in cerebellar Purkinje cells induces long-term changes in synaptic efficacy *in vitro*. *Journal Of Physiology-London* **432**, 123-141.

Crepel, F. & Krupa, M. (1988). Activation of protein kinase C induces a long-term depression of glutamate sensitivity of cerebellar Purkinje cells. An *in vitro* study. *Brain Research* **458**, 397-401.

Cuttle, M. F., Tsujimoto, T., Forsythe, I. D., & Takahashi, T. (1998). Facilitation of the presynaptic calcium current at an auditory synapse in rat brainstem. *Journal Of Physiology-London* **512**, 723-729.

Daly, J. W., Padgett, W., Shamim, M. T., Butts-Lamb, P., & Waters, J. (1985). 1,3-Dialkyl-8-(p-sulfophenyl)xanthines: potent water-soluble antagonists for A1- and A2-adenosine receptors. *Journal Of Medicinal Chemistry* **28**, 487-492.

Daniel, H., Hemart, N., Jaillard, D., & Crepel, F. (1993). Long-term depression requires nitric oxide and guanosine 3' 5'cyclic monophosphate production in rat cerebellar Purkinje cells. *European Journal Of Neuroscience* **5**, 1079-1082.

Daniel, H., Levenes, C., Fagni, L., Conquet, F., Bockaert, J., & Crepel, F. (1999). Inositol-1,4,5-trisphosphate-mediated rescue of cerebellar long-term depression in subtype 1 metabotropic glutamate receptor mutant mouse. *Neuroscience* **92**, 1-6.

de Rooij, J., Zwartkruis, F. J., Verheijen, M. H., Cool, R. H., Nijman, S. M., Wittinghofer, A., & Bos, J. L. (1998). Epac is a Rap1 guanine-nucleotide-exchange factor directly activated by cyclic AMP. *Nature* **396**, 474-477.

del Castillo, J. & Katz, B. (1954). Quantal components of the end-plate potential. *Journal Of Physiology-London* **124**, 560-573.

DeSchutter, E. (1995). Cerebellar long-term depression might normalize excitation of Purkinje cells, a hypothesis. *Trends In Neurosciences* **18**, 291-295.

Detre, J. A., Nairn, A. C., Aswad, D. W., & Greengard, P. (1984). Localization in mammalian brain of G-substrate, a specific substrate for guanosine 3',5'-cyclic monophosphate-dependent protein kinase. *Journal Of Neuroscience* **4**, 2843-2849.

DeZeeuw, C. I., Hansel, C., Bian, F., Koekkoek, S. E., VanAlphen, A. M., Linden, D. J., & Oberdick, J. (1998). Expression of a protein kinase C inhibitor in Purkinje cells blocks cerebellar LTD and adaptation of the vestibulo-ocular reflex. *Neuron* **20**, 495-508.

DiGregorio, D. A., Nusser, Z., & Silver, R. A. (2002). Spillover of glutamate onto synaptic AMPA receptors enhances fast transmission at a cerebellar synapse. *Neuron* **35**, 521-533.

Dittman, J. S., Kreitzer, A. C., & Regehr, W. G. (2000). Interplay between facilitation, depression, and residual calcium at three presynaptic terminals. *Journal Of Neuroscience* **20**, 1374-1385.

Dittman, J. S. & Regehr, W. G. (1996). Contributions of calcium-dependent and calcium-independent mechanisms to presynaptic inhibition at a cerebellar synapse. *Journal Of Neuroscience* **16**, 1623-1633.

Dong, H., O'Brien, R. J., Fung, E. T., Lanahan, A. A., Worley, P. F., & Huganir, R. L. (1997). GRIP: a synaptic PDZ domain-containing protein that interacts with AMPA receptors. *Nature* **386**, 279-284.

Dow, R. S. & Moruzzi, G. (1958). *The Physiology and Pathology of the Cerebellum* University of Minneapolis, Minneapolis.

Dumuis, A., Sebben, M., Fagni, L., Prezeau, L., Manzoni, O., Cragoe, E. J., & Bockaert, J. (1993). Stimulation by glutamate receptors of arachidonic-acid release depends on the Na^+/Ca^{2+} exchanger in neuronal cells. *Molecular Pharmacology* **43**, 976-981.

Eccles, J. C., Ito, M., & Szentagothai, J. (1967). *The Cerebellum as a Neuronal Machine* Springer Verlag, New York.

Eccles, J. C., Llinas, R., & Sasaki, K. (1966a). Parallel fiber stimulation and the responses induced thereby in the Purkinje cells of the cerebellum. *Experimental Brain Research* **1**, 17-39.

Eccles, J. C., Llinas, R., & Sasaki, K. (1966b). The excitatory synaptic action of climbing fibres on the Purkinje cells of the cerebellum. *Journal Of Physiology-London* **182**, 268-296.

Eccles, J. C., Sabah, N. H., Schmidt, R. F., & Taborikova, H. (1972). Integration by Purkyne cells of mossy and climbing fiber inputs from cutaneous mechanoreceptors. *Experimental Brain Research* **15**, 498-520.

Edwards, F. A., Konnerth, A., Sakmann, B., & Takahashi, T. (1989). A thin slice preparation for patch clamp recordings from neurons of the mammalian central nervous-system. *Pflugers Archiv-European Journal Of Physiology* **414**, 600-612.

Eilers, J., Augustine, G. J., & Konnerth, A. (1995). Subthreshold synaptic Ca^{2+} signalling in fine dendrites and spines of cerebellar Purkinje neurons. *Nature* **373**, 155-158.

Eilers, J., Takechi, H., Finch, E. A., Augustine, G. J., & Konnerth, A. (1997). Local dendritic Ca^{2+} signaling induces cerebellar long-term depression. *Learning & Memory* **4**, 159-168.

Ekerot, C. F. & Jorntell, H. (2001). Parallel fibre receptive fields of Purkinje cells and interneurons are climbing fibre-specific. *European Journal Of Neuroscience* **13**, 1303-1310.

Ekerot, C. F. & Kano, M. (1989). Stimulation parameters influencing climbing fiber induced long-term depression of parallel fiber synapses. *Neuroscience Research* **6**, 264-268.

Endo, S., Nairn, A. C., Greengard, P., & Ito, M. (2003). Thr123 of rat G-substrate contributes to its action as a protein phosphatase inhibitor. *Neuroscience Research* **45**, 79-89.

Endo, S., Suzuki, M., Sumi, M., Nairn, A. C., Morita, R., Yamakawa, K., Greengard, P., & Ito, M. (1999). Molecular identification of human G-substrate, a possible downstream component of the cGMP-dependent protein kinase cascade in cerebellar Purkinje cells. *Proceedings Of The National Academy Of Sciences Of The United States Of America* **96**, 2467-2472.

Erecinska, M. & Silver, I. A. (1992). Relationship between ions and energy metabolism: cerebral calcium movements during ischaemia and subsequent recovery. *Canadian Journal Of Physiology and Pharmacology* **70 Suppl**, S190-S193.

Feil, R., Hartman, J., Luo, C. D., Wolfsgruber, W., Schilling, K., Feil, S., Barski, J. J., Meyer, M., Konnerth, A., De Zeeuw, C. I., & Hofmann, F. (2003). Impairment of LTD and cerebellar learning by Purkinje cell-specific ablation of cGMP-dependent protein kinase I. *Journal Of Cell Biology* **163**, 295-302.

Finch, E. A. & Augustine, G. J. (1998). Local calcium signalling by inositol-1,4,5-trisphosphate in Purkinje cell dendrites. *Nature* **396**, 753-756.

Freeman, J. H., Shi, T., & Schreurs, B. G. (1998). Pairing-specific long-term depression prevented by blockade of PKC or intracellular Ca2+. *NeuroReport* **9**, 2237-2241.

Gabbiani, F., Midtgaard, J., & Knopfel, T. (1994). Synaptic integration in a model of cerebellar granule cells. *Journal Of Neurophysiology* **72**, 999-1009.

Gandhi, S. P. & Stevens, C. F. (2003). Three modes of synaptic vesicular receycling revealed by single-vesicle imaging. *Nature* **423**, 607-613.

Garwicz, M. & Andersson, G. (1992). Spread of synaptic activity along parallel fibres in cat cerebellar anterior lobe. *Experimental Brain Research* **88**, 615-622.

Gill, R., Nordholm, L., & Lodge, D. (1992). The neuroprotective actions of 2,3-dihydroxy-6-nitro-7-sulfamoyl-benzo(F)quinoxaline (NBQX) in a rat focal ischaemia model. *Brain Research* **580**, 35-43.

Glaum, S. R., Slater, N. T., Rossi, D. J., & Miller, R. J. (1992). Role of metabotropic glutamate (t-ACPD) receptors at the parallel fiber-Purkinje cell synapse. *Journal Of Neurophysiology* **64**, 1453-1462.

Goossens, J., Daniel, H., Rancillac, A., van der, S. J., Oberdick, J., Crepel, F., De Zeeuw, C. I., & Frens, M. A. (2001). Expression of protein kinase C inhibitor blocks cerebellar long-term depression without affecting Purkinje cell excitability in alert mice. *Journal Of Neuroscience* **21**, 5813-5823.

Grassi, S. & Pettorossi, V. E. (2000). Role of nitric oxide in long-term potentiation of the rat medial vestibular nuclei. *Neuroscience* **101**, 157-164.

Griffiths, C. & Garthwaite, J. (2001). The shaping of nitric oxide signals by a cellular sink. *Journal Of Physiology-London* **536**, 855-862.

Griffiths, C., Yamini, B., Hall, C., & Garthwaite, J. (2002). Nitric oxide inactivation in brain by a novel O^2-dependent mechanism resulting in the formation of nitrate ions. *Biochemical Journal* **362**, 459-464.

Gundappa-Sulur, G., De Schutter, E., & Bower, J. M. (1999). Ascending granule cell axon: an important component of cerebellar cortical circuitry. *Journal Of Comparative Neurology* **408**, 580-596.

Haley, J. E., Wilcox, G. L., & Chapman, P. F. (1992). The role of nitric oxide in hippocampal long-term potentiation. *Neuron* **8**, 211-216.

Hall, K. U., Collins, S. P., Gamm, D. M., Massa, E., DePaoliRoach, A. A., & Uhler, M. D. (1999). Phosphorylation-dependent inhibition of protein phosphatase-1 by G- substrate - A Purkinje cell substrate of the cyclic GMP-dependent protein kinase. *Journal Of Biological Chemistry* **274**, 3485-3495.

Hamill, O. P., Marty, A., Neher, E., Sakmann, B., & Sigworth, F. J. (1981). Improved patch-clamp techniques for high-resolution current recording from cells and cell-free membrane patches. *Pflugers Archiv-European Journal Of Physiology* **391**, 85-100.

Harris, K. M. & Stevens, J. K. (1988). Dendritic spines of rat cerebellar Purkinje cells: serial electron microscopy with reference to their biophysical characteristics. *Journal Of Neuroscience* **8**, 4455-4469.

Harris, K. M. & Sultan, P. (1995). Variation in the number, locations and size of synaptic vesicles provides an anatomical basis for the nonuniform probability of release at hippocampal CA1 synapses. *Neuropharmacology* **34**, 1387-1395.

Harrison, J. & Jahr, C. E. (2003). Receptor occupancy limits synaptic depression at climbing fiber synapses. *Journal Of Neuroscience* **23**, 377-383.

Hartell, N. A. (1994a). cGMP acts within cerebellar Purkinje cells to produce long term depression via mechanisms involving PKC and PKG. *NeuroReport* **5**, 833-836.

Hartell, N. A. (1994b). Induction of cerebellar long-term depression requires activation of glutamate metabotropic receptors. *NeuroReport* **5**, 913-916.

Hartell, N. A. (1996). Strong activation of parallel fibers produces localized calcium transients and a form of LTD that spreads to distant synapses. *Neuron* **16**, 601-610.

Hartell, N. A. (2000). Receptors, second messengers and protein kinases required for heterosynaptic cerebellar long-term depression. *Neuropharmacology* **40**, 148-161.

Hartell, N. A., Furuya, S., Jacoby, S., & Okada, D. (2001). Intercellular action of nitric oxide increases cGMP in cerebellar Purkinje cells. *NeuroReport* **12**, 25-28.

Harvey, R. J. & Napper, R. M. (1988). Quantitative study of granule and Purkinje cells in the cerebellar cortex of the rat. *Journal Of Comparative Neurology* **274**, 151-157.

Hausser, M. & Roth, A. (1997). Dendritic and somatic glutamate receptor channels in rat cerebellar Purkinje cells. *Journal Of Physiology-London* **501**, 77-95.

Hayashi, T., Umemori, H., Mishina, M., & Yamamoto, T. (1999). The AMPA receptor interacts with and signals through the protein tyrosine kinase Lyn. *Nature* **397**, 72-76.

Hebb, D. O. (1949). *The Organisation of Behaviour* Wiley, New York.

Heck, D. (1995). Sequential stimulation of guinea pig cerebellar cortex in vitro strongly affects Purkinje cells via parallel fibres. *Naturwissenschaften* **82**, 201-203.

Hemart, N., Daniel, H., Jaillard, D., & Crepel, F. (1994). Properties of glutamate receptors are modified during long-term depression in rat cerebellar Purkinje cells. *Neuroscience* **19**, 213-221.

Hemart, N., Daniel, H., Jaillard, D., & Crepel, F. (1995). Receptors and second messengers involved in long-term depression in rat cerebellar slices *in vitro*: a reappraisal. *European Journal Of Neuroscience* **7**, 45-53.

Hirai, H. (2001). Modification of AMPA receptor clustering regulates cerebellar synaptic plasticity. *Neuroscience Research* **39**, 261-267.

Hirai, H., Launey, T., Mikawa, S., Torashima, T., Yangihara, D., Kasaura, T., Miyamoto, A., & Yuzaki, M. (2003). New role of delta 2-glutamate receptors in AMPA receptor trafficking and cerebellar function. *Nature Neuroscience* **6**, 869-876.

Hirano, T. (1990). Depression and potentiation of the synaptic transmission between a granule cell and a purkinje-cell in rat cerebellar culture. *Neuroscience Letters* **119**, 141-144.

Hirano, T., Kasono, K., Araki, K., & Mishina, M. (1995). Suppression of LTD in cultured Purkinje cells deficient in the glutamate receptor d2 subunit. *NeuroReport* **6**, 534-526.

Hirano, T., Kasono, K., Araki, K., Shinozuka, K., & Mishina, M. (1994). Involvement of the glutamate-receptor delta-2 subunit in the long- term depression of glutamate responsiveness in cultured rat purkinje- cells. *Neuroscience Letters* **182**, 172-176.

Ho, N., Liauw, J. A., Blaeser, F., Wei, F., Hanissian, S., Muglia, L. M., Wozniak, D. F., Nardi, A., Arvin, K. L., Holtzman, D. M., Linden, D. J., Zhuo, M., Muglia, L. J., & Chatila, T. A. (2000). Impaired synaptic plasticity and cAMP response element-binding protein activation in Ca2+/calmodulin-dependent protein kinase type IV/Gr- deficient mice. *Journal Of Neuroscience* **20**, 6459-6472.

Ichikawa, R., Miyazaki, T., Kano, M., Hashikawa, T., Tatsumi, H., Sakimura, K., Mishina, M., Inoue, Y., & Watanabe, M. (2002). Distal extension of climbing fiber territory and multiple innervation caused by aberrant wiring to

adjacent spiny branchlets in cerebellar Purkinje cells lacking glutamate receptor delta 2. *Journal Of Neuroscience* **22**, 8487-8503.

Inada, H., Shindo, H., Tawata, M., & Onaya, T. (1998). cAMP regulates nitric oxide production and ouabain sensitive Na^+, K^+-ATPase activity in SH-SY5Y human neuroblastoma cells. *Diabetologia* **41**, 1451-1458.

Inada, H., Shindo, H., Tawata, M., & Onaya, T. (1999). Cilostazol, a cyclic AMP phosphodiesterase inhibitor, stimulates nitric oxide production and sodium potassium adenosine triphosphatase activity in SH-SY5Y human neuroblastoma cells. *Life Sciences* **65**, 1413-1422.

Isope, P. & Barbour, B. (2002). Properties of unitary granule cell-->Purkinje cell synapses in adult rat cerebellar slices. *Journal Of Neuroscience* **22**, 9668-9678.

Ito, M. (1982). Cerebellar control of the vestibulo-ocular reflex around the flocculus hypothesis. *Annual Review Of Neuroscience* **5**, 0-96.

Ito, M. (1984). *The cerebellum and neuronal control* Raven, New York.

Ito, M. (1989). Long-term depression. *Annual Review Of Neuroscience* **12**, 85-102.

Ito, M. (1998). Cerebellar learning in the vestibulo-ocular reflex. *Trends In Cognitive Sciences* **2**, 313-321.

Ito, M. (2001). Cerebellar long-term depression: characterisation, signal transduction, and functional roles. *Physiological Reviews* **81**, 1143-1195.

Ito, M. & Kano, M. (1982). Long-lasting depression of parallel fiber-Purjkinje cell transmission induced by conjunctive stimulation of parallel fibres and climbing fibers in the cerebellar cortex. *Neuroscience Letters* **33**, 253-258.

Ito, M. & Karachot, L. (1990). Messengers mediating long-term desensitization in cerebellar Purkinje cells. *NeuroReport* **1**, 129-132.

Ito, M. & Karachot, L. (1992). Protein kinases and phosphatase inhibitors mediating long-term desensitization of glutamate receptors in cerebellar Purkinje cells. *Neuroscience* **14**, 27-38.

Ito, M., Sakurai, M., & Tongroach, P. (1982). Climbing fiber induced depression of both mossy fiber responsiveness and glutamate sensitivity of cerebellar Purkinje cells. *Journal Of Physiology-London* **324**, 113-134.

Jacoby, S. (2001). *On the mechanisms of synaptic plasticity in the cerebellum*. Aston University.

Jacoby, S. & Hartell, N. A. (1999). Raised frequency parallel fibre stimulation can produce both nitric oxide-dependent LTP and LTD in the rat cerebellar cortex. *Journal Of Physiology-London* **520**, 38P.

Jacoby, S., Sims, R. E., & Hartell, N. A. (2001). Nitric Oxide is required for the induction and heterosynaptic spread of cerebellar LTP. *Journal Of Physiology-London* **535**, 825-839.

Jeromin, A., Huganir, R. L., & Linden, D. J. (1996). Suppression of the glutamate-receptor delta-2 subunit produces a specific impairment in cerebellar long-term depression. *Journal Of Neurophysiology* **76**, 3578-3583.

Jorntell, H. & Ekerot, C. F. (2002). Reciprocal bidirectional plasticity of parallel fiber receptive fields in cerebellar Purkinje cells and their afferent interneurons. *Neuron* **34**, 797-806.

Karachot, L., Kado, R. T., & Ito, M. (1995). Stimulus parameters for induction of long-term depression in *in vitro* rat Purkinje cells. *Neuroscience Research* **21**, 161-168.

Karachot, L., Shirai, Y., Vigot, R., Yamamori, T., & Ito, M. (2001). Induction of long-term depression in cerebellar Purkinje cells requires a rapidly turned over protein. *Journal Of Neurophysiology* **86**, 280-289.

Kashiwabuchi, N., Ikeda, K., Araki, K., Hirano, T., Shibuki, K., Katsuwada, T., Yagi, T., Kang, Y. A., & Mishina, M. (1995). Impairment of motor coordination, Purkinje cell synapse formation, and cerebellar long-term depression in Glurd2 mutant mice. *Cell* **81**, 245-252.

Kasono, K. & Hirano, T. (1994). Critical role of postsynaptic calium in cerebellar long-term depression. *NeuroReport* **6**, 17-20.

Kato, K., Clark, G. D., Bazan, N. G., & Zorumski, C. F. (1994). Platelet-activating-factor as a potential retrograde messenger in ca1 hippocampal long-term potentiation. *Nature* **367**, 175-179.

Katoh, A., Kitazawa, S., Itohara, S., & Nagao, S. (1998). Dynamic characteristics and adaptability of mouse vestibulo-ocular and optokinetic response eye movements and the role of the flocculo-olivary system revealed by chemical lesions. *Proceedings Of The National Academy Of Sciences Of The United States Of America* **95**, 7705-7710.

Katoh, A., Kitazawa, S., Itohara, S., & Nagao, S. (2000). Inhibition of nitric oxide synthesis and gene-knockout of neuronal nitric oxide synthase impaired adaptation of mouse optokinetic eye movements. *Learning & Memory* **7**, 220-226.

Kawasaki, H., Springett, G. M., Mochizuki, N., Toki, S., Nakaya, M., Matsuda, M., Housman, D. E., & Graybiel, A. M. (1998). A family of cAMP-binding proteins that directly activate Rap1. *Science* **282**, 2275-2279.

Khodakhah, K. & Armstrong, C. M. (1997). Induction of long-term depression and rebound potentiation by inositol trisphosphate in cerebellar Purkinje neurons. *Proceedings Of The National Academy Of Sciences Of The United States Of America* **94**, 14009-14014.

Kim, J. & Alger, B. E. (2001). Random response fluctuations lead to spurious paired-pulse facilitation. *Journal Of Neuroscience* **21**, 9608-9618.

Kimura, S., Uchiyama, S., Takahashi, H. E., & Shibuki, K. (1998). cAMP-dependent long-term potentiation of nitric oxide release from cerebellar parallel fibers in rats. *Journal Of Neuroscience* **18**, 8551-8558.

Kitazawa, S. (2002). Optimization of goal-directed movements in the cerebellum: a random walk hypothesis. *Neuroscience Research* **43**, 289-294.

Kitazawa, S., Katoh, A., Yagi, T., & Nagao, S. (2000). Dynamic characteristics and adaptability of reflex eye movements of Fyn-kinase-deficient mice. *Neuroscience Letters* **280**, 179-182.

Kitazawa, S., Kimura, T., & Yin, P. B. (1998). Cerebellar complex spikes encode both destinations and errors in arm movements. *Nature* **392**, 494-497.

Kocsis, J. D., Malenka, R. C., & Waxman, S. G. (1983). Effects of extracellular potassium concentration on the excitability of the parallel fibres of the rat cerebellum. *Journal Of Physiology-London* **334**, 225-244.

Kohda, K., Inoue, T., & Mikoshiba, K. (1995). Ca2+ release from Ca2+ stores, particularly from ryanodine-sensitive Ca2+ stores, is required for the induction of LTD in cultured cerebellar Purkinje cells. *Journal Of Neurophysiology* **74**, 2184-2189.

Kohler, T., Kamiya, Y., Matsuda, S., Kato, K., Umemori, H., & Yuzaki, M. (2003). Heteromer formation of delta 2 glutamate receptors with AMPA or kainate receptors. *Molecular Brain Research* **110**, 27-37.

Konnerth, A., Dreessen, J., & Augustine, G. J. (1992). Brief dendritic calcium signals initiate long-lasting synaptic depression in cerebellar Purkinje cells. *Proceedings Of The National Academy Of Sciences Of The United States Of America* **89**, 7051-7055.

Konnerth, A., Llano, I., & Armstrong, C. M. (1990). Synaptic currents in cerebellar Purkinje cells. *Proceedings Of The National Academy Of Sciences Of The United States Of America* **87**, 2662-2665.

Korn, H. & Faber, D. S. (1991). Quantal analysis and synaptic efficacy in the CNS. *Trends In Neurosciences* **14**, 439-445.

Korn, H., Mallet, A., & Triller, A. (1982). Transmission at a central inhibitory synapse .2. Quantal description of release, with a physical correlate for binomial-n. *J Neurophysiol.* **48**, 679-707.

Kreitzer, A. C. & Regehr, W. G. (2001). Retrograde inhibition of presynaptic calcium influx by endogenous cannabinoids at excitatory synapses onto Purkinje cells. *Neuron* **29**, 717-727.

Kullmann, D. M., Perkel, D. J., Manabe, T., & Nicoll, R. A. (1992). Ca^{2+} entry via postsynaptic voltage-sensitive Ca2+ channels can transiently potentiate excitatory synaptic transmission in the hippocampus. *Neuron* **9**, 1175-1183.

Lev-Ram, V., Jiang, T., Wood, J., Lawrence, D. S., & Tsien, R. Y. (1997a). Synergies and coincidence requirements between NO, cGMP, and Ca^{2+} in the induction of cerebellar long-term depression. *Neuron* **18**, 1025-1038.

Lev-Ram, V., Makings, L. R., Keitz, P. F., Kao, J. Y., & Tsien, R. Y. (1995). Long-term depression in cerebellar Purkinje neurons results from coincidence of nitric oxide and depolarization-induced Ca^{2+} transients. *Neuron* **15**, 407-415.

Lev-Ram, V., Nebyelul, Z., Ellisman, M. H., Huang, P. L., & Tsien, R. Y. (1997b). Absence of cerebellar long-term depression in mice lacking neuronal nitric oxide synthase. *Learning & Memory* **3**, 167-177.

Lev-Ram, V., Wong, S. T., Storm, D. R., & Tsien, R. Y. (2002). A new form of cerebellar long-term potentiation is postsynaptic and depends on nitric oxide but not cAMP. *Proceedings Of The National Academy Of Sciences Of The United States Of America* **99**, 8389-8393.

Li, J., Smith, S. S., & McElliot, J. G. (1995). Cerebellar Nitric Oxide is necessary for vestibulo-ocular reflex adaptation, a sensory model of learning. *Journal Of Neurophysiology* **74**, 489-494.

Linden, D. J. (1995). Phospholipase A2 controls the induction of short-term versus long-term depression in the cerebellar Purkinje neuron in culture. *Neuron* **15**, 1393-1401.

Linden, D. J. (1996). A protein synthesis-dependent late phase of cerebellar long-term depression. *Neuron* **17**, 483-490.

Linden, D. J. (2001). The expression of cerebellar LTD in culture is not associated with changes in AMPA-receptor kinetics, agonist affinity, or unitary conductance. *Proceedings Of The National Academy Of Sciences Of The United States Of America* **98**, 14066-14071.

Linden, D. J. & Connor, J. A. (1991). Participation of postsynaptic PKC in cerebellar long-term depression in culture. *Science* **254**, 1656-1659.

Linden, D. J. & Connor, J. A. (1992). Long-term depression of glutamate currents in cultured cerebellar Purkinje neurons does not require nitric oxide signalling. *European Journal Of Neuroscience* **4**, 10-15.

Linden, D. J., Dawson, T. M., & Dawson, V. L. (1995). An evaluation of the nitric oxide/cGMP-dependent protein kinase cascade in the induction of cerebellar long-term depression in culture. *Journal Of Neuroscience* **15**, 5098-5105.

Linden, D. J., Dickenson, M. H., Smeyne, M., & Connor, J. A. (1991). A long-term depression of AMPA currents in cultured cerebellar Purkinje neurons. *Neuron* **7**, 81-89.

Linden, D. J., Smeyne, M., & Connor, J. A. (1993). Induction of cerebellar long-term depression in culture requires postsynaptic action of sodium ions. *Neuron* **11**, 1093-1110.

Linden, D. J., Smeyne, M., & Connor, J. A. (1994). Trans-ACPD, a metabotropic receptor agonist, produces calcium mobilization and an inward current in cultured cerebellar Purkinje neurons. *Journal Of Neurophysiology* **71**, 1992-1998.

Llinas, R. (1982). General Discussion: radial connectivity in the cerebellar cortex: a novel view regarding the functional organisation of the molecular layer. In *The cerebellum: new vistas [Exp. Brain Res, vol 6 (Suppl.)]*, eds. Palay, S. L. & Chan-Palay, V., pp. 189-194. Springer Verlag, New York.

Lombardi, G., Leonardi, P., & Moroni, F. (1996). Metabotropic glutamate receptors, transmitter output and fatty acids: studies in rat brain slices. *British Journal Of Pharmacology* **117**, 189-195.

Luthi, A., Chittajallu, R., Duprat, F., Palmer, M. J., Benke, T. A., Kidd, F. L., Henley, J. M., Isaac, J. T. R., & Collingridge, G. L. (1999). Hippocampal LTD expression involves a pool of AMPARs regulated by the NSF-GluR2 interaction. *Neuron* **24**, 389-399.

Maeda, N., Ninobe, M., & Mikoshiba, K. (1990). A cerebellar Purkinje cell marker P400 protein is an inositol 1,4,5-trisphosphate ($InsP_3$) receptor protein. Purification and characterisation of $InsP_3$ receptor complex. *European Molecular Biology Organization Journal* **9**, 61-67.

Markram, H., Wang, Y., & Tsodyks, M. (1998). Differential signaling via the same axon of neocortical pyramidal neurons. *Proceedings Of The National Academy Of Sciences Of The United States Of America* **95**, 5323-5328.

Marr, D. (1969). A theory of cerebellar cortex. *Journal Of Physiology-London* **202**, 437-470.

Matsuda, S., Launey, T., Mikawa, S., & Hirai, H. (2000). Disruption of AMPA receptor GluR2 clusters following long-term depression induction in cerebellar Purkinje neurons. *European Molecular Biology Organization Journal* **19**, 2765-2774.

Meffert, M. K., Calakos, N. C., Scheller, R. H., & Schulman, H. (1996). Nitric oxide modulates synaptic vesicle docking fusion reactions. *Neuron* **16**, 1229-1236.

Meffert, M. K., Premack, B. A., & Schulman, H. (1994). Nitric oxide stimulates Ca^{2+}-independent synaptic vesicle release. *Neuron* **12**, 1235-1244.

Merrill, E. G., Wall, P. D., & Yaksh, T. L. (1978). Properties of two unmyelinated fibre tracts of the central nervous system: lateral Lissauer tract, and parallel fibres of the cerebellum. *Journal Of Physiology-London* **284**, 127-145.

Miyata, M., Okada, D., Hashimoto, K., Kano, M., & Ito, M. (1999). Corticotropin-releasing factor plays a permissive role in cerebellar long-term depression. *Neuron* **22**, 763-775.

Mocanu, O. D., Oliver, J., Santamaria, F., & Bower, J. M. (2002). Branching point effects on the passive properties of the cereballar granule cell axon. *Neurocomputing* **32-33**, 207-212.

Montague, P. R. & Sejnowski, T. J. (1994). The predictive brain: temporal coincidence and temporal order in synaptic learning mechanisms. *Learning & Memory* **1**, 1-33.

Morgan, J. I. & Curran, T. (1989). Stimulus-transcription coupling in neurons: role of cellular immediate-early genes. *Trends In Neurosciences* **12**, 459-462.

Mugnaini, E. (1972). The histology and cytology of the cerebellar cortex. In *The comparative anatomy and histology of the cerebellum: the human cerebellum, cerebellar connections, and cerebellar cortex.*, eds. Larsell, O. & Jansen, J., pp. 201-262. University of Minnesota Press, Minneapolis.

Murthy, V. N., Sejnowski, T. J., & Stevens, C. F. (1997). Heterogeneous release properties of visualized individual hippocampal synapses. *Neuron* **18**, 599-612.

Nagao, S. (1988). Behaviour of floccular Purkinje cells correlated with adaptation of horizontal optokinetic eye movement response in pigmented rabbits. *Experimental Brain Research* **73**, 489-497.

Nagao, S. & Ito, M. (1991). Subdural application of hemoglobin to the cerebellum blocks vestibulooccular reflex adaptation. *NeuroReport* **2**, 193-196.

Nakanishi, S. (1994). Metabotropic glutamate receptors - synaptic transmission, modulation, and plasticity. *Neuron* **13**, 1031-1037.

Nakazawa, K., Karachot, Nakabeppu, Y., & Yamamori, T. (1993). The conjunctive stimuli that cause long-term desensitization also predominantly induce c-Fos and Jun-B in cerebellar Purkinje cells. *NeuroReport* **4**, 1275-1278.

Namba, T., Morimoto, K., Sato, K., Yamada, N., & Kuroda, S. (1994). Antiepileptogenic and anticonvulsant effects of NBQX, a selective AMPA receptor antagonist, in the rat kindling model of epilepsy. *Brain Res.* **638**, 36-44.

Napper, R. M. & Harvey, R. J. (1988). Number of parallel fiber synapses on an individual Purkinje cell in the cerebellum of the rat. *Journal Of Comparative Neurology* **274**, 168-177.

Narasimhan, K., Pessah, I. N., & Linden, D. J. (1998). Inositol-1,4,5-trisphosphate receptor-mediated Ca mobilization is not required for cerebellar long-term depression in reduced preparations. *Journal Of Neurophysiology* **80**, 2963-2974.

Neher, E. (1992). Ion channels for communication between and within cells (Nobel lecture). *Angewandte Chemie-International Edition In English* **31**, 824-829.

Neher, E. & Sakmann, B. (1992). The patch clamp technique. *Scientific American* **266**, 28-35.

Nguyen, P. V., Abel, T., & Kandel, E. R. (1994). Requirement of a critical period of transcription for induction of a late-phase of ltp. *Science* **265**, 1104-1107.

Nieto-Bona, M. P., Garcia-Segura, L. M., & Torres-Aleman, I. (1997). Transynaptic modulation by insulin-like growth factor I of dendritic spines in Purkinje cells. *International Journal Of Developmental Neuroscience* **15**, 749-754.

Nishimune, A., Isaac, J. T. R., Molnar, E., Noel, J., Nash, S. R., Tagaya, M., Collingridge, G. L., Nakanishi, S., & Henley, J. M. (1998). NSF binding to GluR2 regulates synaptic transmission. *Neuron* **21**, 87-97.

Nowicky, A. V. & Bindman, L. J. (1993). The nitric oxide synthase inhibitor, N-monomethyl-L-arginine blocks induction of a long-term potentiation-like phenomenon in rat medial frontal cortical neurons in vitro. *Journal Of Neurophysiology* **70**, 1255-1259.

Okada, D. (1995). Protein kinase C modulates calcium sensitivity of nitric oxide synthase in cerebellar slices. *Journal Of Neurochemistry* **64**, 1298-1304.

Oleskevich, S., Clements, J. D., & Walmsley, B. (2000). Release probability modulates short-term plasticity at a rat giant terminal. *Journal Of Physiology-London* **524**, 513-523.

Oscarsson, O. (1979). Functional units of the cerebellum - sagittal zones and microzones. *Trends In Neurosciences* **2**, 143-145.

Osoegawa, K., Tateno, M., Woon, P. Y., Frengen, E., Mammoser, A. G., Catanese, J. J., Hayashizaki, Y., & de Jong, P. J. (2000). Bacterial artificial chromosome libraries for mouse sequencing and functional analysis. *Genome Research* **10**, 116-128.

Palay, S. L. & Chan-Palay, V. (1974). *The Cerebellar Cortex* Springer-Verlag, New York.

Park, J. H., Straub, V. A., & Oshea, M. (1998). Anterograde signaling by nitric oxide: Characterization and in vitro reconstitution of an identified nitrergic synapse. *Journal Of Neuroscience* **18**, 5463-5476.

Philippides, A., Husbands, P., & O'Shea, M. (2000). Four-dimensional neuronal signaling by nitric oxide: A computational analysis. *Journal Of Neuroscience* **20**, 1199-1207.

Pitchitpornchai, C., Rawson, J. A., & Rees, S. (1994). Morphology of parallel fibres in the cerebellar cortex of the rat: an experimental light and electron microscopic study with biocytin. *Journal Of Comparative Neurology* **342**, 206-220.

Rao, K. V., Vaidvanathan, V. V., & Sastry, P. S. (1994). Diacylglycerol kinase is stimulated by archidonic acid in neural membranes. *Journal Of Neurochemistry* **63**, 1454-1459.

Rapp, M., Segev, I., & Yarom, Y. (1994). Physiology, morphology and detailed passive models of guinea-pig cerebellar Purkinje cells. *Journal Of Physiology-London* **474**, 101-118.

Redman, S. (1990). Quantal analysis of synaptic potentials in neurons of the central nervous system. *Physiological Reviews* **70**, 165-198.

Reynolds, T. & Hartell, N. A. (1998). Long-term depression in rat cerebellar slices lacks input specificity. *Journal Of Physiology-London* **509**, 57P.

Reynolds, T. & Hartell, N. A. (2000). An evaluation of the synapse-specificity of long-term depression induced in rat cerebellar slices. *Journal Of Physiology-London* **527**, 563-577.

Reynolds, T. & Hartell, N. A. (2001). Roles for nitric oxide and arachidonic acid in the induction of heterosynaptic cerebellar LTD. *NeuroReport* **12**, 133-136.

Rodrigo, J., Springall, D. R., Uttenthal, O., Bentura, M. L., Abadia-Molina, F., Riveros-Moreno, V., Martinez-Murillo, R., Polak, J. M., & Moncada, S. (1994). Localization of nitric-oxide synthase in the adult-rat brain. *Philosophical Transactions of the Royal Society of London - Series B: Biological Sciences* **345**, 175-221.

Ross, W. N. & Werman, R. (1987). Mapping calcium transients in the dendrites of Purkinje-cells from the guinea-pig cerebellum *in vitro*. *Journal Of Physiology-London* **389**, 319-336.

Roth, A. & Hausser, M. (2001). Compartmental models of rat cerebellar Purkinje cells based on simultaneous somatic and dendritic patch-clamp recordings. *Journal Of Physiology-London* **535**, 445-472.

Sakmann, B. & Neher, E. (1984). Patch clamp techniques for studying ionic channels in excitable membranes. *Annual Review of Physiology* **46**, 455-472.

Sakurai, M. (1987). Synaptic modification of parallel fibre-Purkinje cell transmission in *in vitro* guinea-pig cerebellar slices. *Journal Of Physiology-London* **394**, 463-480.

Sakurai, M. (1990). Calcium is an intracellular mediator of the climbing fibre induction of cerebellar long-term depression. *Proceedings Of The National Academy Of Sciences Of The United States Of America* **87**, 3383-3385.

Salin, P. A., Malenka, R. C., & Nicoll, R. A. (1996). Cyclic-AMP mediates a presynaptic form of LTP at cerebellar parallel fiber synapses. *Neuron* **16**, 797-803.

Scheuss, V. & Neher, E. (2001). Estimating synaptic parameters from mean, variance, and covariance in trains of synaptic responses. *Biophysical Journal* **81**, 1970-1989.

Scheuss, V., Schneggenburger, R., & Neher, E. (2002). Separation of presynaptic and postsynaptic contributions to depression by covariance analysis of successive EPSCs at the calyx of Held synapse. *Journal Of Neuroscience* **22**, 728-739.

Schikorski, T. & Stevens, C. F. (1997). Quantitative ultrastructural analysis of hippocampal excitatory synapses. *Journal Of Neuroscience* **17**, 5858-5867.

Schikorski, T. & Stevens, C. F. (2001). Morphological correlates of functionally defined synaptic vesicle populations. *Nature Neuroscience* **4**, 391-395.

Schlichter, D. J., Casnellie, J. E., & Greengard, P. (1978). An endogenous substrate for cGMP-dependent protein kinase in mammalian cerebellum. *Nature* **273**, 61-62.

Schlichter, D. J., Detre, J. A., Aswad, D. W., Chehrazi, B., & Greengard, P. (1980). Localization of cyclic GMP-dependent protein kinase and substrate in mammalian cerebellum. *Proceedings Of The National Academy Of Sciences Of The United States Of America* **77**, 5537-5541.

Schoepp, D. D. & Conn, P. J. (1993). Metabotropic glutamate receptors in brain function and pathology. *Trends In Pharmacological Sciences* **14**, 13-20.

Schreurs, B. G. & Alkon, D. L. (1993). Rabbit cerebellar slice analysis of long-term depression and its role in classical conditioning. *Brain Research* **631**, 23-240.

Schreurs, B. G., Oh, M., & Alkon, D. L. (1996). Pairing-specific long-term depression of Purkinje cell excitatory postsynaptic potentials results from a classical conditioning proceedure in the rabbit cerebellar slice. *Journal Of Neurophysiology* **753**, 1051-1060.

Schuman, E. M. & Madison, D. V. (1994a). Locally distributed synaptic potentiation in the hippocampus. *Science* **263**, 532-536.

Schuman, E. M. & Madison, D. V. (1994b). Nitric oxide and synaptic function. *Annual Review Of Neuroscience* **17**, 153-183.

Schweighofer, N., Doya, K., & Lay, F. (2001). Unsupervised learning of granule cell sparse codes enhances cerebellar adaptive control. *Neuroscience* **103**, 35-50.

Schweighofer, N. & Ferriol, G. (2000). Diffusion of nitric oxide can facilitate cerebellar learning: A simulation study. *Proceedings Of The National Academy Of Sciences Of The United States Of America* **97**, 10661-10665.

Shambes, G. M., Gibson, I. M., & Welker, W. (1978). Fractured somatotopy in granule cell tactile areas of rat cerebellar hemispheres revealed by micromapping. *Brain Behaviour And Evolution* **15**, 94-140.

Shearman, M. S., Naor, Z., Sekiguchi, K., Kishimoto, A., & Nishizuka, Y. (1989). Selective activation of the gamma-subspecies of protein kinase-C from bovine cerebellum by arachidonic-acid and its lipoxygenase metabolites. *FEBS Letters* **243**, 177-182.

Shepherd, G. M., Raastad, M., & Andersen, P. (2002). General and variable features of varicosity spacing along unmyelinated axons in the hippocampus and cerebellum. *Proceedings Of The National Academy Of Sciences Of The United States Of America* **99**, 6340-6345.

Shibuki, K. & Kimura, S. (1997). Dynamic properties of nitric oxide release from parallel fibres in rat cerebellar slices. *Journal Of Physiology-London* **498**, 443-452.

Shibuki, K. & Okada, D. (1991). Endogenous nitric oxide release required for long-tern synaptic depression in the cerebellum. *Nature* **349**, 326-328.

Shibuki, K. & Okada, D. (1992). Cerebellar long-term potentiation under supressed postsynaptic Ca^{2+} activity. *NeuroReport* **3**, 231-234.

Shigemoto, R., Abe, T., Nomura, S., Nakanishi, S., & Hirano, T. (1994). Antibodies inactivating mGluR1 metabotropic glutamate receptor block long-term depression in cultured Purkinje cells. *Neuron* **12**, 1245-1255.

Shinomura, T., Asaoka, Y., Oka, M., Yoshida, K., & Nishizuka, Y. (1991). Synergistic action of diacylglyerol and unsaturated fatty acid for protein kinase C activation: its possible implicationd. *Proceedings Of The National Academy Of Sciences Of The United States Of America* **88**, 5149-5153.

Siesjo, B. K. (1992). Pathophysiology and treatment of focal cerebral ischemia. Part I: Pathophysiology. *Journal Of Neurosurgery* **77**, 169-184.

Silver, R. A., Momiyama, A., & Cull-Candy, S. G. (1998). Locus of frequency-dependent depression identified with multiple- probability fluctuation analysis

at rat climbing fibre-Purkinje cell synapses. *Journal Of Physiology-London* **510 (Pt 3)**, 881-902.

Son, H., Hawkins, R. D., Martin, K., Kiebler, M., Huang, P. L., Fishman, M. C., & Kandel, E. R. (1996). Long-term potentiation is reduced in mice that are doubly mutant in endothelial and neuronal nitric oxide synthase. *Cell* **87**, 1015-1023.

Southam, E., Morris, R., & Garthwaite, J. (1992). Sources and targets of nitric oxide in rat cerebellum. *Neuroscience* **137**, 241-244.

Sudhof, T. C. (1995). The synaptic vesicle cycle: a cascade of protein-protein interactions. *Nature* **375**, 645-653.

Sugimori, M. & Llinas, R. R. (1990). Real-time imaging of calcium influx in mammalian cerebellar Purkinje cells *in vitro*. *Proceedings Of The National Academy Of Sciences Of The United States Of America* **87**, 5084-5088.

Takechi, H., Eilers, J., & Konnerth, A. (1998). A new class of synaptic response involving calcium release in dendritic spines. *Nature* **396**, 757-760.

Tempia, F., Kano, M., Schneggenburger, R., Schirra, C., Garaschuk, O., Plant, T., & Konnerth, A. (1996). Fractional calcium current through neuronal AMPA-receptor channels with a low-calcium permeability. *Journal Of Neuroscience* **16**, 456-466.

Thatch, W. T. (1967). Somatosensory receptive fields of single units in cat cerebellar cortex. *Journal Of Neurophysiology* **30**, 675-696.

Thomson, A. M. (2000). Facilitation, augmentation and potentiation at central synapses. *Trends In Neurosciences* **23**, 305-312.

Tremblay, J., Gerzer, R., & Hamet, P. (1988). Cyclic GMP in cell function. *Advances in Second Messenger and Phosphorylation Research, 22.Eds.Greengard P and Robison GA.Raven press, New York.*

Tsunoda, R., Okumura, K., Ishizaka, H., Matsunaga, T., Tabuchi, T., Yasue, H., Akaike, T., Sato, K., & Maeda, H. (1994). Vasodilator effect of carboxy-2-phenyl-4,4,5,5-tetramethylimidazoline-1-oxyl in the coronary circulation: in vivo and in vitro studies. *European Journal Of Pharmacology* **262**, 55-63.

Ukena, D., Schudt, C., & Sybrecht, G. W. (1993). Adenosine receptor-blocking xanthines as inhibitors of phosphodiesterase isozymes. *Biochemical Pharmacology* **45**, 847-851.

Umemori, H., Hayashi, T., Inoue, T., Nakanishi, S., Mikoshiba, K., & Yamamoto, T. (1999). Involvement of protein tyrosine phosphatases in activation of the trimeric protein $G_{q/11}$. *Oncogene* **18**, 7399-7402.

Voronin, L. L. (1994). Quantal analysis of hippocampal long-term potentiation. *Reviews in the Neurosciences* **5**, 141-170.

Vranesic, I., Iijima, T., Ichikawa, M., Matsumoto, G., & Knopfel, T. (1994). Signal transmission in the parallel fiber-Purkinje cell system visualized by high-resolution imaging. *Proceedings Of The National Academy Of Sciences Of The United States Of America* **91**, 13014-13017.

Wang, S. S., Denk, W., & Hausser, M. (2000a). Coincidence detection in single dendritic spines mediated by calcium release. *Nature Neuroscience* **3**, 1266-1273.

Wang, S. S., Khiroug, L., & Augustine, G. J. (2000b). Quantification of spread of cerebellar long-term depression with chemical two-photon uncaging of glutamate. *Proceedings Of The National Academy Of Sciences Of The United States Of America* **97**, 8635-8640.

Wang, Y. T. & Linden, D. J. (2000). Expression of cerebellar long-term depression requires postsynaptic clathrin-mediated endocytosis. *Neuron* **25**, 635-647.

Wood, J. & Garthwaite, J. (1994). Models of the diffusional spread of nitric-oxide - implications for neural nitric-oxide signaling and its pharmacological properties. *Neuropharmacology* **33**, 1235-1244.

Xia, J., Chung, H. J., Wihler, C., Huganir, R. L., & Linden, D. J. (2000). Cerebellar long-term depression requires PKC-regulated interactions between GluR2/3 and PDZ domain-containing proteins. *Neuron* **28**, 499-510.

Xu-Friedman, M. A., Harris, K. M., & Regehr, W. G. (2001). Three-dimensional comparison of ultrastructural characteristics at depressing and facilitating synapses onto cerebellar Purkinje cells. *Journal Of Neuroscience* **21**, 6666-6672.